



Jimma University

School of Graduate Studies

Jimma Institute of Technology

School of Civil and Environmental Engineering

Department of Civil Engineering

Structural Engineering Stream

CAUSE AND CONTROL OF CRACKING IN REINFORCED CONCRETE HIGHWAY
BRIDGE DECK: A CASE STUDY IN BONGA TOWN, SHETA RIVER BRIDGE DECK

A thesis submitted to the school of graduate studies of Jimma Institute of Technology in
partial fulfilment of the requirement for the degree of Master of Science in Civil
Engineering (Major Structural Engineering)

Berhanu Tefera

August 2016

Jimma, Ethiopia



Jimma University

School of Graduate Studies

Jimma Institute of Technology

School of Civil and Environmental Engineering

Department of Civil Engineering

Structural Engineering Stream

CAUSE AND CONTROL OF CRACKING IN REINFORCED CONCRETE HIGHWAY
BRIDGE DECK: A CASE STUDY IN BONGA TOWN, SHETA RIVER BRIDGE DECK

A thesis submitted to the school of graduate studies of Jimma Institute of Technology in
partial fulfilment of the requirement for the degree of Master of Science in Civil
Engineering (Major Structural Engineering)

Berhanu Tefera

Dr. Ing. Abrham Gebre (PhD)

Advisor

Eng. Kabtamu Getachew (MSc)

Co – Advisor

August 2016

Jimma, Ethiopia

CAUSE AND CONTROL OF CRACKING IN REINFORCED CONCRETE HIGHWAY
BRIDGE DECK: A CASE STUDY IN BONGA TOWN, SHETA RIVER BRIDGE DECK

Berhanu Tefera

A thesis submitted to the school of graduate studies of Jimma Institute of Technology in
partial fulfilment of the requirement for the degree of Master of Science in Civil
Engineering (Major Structural Engineering)

August 2016

Jimma, Ethiopia

Approved by Board of Examiners

Dr. Ing. Abrham Gebre (PhD)

Advisor

Signature

Date

Eng. Kabtamu Getachew (MSc)

Co – Advisor

Signature

Date

External examiner

Signature

Date

Internal examiner

Signature

Date

Chairman

Signature

Date

ABSTRACT

Cracking in concrete bridge deck is widely regarded as a long-term durability and maintenance problem that requires attention. Once a crack has developed in a bridge deck create a path for water and de-icing salts to reach the steel, often leading to corrosion of the reinforcement, greatly reducing the service life of the bridge deck. The focus of this study was to investigate the causes of cracking in reinforced concrete highway bridge deck related to transverse deck cracking. This study selected a single-span RC deck girder bridge crossing Sheta River with a service life of 50 years, located at Kaffa Zone, Bonga town. The study used both primary and secondary data. The primary data was collected from in place non-destructive tests in conjunction with completing visual bridge inspection formats. The secondary data was collected from ERA previous inspection & inventory reports and data on similarly constructed RC deck girder bridge (Bitino River Bridge). ACI 209R-92 model and ASHTO-2011 second edition manual for bridge evaluation were used to analyze the collected data to measure predicted compressive strength at any time and performance evaluation of Sheta River Bridge deck, respectively.

The study finding revealed that the major causes of Sheta River Bridge deck cracking are environment & site conditions, materials properties, structural design parameters, excessive traffic overloading and age of the bridge. The finding of this study also shows that the structural conditions of the bridge are at reasonably good condition and almost all manifested cracking in Sheta River Bridge deck are non-structural cracks. Therefore, the researcher recommends that concerned body shall use gravity filling crack repair mechanism with association of lower viscosity gravity feed product and strengthen a girder of the bridge solutions in order to prolonging the span life of Sheta River Bridge deck.

Key words

Bridge deck, reinforced concrete, cracking, cause of crack, control of crack

DECLARATION

I, the undersigned, declare that this thesis entitled “*Cause and control of cracking in reinforced concrete highway bridge deck: A case study in Bonga town, Sheta River Bridge deck*” is my original work. The work has not been presented by any other person for a degree in this or any other University and all sources of material used for this thesis have been duly acknowledged.

Candidate:

Mr. Berhanu Tefera

Signature: _____

Place: Jimma Institute of Technology

Date of Submission: August, 2016

This thesis work is dedicated to my family

ACKNOWLEDGMENT

First of all I would like to thank the almighty God for helping me on every aspect during my stay at the university and the accomplishment of this thesis. Next to this I also would like to take this opportunity to express my sincere appreciation to my advisor Dr.-Ing Abrham Gebre (PhD), Addis Ababa University, Addis Ababa Institute of Technology for his professional, genuine guidance and valuable advice to accomplish the thesis on time. And also I would like to extend my heart gratitude and sincere appreciation to my co–advisor Engineer Kabtamu Getachew, structural engineering chair in Jimma University, Jimma Institute of Technology for his continuous assistance, suggestions and follow up to accomplish my thesis. Besides, I would like thank for my dear wife Tsiyon Zegeye, whose love and moral support made life fun and attractive. Last but not least I would like to thank my family who has always been there for me.

TABLE OF CONTENTS

List of Tables	VII
List of Figures	VIII
List of Abbreviations and Symbols	IX
CHAPTER ONE	
1. INTRODUCTION	1
1.1 Background of the Study	1
1.2 Statement of the Problem.....	3
1.3 Research Questions.....	4
1.4 Objectives of the Study.....	4
1.4.1 General Objective of the Study.....	4
1.4.2 Specific Objectives of the study	4
1.5 Scope of the Study.....	4
1.6 Significance of the Study.....	5
1.7 Organization of the Study	5
CHAPTER TWO	
2. LITRUTURE REVIEW	6
2.1 General.....	6
2.2 Reinforced concrete bridge deck cracking.....	6
2.3 Classification of cracks in reinforced concrete bridge deck.....	6
2.4 Overview transverse cracking of bridge deck.....	9
2.5 Non-destructive tests for bridge deck condition evaluation	9
2.6 Crack width.....	14
2.7 Factors influencing transverse cracking	15
CHAPTER THREE	
3. RESEARCH METHODOLOGY.....	22
3.1 Study area	22
3.2 Study design.....	23
3.3 Variables of the study	23
3.4 Data collection process	13
3.5 Data processing and analysis	25
3.6 Limitations of the study	26
3.7 Operational definitions	26

CHAPTER FOUR

4. RESULTS AND DISCUSSION	27
4.1 General.....	27
4.2 Field investigation.....	27
4.2.1 Visual inspection.....	28
4.2.2 Crack width.....	31
4.2.3 Rebound hammer test	32
4.2.4 Hammer Sounding	35
4.2.5 Pachometer survey	36
4.2.6 Chloride content analysis	37
4.3 Cause of time - dependent concrete bridge deck cracking	38
4.3.1 Environment and Site conditions	38
4.3.2 Material properties	40
4.3.2.1 Shrinkage	40
4.3.2.2 Creep	41
4.3.3 Structural design parameters.....	42
4.3.3.1 Deck thickness	42
4.3.3.2 Concrete cover	42
4.3.3.3 Design vehicle load.....	43
4.3.3.4 Girder end restraint condition	44
4.3.4 Excessive traffic overloading and Age of bridge.....	45
4.5 Comparision of study with others	46
4.6 Major findings	47

CHAPTER FIVE

5. CONCLUSIONS AND RECOMMENDATIONS	51
5.1 Conclusions.....	51
5.2 Recommendations	52
References	53
Appendix	56

LIST OF TABLES

Table 1.1: Condition of Bridges on Federal Road Network	1
Table 2.1: Tolerable crack widths in reinforced concrete structures	14
Table 3.1: Data processing and analysis methods	25
Table 4.1: General information of existing Sheta River Bridge	27
Table 4.2: Rebound test hammer results for Sheta River Bridge deck	33
Table 4.3 Values of the constant a and b	34
Table 4.4: Chloride ion content analysis	37

LIST OF FIGURES

Figure 1.1: Bridges age distribution of federal road network	2
Figure 2.1: Transverse cracking.....	7
Figure 2.2: Longitudinal cracking	8
Figure 2.3: Diagonal cracking	8
Figure 2.4: Map/Pattern cracking	9
Figure 2.5: Typical crack width measurement on bridge deck	11
Figure 2.6: Operation of the rebound hammer	11
Figure 2.7: Pachometer used to locate reinforcing in bridge deck	13
Figure 2.8: Electro – chemical corrosion in the presence of chlorides.....	13
Figure 2.9: Shrinkage warping in a singly reinforced beam.....	16
Figure 2.10: Concrete strain components subjected to a sustained load	16
Figure 2.11: Epoxy crack injection.....	19
Figure 2.12: Repair of Crack by routing and Sealing	20
Figure 2.13: Application of a gravity feed repair method	21
Figure 3.1: Existing road map of Kaffa Zone	22
Figure 3.2: Typical ERA – BMS datasheet	24
Figure 4.1: Visible transverse bridge deck cracking& deposited silt	28
Figure 4.2: Visible leakage at cracks underneath of deck slab	29
Figure 4.3: Cracking severity of Sheta Bridge deck.....	31
Figure 4.4: Smoothing with a carborundum stone of underneath deck test surface	32
Figure 4.5: Measuring bare undeformed reinforcement bar	32
Figure 4.6: Marked delaminated areas of Sheta River Bridge deck.....	32
Figure 4.7: Measuring bare undeformed steel reinforcement bars.....	32
Figure 4.8: Maximum temperature in Kaffa Zone Bonga town	39
Figure 4.9: Maximum low relative humidity in Kaffa Zone Bonga town	40
Figure 4.10: Total shrinkage strain predictions	41
Figure 4.11: Undeformed bare rebar.....	42
Figure 4.12: Girder end restraint condition	44
Figure 4.13: Corrosion of end plate bearing	44
Figure 4.14: HS20-44 Truck.....	46

LIST OF ABBREVIATIONS AND SYMBOLS

AASHTO	=	American Association State of Highway and Transportation Official
ACI	=	American Concrete Institute
ASTM	=	American Society for Testing and Materials
BMS	=	Bridge Management System
EC	=	Europe Code
ERA	=	Ethiopian Road Authority
JIT	=	Jimma Institute of Technology
LFD	=	Load Factor Design
LRFD	=	Load Resistance and Factor Design
RC	=	Reinforced Concrete
a, b	=	Constants used to describe the strength gain development of the concrete
E	=	Modulus of elasticity, MPa
E_{cm}	=	Mean modulus of elasticity of Concrete, MPa
E_{cm28}	=	Mean modulus of elasticity of concrete at 28 days, MPa
E_{cmt}	=	Mean modulus of elasticity of Concrete at age t , MPa
E_{cmt_0}	=	Mean modulus of elasticity of Concrete when loading starts at age t_0 , MPa
f_{cm}	=	Concrete mean compressive cylinder strength, MPa
f_{cm28}	=	Concrete mean compressive cylinder strength at 28 days, MPa
f_{cmt}	=	Concrete mean compressive cylinder strength at age t , MPa
f_{cmt_c}	=	Concrete mean compressive cylinder strength when drying starts at age t_c , MPa
f'_c	=	Concrete specified cylinder strength at 28 days, MPa
h	=	Relative humidity expressed as a decimal
$\beta_{RH}(h)$	=	Correction term for effect of humidity on shrinkage
$\beta_s(t - t_c)$	=	Correction term for effect of time on shrinkage
T	=	Temperature, °C.
$T(\Delta t_i)$	=	Temperature, °C during the time period Δt_i ,
Δt_i	=	Number of days where a temperature T prevails, n is the number of time intervals considered
t	=	Age of Concrete, days
$t - t_c$	=	Duration of drying, days
t_0	=	Age of Concrete at loading, days

t_o, T	=	Temperature-adjusted age of Concrete at loading, in days
V/S	=	Volume-surface ratio, mm
α_1 or k	=	Shrinkage constant as function of cement type
α_2	=	Shrinkage constant related to curing conditions
α_3	=	Coefficient that depends on the mean compressive strength of Concrete
$\alpha_{as}, \alpha_{ds1}$ and α_{ds2}	=	Correction coefficients for effect of cement type on autogenous and drying shrinkage
$\beta(t_o)$	=	Factor to allow for the effect of concrete age at loading on notational creep coefficient
$\beta_{as}(t)$	=	Function describing time development of autogenous shrinkage
$\beta_c(t - t_o)$	=	Correction term for effect of time on creep coefficient
$\beta_{ds}(t - t_c)$	=	Function describing time development of drying shrinkage
β_e	=	Factor relating strength development to cement type
$\beta(f_{cm28})$	=	Factor to allow for the effect of concrete strength on notational creep coefficient
$\beta_{RH}(h)$	=	Coefficient that takes the effect of relative humidity on drying shrinkage
β_H	=	Coefficient depending on the relative humidity (RH in %)
$\beta_{RH,T}$	=	Correction coefficient to account for effect of temperature on notional shrinkage
β_{sc}	=	Correction coefficient that depends on type of cement
$\varepsilon_{cas}(t)$	=	Autogenous shrinkage strain at Concrete age t, mm/mm
ε_{cso}	=	Notional shrinkage coefficient, mm/mm
$\varepsilon_{caso}(f_{cm28})$	=	Notional autogenous shrinkage coefficient, mm/mm
$\varepsilon_{cdso}(f_{cm28})$	=	Notional drying shrinkage coefficient, mm/mm
$\varepsilon_{sh}(t, t_c)$	=	Shrinkage strain at Concrete age t since the start of drying at age t_c , mm/mm
ε_{shu} or $\varepsilon_{sh\infty}$	=	Notional ultimate shrinkage strain, mm/mm
$\varphi(t, t_o)$	=	Creep coefficient (dimensionless)
$\varphi_{28}(t, t_o)$	=	28-day creep coefficient (dimensionless)
φ_o	=	Notional creep coefficient (dimensionless),
$\varphi_{RH}(h)$	=	Correction term for effect of relative humidity on notional creep coefficient
φ_u	=	Ultimate (in time) creep coefficient
γ_c	=	Unit weight of Concrete, kg/m ³

CHAPTER ONE

INTRODUCTION

1.1. Background of the Study

Bridges crossing the rivers and valleys are vital components of the road network that contributes greatly to the national development and public daily life. Any damage or collapse of bridge can risk the lives of road users as well as create serious influence to the entire country. Additionally, the reconstruction of the bridge needs considerable amount of money and time. The Ethiopian Roads Authority is responsible for the operation and maintenance of the federal road network. Presently more than 20,000 km of federal road administered by ERA and the road network contains about 3,000 bridges and more than 27,000 small drainage structures. Among them about 35% of Ethiopian bridges were constructed more than 60 years ago showing signs of severe deterioration due to that they have not been properly maintained since their construction. They are suffering from the rapid increase of traffic volume and excessive overloads that were not expected in their design stages. In 2006 year ERA has, for the first time in Ethiopia, conducted inventory and inspection of bridges along the federal roads network. The following bridge data is extracted from the ERA–BMS reports [1].

Table 1.1: Condition of Bridges on Federal Road Network

TR	Section	Total Bridges	Good *Bridges	Need Repair Bridges	Need Replacement Bridges
A1	AA – Mekele	284	250	81	19
A2	AA – Axum	525	505	115	12
A3	AA – Gonder	226	220	68	5
A4	AA – Gimbi	198	170	49	17
A5	AA – Metu	88	81	83	1
A6	Jimma – Mizan Teferi	13	12	3	1
A7	Modjo – Arba Minch	43	36	5	0
A8	Shashemene – Agre Maryam	26	25	6	0
A9	Nazareth – Asela	7	5	3	0
A10	Awash – Dengego – Degah Bur	67	57	25	0
Link Roads		571	539	210	31
M. Access Roads		405	366	123	13
Collector Roads		330	323	78	3
Feeder Roads		172	154	38	5
Grand Total		2,955	2,743	887	107

***Remark:** Some bridges are in good condition but they need repair / rehabilitation due to hydrological problems.

Presently, there are 2,955 bridges along the federal road network. There are 13 different types of bridges are located on the trunk road of A6 at section from Jimma to Mizan Teferi road. Out of which, three bridges needs repair in this trunk road inclusive of Sheta River Bridge. Furthermore, according to the 2006 year ERA–BMS reports has 2,955 total numbers of bridges registered in federal road network out of which 632 are reinforced concrete deck girder bridges [1].

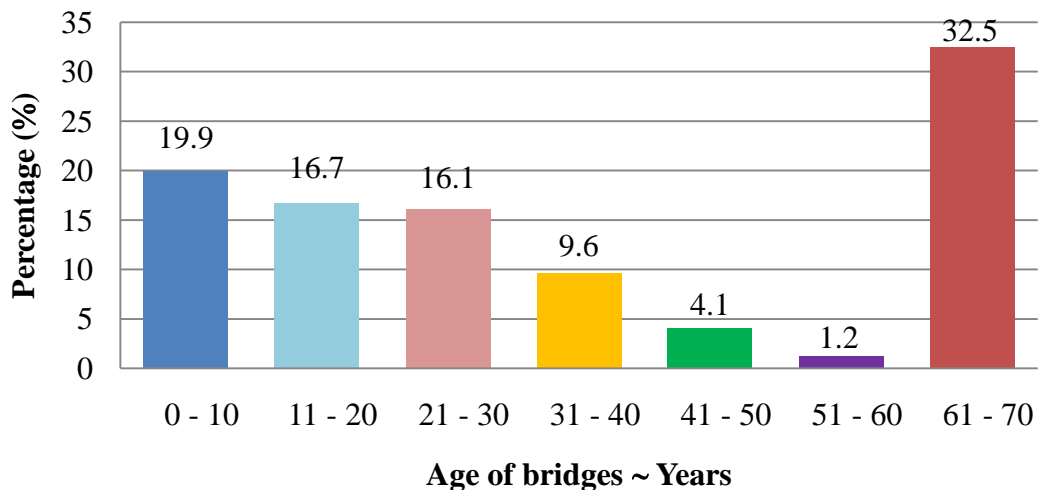


Figure 1.1: Bridges age distribution of federal road network

In fact, Ethiopia has experienced many cases of bridge collapse and their serious consequences over decades. One of the major cause leads to bridge collapse is time dependent cracks growth and fracture on bridge deck. The presence of these cracks in concrete bridge deck can allow rapid ingress of moisture and chloride ions into concrete interior leading to accelerated corrosion of rebar, deterioration and leaching of concrete. The adverse effects of concrete bridge deck cracking can be greatly reduces the service life of deck, leads to a loss of functionality, loss of stiffness, ultimately the loss of structural safety and increase maintenance costs, which is of most importance in highway maintenance activities. According to the study report of DANA and Associates Engineering Consultants P.L.C., to Western Region Contract Management Directorate Director of Ethiopian Road Authority, under the scope of the works contract of Bonga–Felege Selam road project for reconstruction one of the defects of Sheta River Bridge was transverse deck cracking, peel off and honeycomb observed at the bottom of the deck slab and girders [2].

The condition bridge deck assessment methods used for this study include visual inspection, hammer sounding, pachometer survey, rebound test hammer, and chloride concentration analysis. Research performed in this study, a single-span RC deck girder bridge crossing Sheta River with a service life of almost 50 years, located at Kaffa Zone, Bonga town.

1.2. Statement of the Problem

According to United States Transportation Research Board reports showed that transverse cracking was the predominant type of cracking in reinforced concrete bridge deck slabs [8]. Transverse cracks can accelerate corrosion of reinforcing steel, deteriorate deck concrete, possibly cause damage to underneath components of the bridge and damage bridge aesthetic. As a result of these adverse effects of transverse cracking, the maintenance costs will increase and ultimately the service life of the bridge system will be shortened [9]. There have been significant numbers of time-dependent causes of transverse deck cracking, as it will be discussed in the chapter four. However, the time-dependent causes are not yet fully understood and the problem still exists. Previous studies [3,5 and 11] were mostly focused on early-age of transverse deck cracking of new constructed reinforced concrete bridge decks and most of them by concrete mix design & improvement through changes to construction practices to alleviate early-age transverse deck cracking.

In many instances there are major disagreements on the factors affecting transverse cracking indicating the need for further research. For examples, according to Dakhil et al. report a direct relationship between an increase in cracking and an increase in concrete slump while Cheng and Johnston have observed a decrease in transverse cracking in concrete bridge decks with increasing slump [9]. Contradiction on the effect of girder type and end restrained condition is another important example on the lack of full understanding of the causes of this phenomenon. Transverse cracking of ageing reinforced concrete highway bridge decks was not researched in Ethiopia. However, transverse cracking are observed on Sheta River Bridge deck indicating the contribution of other factors and the need for further study to identify these factors and propose mitigation strategies to reduce transverse bridge deck cracking. This study is intended to fill the gap of information on the causes of transverse cracking on aging reinforced concrete bridge deck in the study area.

1.3. Research Questions

This research was aimed at addressing the following basic research questions;

1. What are the potential time-dependent causes of the reinforced concrete bridge deck cracking on Sheta River Bridge?
2. What are the effects of cracks on the performance reinforced concrete bridge deck on Sheta River Bridge?
3. What mitigation strategies are appropriate to reduce transverse cracking on Sheta River Bridge deck?

1.4. Objectives of the Study

1.4.1. General Objective of the Study

The main objective of this study was to investigate cause of concrete bridge deck cracking and mitigation strategies to reduce cracks in the Sheta River Bridge deck.

1.4.2. Specific Objectives of the Study

- ⊕ To investigate potential time-dependent causes of the reinforced concrete bridge deck cracking.
- ⊕ To describe the effect of cracks on the performance reinforced concrete bridge deck.
- ⊕ To identify mitigation strategies to reduce transverse cracking on Sheta River Bridge deck.

1.5. Scope of the Study

Although the issue of aging concrete bridge deck cracking is very broad and the problem occurred on different type of bridge super-structures with different cracking orientation, due to lack of advanced cracks detecting and field test instruments, the study was limited only on single span, simply supported and cast monolithically reinforced concrete highway T-girder bridge deck transverse cracking. Certified ERA officials conduct reinforced concrete bridges inspections at every two years. Although inspection reports provide information for all of the components of a bridge, this study considered only the bridge deck. These are the main reasons why the research is delimited to above cases.

1.6. Significance of the Study

This study is believed to contribute a lot for different potential beneficiaries in the following way. Firstly, the study on cause and control of transverse cracking will provide an insight and relevant information on the Sheta River Bridge deck at Bonga town, Ethiopia. Secondly, knowing the update information on the evaluation and repair deck cracking will enable the owner of the bridge/ ERA to make choice on an appropriate measure to bridge asset management and maintenance. Thirdly, this study will serve as a reference for future researchers in this regard.

1.7. Organization of the Study

This thesis is divided into five chapters.

1. Chapter one included an introduction to the topic of concrete bridge deck transverse cracking along with the research statement of the problem, research questions, objective of the study, scope of the study and significance of the study.
2. Chapter two presents literature review related to cause and control of time dependent cracking of bridge deck.
3. Chapter three elaborates the methodology of the research, which are includes study area, study design, variables of the study, data collection process, data processing & analysis, limitation of the study and operation definitions.
4. Chapter four included results and discussion of the research along with site investigation, cause of transverse bridge deck cracking and control of cracking in bridge deck with the concept of mitigation strategies to reduce transverse deck cracking.
5. Chapter five which enumerates the conclusions and recommendations based on the results obtained. Finally, Appendix A and B elaborates the results of field investigation and strength analysis of existing Sheta River Bridge deck, respectively.

CHAPTER TWO

LITERATURE REVIEW

2.1. General

After reviewing different research findings, bridge engineering handbooks, structural engineering journals, and locally available unpublished ERA–BMS reports, the researcher review latest and relevant related literature.

2.2. Reinforced concrete bridge deck cracking

Concrete bridge deck may develop cracks whenever the tensile stresses (induced by either internal or external sources) exceed the tensile strength of the concrete. Service and excessive traffic overloads may help to activate or accelerate several of these mechanisms (such as deck flexure/deflection and reflection cracking), and can induce fatigue cracking in longer view. Cracking in reinforced concrete may also result in steel reinforcement bars being exposed to the environment, resulting in corrosion of the steel. Moreover, cracks may reduce the bending stiffness of reinforced concrete members, which may lead to excessive deflection.

2.3. Classification of cracks in reinforced concrete bridge deck

The literature review showed that reinforced concrete bridge decks cracks could be classified in three different ways: cracks that are dependent on applied loading (i.e. flexural cracks and inclined shear cracks), cracks independent of loading (i.e. shrinkage or temperature change), and cracks based on traffic orientation. According ACI Committee 345R-91, most concrete bridge decks cracks may be classified according to their orientation in the relation to the direction of traffic as longitudinal, transverse, diagonal and map/pattern cracking.

Transverse cracks are cracks that are perpendicular to the longitudinal axis of the bridge deck, and they are the main type of cracking found on reinforced concrete bridge decks. These cracks generally form at the surface of the bridge deck under which the transverse reinforcement is placed [3]. Cracks widths often exceed 0.05 mm and can reach widths 0.6 mm, leading to an increased probability of water and chloride ion penetration. Transverse cracking develop when longitudinal tensile stresses in the deck exceed the tensile strength of the concrete. The tensile stresses are caused by temperature changes, concrete shrinkages and bending from self–weight and over traffic loading [4].



Figure 2.1: Transverse cracking [4]

A combination of shrinkage and thermal stresses causes most of the transverse cracking found in concrete bridge decks [5]. Transverse cracks form above the transverse reinforcement, providing a direct path for de-icing chemicals from the deck's surface to the reinforcement steel. Therefore, transverse cracks critically affect the corrosion of the reinforcement steel.

Longitudinal cracking is parallel to the longitudinal direction of the bridge deck. Like transverse cracks, longitudinal cracks have also been shown to occur directly above top main longitudinal reinforcement. According to Curtis R. H. and White H. discovered that longitudinal cracking is caused by the differential movements along the girders, and they believe the cause of the differential movement is from the rotation of the beams about their longitudinal axis [6]. However, based on their research, that longitudinal deck cracking typically occurs above the edge of the girders.



Figure 2.2: Longitudinal cracking [5].

Although diagonal cracks can be found in all types of concrete bridge decks, these cracks are commonly associated with bridge decks with a skew. Through their research, decks with a skew have much more of a tendency to have diagonal cracking than their straight counterparts. In bridge decks with a skew, diagonal cracking occurs more in the corner areas as a result of restraint provided by the abutments and piers [5]. These cracks typically start with a right angle to the deck edge that is along the direction of the supports.



Figure 2.3: Diagonal cracking [8]

Map cracking forms in a random pattern of intersecting transverse, longitudinal and diagonal cracks. For this reason, map cracking is also referred to as pattern cracking. These cracks begin at the bottom of the deck and move upwards through the deck towards the surface [12]. Map or pattern cracks are often the product of improper curing because the surface moisture on the concrete evaporates too quickly, and the volumetric change of the concrete is restrained [7]. However, it must be noted that there are secondary effects map cracking such as delaminating and concrete spalling.



Figure 2.4: Map/Pattern cracking [5]

2.4. Overview transverse cracking of bridge deck

United States Transportation Research Board showed that transverse cracking was the predominant type of cracking in bridge deck slabs [8]. This document also analyzed the survey data collected by North American transportation agencies relating to 45 bridges in 38 U.S. states and 7 Canadian provinces. In addition, three out of four transportation agencies that took part in a large-scale survey of more than 225,000 bridges, engaging transportation agencies in North America, Japan, and a number of European countries, reported that transverse cracking was perceived as a significant performance concern in bridges [3]. Furthermore, the data collected from a survey consisting of 24 bridges, built in 1994 in New Jersey, showed that more than 70% of the surveyed structures were subjected to widespread transverse cracking [9].

The primary obstacle to targeting crack control of the transverse cracking phenomenon, as reflected in related research, involves the difficulties in accurately estimating the time-dependent behaviour of concrete. The "State-of-the-Art Report on Control of Cracking in Early Age Concrete", published in Japan[13], discussed several numerical and analytical methods for simulating volumetric changes through specimen modelling, and addressed a number of recently developed methods of controlling early age cracking in high strength concrete through modifying concrete mixture design and construction procedure. A similar research project was also completed by the Michigan Department of Transportation [14], which attempted to predict the effect of thermal strains in deck slabs during the early age of structures. Final concluded that the dominant cracking mode in bridge decks was transverse cracking, and suggested that cracking occurred at the very early age of concrete structures as well as service life.

Overall, predicting the long term behaviour of reinforced concrete structures is subject to a considerable degree of inherent errors. Being a composite heterogeneous material, concrete is rather inconsistent at a local level. Although many methods have been developed in order to predict the characteristics of long term cracking in concrete structures, the high uncertainty involved in the prediction of time dependent material and structural behaviour prevents the calculation of consistent results. An effective approach has yet to be developed. Cracks are formed as a response to the increasing tensile stress in concrete corresponding to the time dependent volumetric change in a restrained specimen. Cracks generally occur at an early age in concrete due to loss of moisture in the material, and widen at latter stages when further shrinkage occurs. When the control of cracking in a bridge is inadequate, the transverse cracking phenomenon can lead to significant reduction of structural durability due to moisture and salt penetration, and corrosion in steel reinforcement. This problem is most critical when the structure is exposed to detrimental substances such as chlorides, causing ingress of corrosive agents. Severe states of transverse cracking can hinder structural performance and substantially shorten a structure's expected lifespan. Therefore, there is an increasing demand for an effective methodology to control the transverse cracking in the bridge decks of T-girder bridges, and, hence to obtain a better understanding of the primary factors contributing to the occurrence of transverse cracking.

2.5. Non-destructive tests for bridge deck condition evaluation

1. Visual inspection:

Visual inspection is the first step in assessing the condition of a bridge deck. During inspection, the type and extent of deterioration are documented, and coloured photographs may be taken to document any significant damage. Prior to the surveying of the bridge, lanes were temporary closed by the assistance research personnel using a simple flag lane closure and using traffic cones to keep the traffic away from the lane that was being inspected. Bridge decks were cleared of any debris and dirt using an air blower or dust brush, so that the cracks could be seen without difficulty [15].



Figure 2.5: Typical crack width measurement on bridge deck [12]

2. Rebound hammer test

The Rebound hammer has been around since the late 1940's and today is a commonly used method for estimating the compressive strength of in-place concrete. Developed in 1948 by a Swiss engineer named Ernst Schmidt, the device measures the hardness of concrete surfaces using the rebound principle. Although the rebound hammer provides a quick in expensive means of checking the uniformity of concrete, it has serious limitations and these must be recognized [15]. The results of the Schmidt rebound hammer test are affected by: smoothness of test surface, size, shape, and rigidity of specimens, age of test specimens, surface and internal moisture conditions of the concrete, type of coarse aggregate, type of cement, and carbonation of the concrete surface. To obtain greater accuracy of test results, tests performed on a rough-textured finish will typically result in crushing of the surface paste, resulting in a lower number.

Alternately, tests performed on the same concrete that has a hard, smooth texture will typically result in a higher R-number [15].

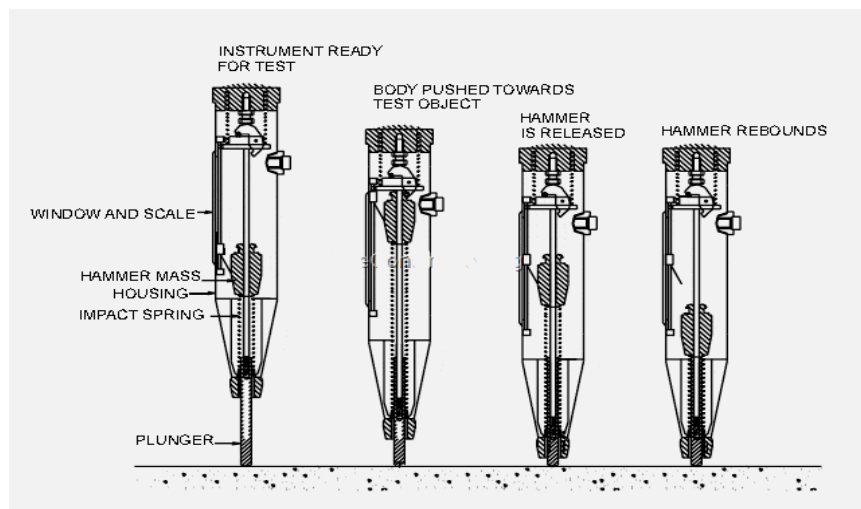


Figure 2.6: Operation of the rebound hammer [15]

3. Hammer Sounding:

Hammer sounding is an acoustic impact method that technicians can use to detect delaminations in concrete by striking the concrete with a hammer or dragging a chain and listening to the response. The operator struck the concrete with a standard carpentry hammer and listened to the response. In this respect, the same limitations that applied to hammer sounding, including the subjective judgment and hearing sense of the operator. Areas of delaminations are then marked directly on the surface of the concrete. After delaminated areas are marked on the bridge deck, the percentage of delaminated areas can be computed [15].

4. Pachometer survey:

Pachometer survey is used to determine the depth of cover by measuring variations in magnetic flux caused by the location of steel. For the pachometer to be accurate, the size of reinforcing steel has to be known so that the readings can be interpreted for depths. Alternative method to determine the depth of cover: by drilling small diameter holes to expose reinforcing steel for direct measurement, or by measuring the cover depth in extracted cores [16].



Fig. 2.7: Pachometer used to locate reinforcing in bridge deck [16]

5. Chloride content analysis:

The principal cause of corrosion of steel reinforcement in bridge decks is due to chloride in the concrete. The chloride originates in the concrete ingredients and from de-icing chemicals applied to the bridge deck. Chloride ions present in the cement paste surrounding the reinforcement react at anodic sites to form hydrochloric acid which destroys the passive protective film on the steel. The surface of the steel then becomes activated locally to form the anode, with passive surface forming the cathode; the ensuing corrosion is in the form of localized pitting [17]. To initiate corrosion in the concrete, the concentration of chloride ions in ordinary Portland cement (type-1) concrete when the maximum water soluble chloride ion (Cl^-) content is greater than 0.3 percent by mass of cement. The presence of chlorides in the steel reinforcement bars, the schematic reactions, as shown in the Figure 2.8 below.

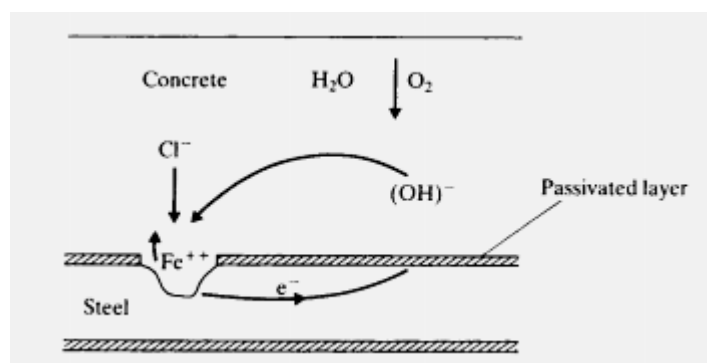
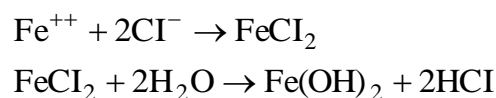


Figure 2.8: Electro-chemical corrosion in the presence of chlorides [17]

When concrete cores are not removed, powder samples can be taken for chloride analyses. This is usually done with a rotary hammer. Samples are taken at various depths, down to and slightly beyond the depth of the steel. Analysis can be done on an acid-soluble or water-soluble basis. Historically, the acid-soluble technique (AASHTO T260-94 or ASTM C1152) has been used, with full awareness of the fact that all of this chloride is not available to support corrosion, due to chemical combination with the cement or because it is tightly held within aggregate particles. The results of water-soluble tests are greatly affected by the degree of grinding of the sample and by the length and temperature of leaching [17]. The currently accepted test for water-soluble chloride is described in ASTM C1218 water-soluble chloride in mortar and concrete. The water soluble chloride content in the concrete, expressed as percentage relative to the weight of sample (% C1), is calculated by the following expressions:

$$C_{\text{AgNO}_3} = \frac{C_{\text{HCl}} \times V_{\text{HCl}}}{V_t}$$

2.6. Crack width

Cracks were identified by their size, location and orientation. Both the lengths and widths of visible cracks were recorded, where the crack width was measured using a crack width comparator card. Crack widths were categorized into three general groups: fine cracks generally less than 1mm; medium cracks—between 1mm and 2 mm and wide cracks—over 2mm [23]. Crack widths can be affected by different factors such as spacing of rebar, stress in the reinforcement, rebar diameter, and the effective depth. According to the ACI 224 report crack width specifications [23], are listed in Table 2.1.

Table 2.1: Tolerable crack widths in reinforced concrete structures [23]

Exposure Condition	Tolerable crack width (mm)
Dry air	0.41
Humidity, Moist air, Soil	0.30
De-icing chemicals/ salts	0.18
Sea water	0.15
Water retaining structures	0.15

Although the ACI 224 report (ACI 224R-01) recommends this table as a practical guide, these values are not a very reliable and conclusive. Thus, it is suggested that engineering judgment and past experience should be taken into consideration for using these values in the field. It must be noted that the factors influencing crack widths are not understood and proven for all conditions, and is a topic of debate among many researchers.

2.7. Factors influencing transverse cracking

The focus of research and studies related to the areas of transverse cracking in bridge deck slabs often falls into one of the three major categories of factors: concrete material behaviour, structural design, and traffic overloading. This section provides a brief discussion on each of the three categories of factors influencing transverse cracking.

2.7.1. Concrete material behaviour

The long term material behaviour of reinforced concrete bridge decks is primarily characterized by two time-dependent variables: shrinkage, and creep.

Shrinkage is one of the most detrimental properties of concrete, which affects the long-term strength and durability. To the practical engineer, the aspect of volume change in concrete is important from the point of view that it causes unsightly cracks in concrete bridge deck. As the concrete shrinks, the reinforcement is compressed and imposes an equal and opposite tensile force on the concrete at the level of the reinforcement. If the reinforcement is not symmetrically placed on a section, a shrinkage-induced curvature develops with time [21]. Shrinkage in an unsymmetrical reinforced concrete bridge deck can produce deflections of significant magnitude, even if the deck is unloaded. For example, consider the unrestrained, singly reinforced, and simply-supported concrete bridge deck slab shown in the Figure 2.9 and the small deck segment of length Δx . The shrinkage induced stresses and strains on an uncracked and on a cracked cross-section are shown in the Figures 2.9b and 2.9c, respectively. Similarly, 30% of the final shrinkage is developed in the first 2-3 weeks.

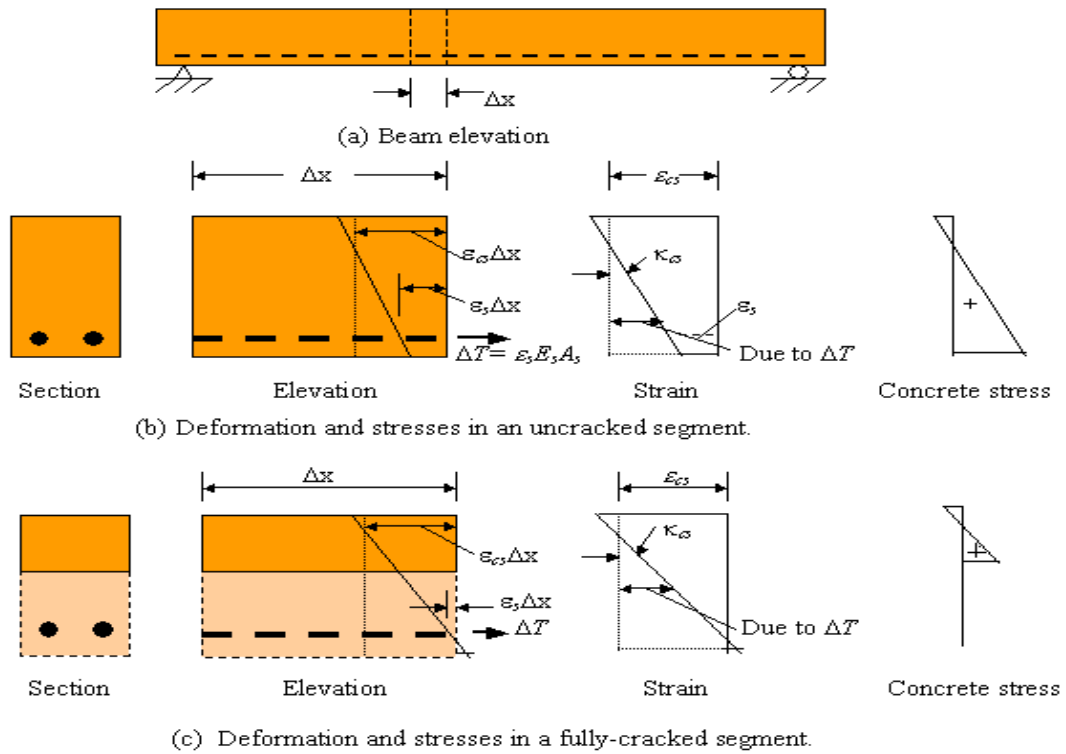


Figure 2.9: Shrinkage warping in a singly reinforced beam [12]

A concrete member subjected to load responds instantaneously and time-dependently. When a concrete member is subjected to a sustained applied load it undergoes an instantaneous deformation at the time of loading followed by a time-dependent one over time. In most of the cases, creep shortening of concrete under permanent loads is generally in the range of 0.5 to 4 times the initial elastic shortening. Creep tends to increase with a decreasing rate over time. As suggested by Gilbert [21], about 50% of the final creep develops in the first 2-3 months and about 90% after 2-3 years.

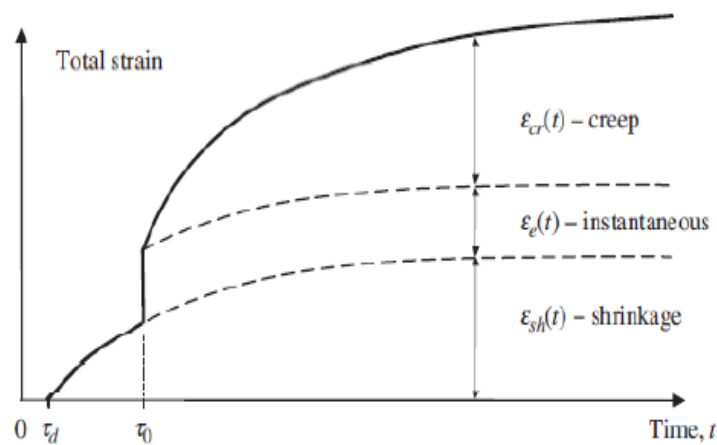


Figure 2.10: Concrete strain components subjected to a sustained load [20]

The magnitude of the creep coefficient is influenced by the environmental conditions (i.e. relative humidity of the environment), composition of concrete, duration of load and the age of the concrete at first loading. As the surface area-to-volume ratio increases, creep increases, and therefore creep is greater in concrete deck member than in thicker members such as girders or piers. As shown in the Figure 2.10 above, concrete loaded at an early age creeps more than concrete loaded at a later age. Concrete is therefore a material that hardens overtime although the tendency to creep never completely disappears, even in very old concrete.

2.7.2. Structural design parameters

The primary structural design parameters of slab-on-girder bridges typically associated with the control of cracking in bridge decks are: concrete design strength, reinforcement ratio, and restraint condition. The design strength of concrete correspondingly affects the concrete tensile strength, which is the maximum amount of stress that concrete can carry before a crack develops.

End condition shows a good correlation between the end fixity and the cracking tendency of the bridge decks. Fixed condition is when the abutment end is fixed (i.e., the end of the girder is built into the abutment wall or integral abutment). The term fixed end should be used with some cautions here. The effect of end condition will be discussed in more detail later in the report. Nevertheless, widespread cracking of bridges with similar end conditions, which actually prompted this research investigation, supports the pronounced effect of end conditions and rotational rigidity on transverse deck cracking.

The average thickness of the cracked decks was about 8.75 in while this average for the un-cracked bridge decks is around 9 in. This shows that an increase in the deck thickness reduces cracking. Similar results are also reported by other researchers [3]. Girder type is considered an important factor by various researchers. Some of the pervious works such as NCHRP Report 380 [3] and Minnesota DOT's research [8], show that decks supported on steel girders are more likely to crack than those supported on concrete girders. The bias in this case is more likely due to the fact that a great number of bridges with reinforced concrete girders had more restraint (fixity) at their supports. As it will be discussed, it appears that it is the relative stiffness of the deck with respect to the girder stiffness that is more important than the girder type.

2.8. Mitigation strategies to reduce transverse deck cracking

The primary reason for providing mitigation strategies is to extend the life of the bridge deck, and to reduce the rate of crack of the concrete bridge deck. Once a crack has developed in a bridge deck, it often propagates with time due to cyclic loading. For the purposes of bridge maintenance, cracks can be categorized as either structural or non structural. Each requires different repair techniques. Typically, structural cracks are repaired to restore structural integrity, and non structural cracks are sealed to minimize the potential for increased cracking. However, cores may be taken to verify crack filling and the depth of penetration measured. Cores can be tested to give an indication of the effectiveness of the repair method. The accuracy of the results may be limited, however, as a function of the crack orientation or due to the presence of reinforcing steel in the core [16].

Structural cracks—Structural cracks are originally created by stress due to live load, dead load, thermal and shrinkage strains. Most structural cracks are active cracks are those the open and close often when the bridge is carrying traffic. Depending on the location, some cracks open under live load, while others close. It is as difficult to predict the amount of movements as it is to predict the types of future loads. Some thermal cracks are active cracks, closing during the day and widening during the night. On concrete bridge decks, they are often located directly above a reinforcing bar, exposing the bar to moisture and chlorides [12].

Non-structural cracks—Non-structural cracks are generally not straight, may be shallow in depth, and take on various patterns depending on their cause. They result primarily from non-structural causes such as plastic drying, autogenous and thermal shrinkage, or alkali-aggregate reaction. They are generally unaffected by live loads, making them easier to repair or seal. Most non-structural cracks are dormant cracks, Methods crack repair include gravity fill, topical applications of sealers, rout and seal, and epoxy injection [12].

a) Epoxy crack injection

Cracks as narrow as 0.3 mm can be bonded by the epoxy injection has been successfully, used in the repair of cracks in bridge deck and other types of concrete structures.

The technique generally consists of establishing entry and venting ports at close intervals along the cracks, sealing the crack on exposed surfaces, and injecting the epoxy under pressure. Epoxy injection requires a high degree of skill for satisfactory execution, and use of the technique may be limited by the ambient temperature. The general procedures involved in epoxy injection are as follows [16]:

- ⊕ Cleaning the cracks
- ⊕ Sealing the surfaces
- ⊕ Installing the entry and venting ports
 - Fittings inserted into drilled holes
 - Bonded flush fitting
 - Interruption in seal
- ⊕ Mixing the epoxy
- ⊕ Injecting the epoxy
- ⊕ Removing the surface seal



Figure 2.11: Epoxy crack injection [16]

b) Routing and sealing of cracks

Routing and sealing method involves enlarging the crack along its exposed face and filling and sealing it with a suitable joint sealant. As shows in the Figure 2.12 below the procedure for repairing a crack was illustrated. This is a common technique for crack treatment and is relatively simple compared with the procedures and the training required for epoxy injection.

The procedure is most applicable to approximately flat horizontal surfaces such as bridge deck. Routing and sealing is used to treat both narrow and wide cracks. A common and effective use is for waterproofing by sealing cracks on the concrete surface where water stands or where hydrostatic pressure is applied. This treatment reduces the ability of moisture to reach the reinforcing steel or pass through the concrete, causing surface stains or other problems. The sealants may be any of several materials, including epoxies, urethanes, silicones, polysulfide, asphaltic materials, or polymer mortars. Cement grouts should be avoided due to the likelihood of cracking [16]. A concrete saw, hand tools or pneumatic tools may be used. The groove is then cleaned by air blasting, sand blasting or water blasting and dried. A sealant is placed into the dry groove and allowed to cure.

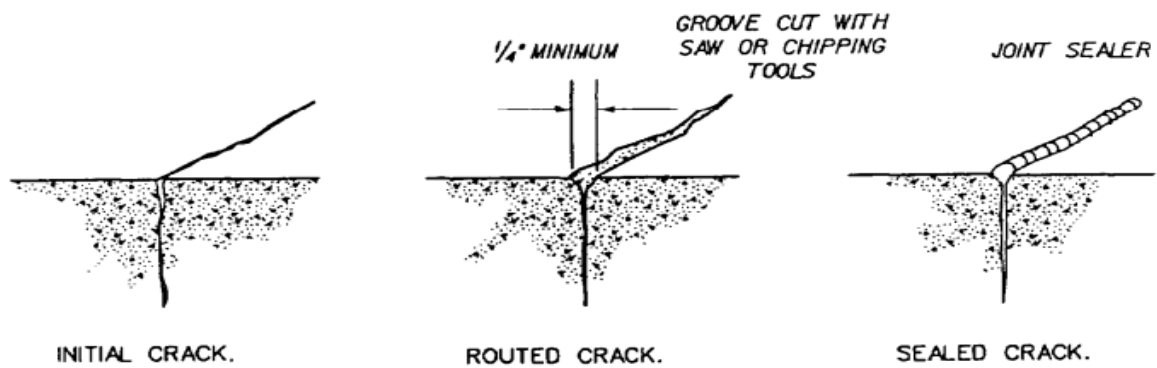


Figure 2.12: Repair of Crack by routing and Sealing [16]

c) Gravity filling of cracks

Low viscosity monomers and resins can be used to seal cracks with width of 0.03 mm to 2 mm by gravity filling. High molecular-weight methacrylates, urethanes and some low viscosity epoxies could be used successfully. Lower the viscosity, finer the cracks that can be filled. The typical procedure is to clean the surface by air blasting, water blasting, or both. Wet surfaces should be permitted to dry for several days to obtain the best crack filling. The monomer or resin can be poured onto the surface and spread with brooms, rollers, or squeegees. The material should be worked back and forth over the cracks to obtain maximum filling because the monomer or resin recedes slowly into the cracks. The use of this method on elevated slabs will require sealing of the cracks on the bottom of the slab to contain material from leaking through the crack. Excess material should be broomed off the surface to prevent slick, shining areas after curing.

If surface friction is important, sand should be broadcast over the surface before the monomer or resin cures [16].



Figure 2.13: Application of a gravity feed repair method [4]

d) Overlay and surface treatments

Cracks in bridge deck may be covered by using either a bonded or unbonded overlay or surface treatment. These methods do not repair cracks, but rather hide or obscure the cracks. By covering the deck surface, overlay repairs obscure the cracks and can prevent chloride penetration. Overlay systems are usually applied by spreading an epoxy across the entire surface and broadcasting a wearing surface of gravel, stone, or large sand particles. Multiple layers may be necessary to properly apply the overlay. Because overlay systems cover cracks rather than repairing them, they are often susceptible to cracking at the location of the original concrete crack. If the overlay has sufficient strength to remaining act under traffic loads, it may be ideal for repair of highly cracked bridge decks. Often it is recommended that overlay repair products be used in conjunction with a gravity feed or epoxy injection crack repair to maximize the effect of both products [4].

CHAPTER THREE

RESEARCH METHODOLOGY

3.1. Study Area

Sheta River Bridge is a simply supported, single span and cast in place T-girder RC deck bridge with a total span length of 20 meter. It is located in Kaffa Zone, Bonga town, a city in the southwest part of Ethiopia around 446 kilometres away from the capital city of Addis Ababa, Ethiopia.

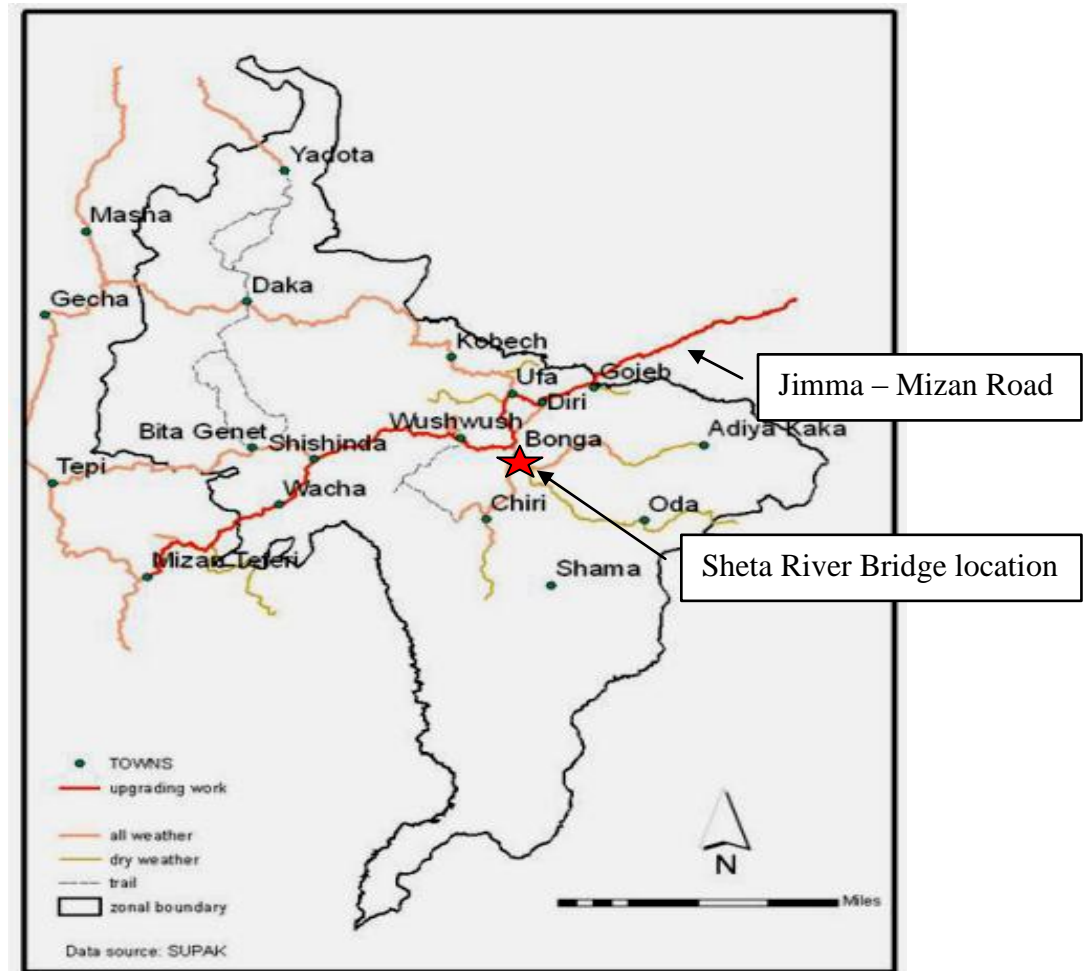


Figure 3.1: Existing road map of Kaffa Zone

3.2. Study Design

The purpose of this study was cause and control of cracking in reinforced concrete highway bridge deck: A case study in Bonga town Sheta River. However, the study type may dictate certain thesis designs. To achieve my study objectives researcher selected a case study research designs type that was most appropriate and most feasible design for my thesis title. Because this study specifically identifies the causes of Sheta River Bridge deck cracking.

3.3. Variables of the Study

Dependent Variable of the Study: Concrete bridge deck cracking

Independent Variables of the Study are: Site & environment conditions, material properties, structural design parameters (deck thickness, girder end condition, concrete cover and design vehicle load), traffic overloading and age of the bridge

3.4. Data Collection Process

3.4.1. Sources of Data

The study used both primary and secondary data. The primary data was collected from in place non-destructive tests in conjunction with completing visual bridge inspection formats. The secondary data was collected from ERA previous inspection & inventory reports, data on similarly constructed RC deck girder bridge (Bitino River Bridge) and weather data logbook. These above mentioned sources of data employed in development of the data base that was consequently used for evaluation aging concrete deck cracking.

3.4.2. Methods of data collection

⊕ Field Investigation

Field investigation the primary source of information about the types and extent of distress presented on the reinforced concrete bridge deck. Additional information, such as colour photos of cracks and damaged structural components, were also collected the bridges in conjunction with completing field investigation forms, which are all included in the Appendix A below.

⊕ As-built drawing / Structural plans

As-built drawing/ structural plans were secondary source of information. It contains bridge dimensions, deck details, and girder details ...etc. However, due to confirmation of ERA-Jimma District staff at the Bureau of Bridge Management, a structural plan of Sheta River Bridge was not available because it's aging and poor documentation practice of ERA. Bridges without plans create a particular challenge to engineers and owner/ ERA when effect of cracks on the performance of bridges have to be rated. Structural properties for bridges without original design plans are not easily obtained. This is especially a problem for older concrete bridges for which the amount of reinforcing steel bars may be unknown.

As a result, the bridge capacity or rating cannot be evaluated easily using traditional methods, based on simplified theoretical models. Therefore, in this study were used similarly constructed bridge (Bitino River Bridge) structural plans for determined the amount steel reinforcement bars.

✦ **ERA – BMS reports**

This datasheet is another secondary source of data, which are completed during the inventory and inspection, contain different data regarding construction and detail of structural dimensions for Sheta River Bridge. This form is part of the documents that ERA–Jimma District holds for each bridge.

Bridge No	E61-1-001		Bridge Name	Sheta		Print	Close		
Location									
District	Jimma	Main Road (Route)	E61	Bonga - Chida	Km from Addis	465.25			
Section	Bonga	Sub Route	E61	Bonga - Chida	Co-Ordinate X	194755	Y 806404		
Road Segmen	Bonga - Felegeselam								
General Information									
Bridge Length(Mt)	18.00	Present water Level (Mt)	1.20	Year Of Construction	1982	<input type="checkbox"/> Before	Road Alignment	Straight	
Bridge Width(Mt)	8.92	Highest Water level (Mt)	2.50	Contractor	Blue Nile Construction			Load Capacity (Tone)	32
River Width(Mt)	7.00	Altitude(Mt)	1,600	Designer/ SuperVisor	ERA			Bridge Cost(Br)	350,000
Area Topography	Rolling		Safety Load Limit Sign		<input type="radio"/> Yes <input checked="" type="radio"/> No			Detour <input checked="" type="radio"/> Yes <input type="radio"/> No	
Super Structure									
Bridge/Structure Type	RC Deck Girder		Carriage Way Width (Mt)	7.30	Number Of Lane	2		No Of Girder (Box)	4.00
No Of Spar	1		Side Walk Width (Mt)	0.80	Span Support Type	Single Span		Depth Of Girder (Box) (Mt)	0.40
Total Span Length (Mt)	18.00				Type of deck Slab	RC		Spacing of Girder(Mt)	2.10
Span Length	1				Slab Thickness(Cm)	40.00		Width Of Box (Mt)	0.41
Abutment									
	Type	Foundation Type	Foundation Size	Height(Mt)	Width (Mt)	Wing Wall Length	Pile Depth	No Of Piles	Soil Type
A1	Masonry	RC Direct/Mat	12x3	28	11.3	2	0	0	Red clay
A2	Masonry	RC Direct/Mat	12x3	26	11.3	2	0	0	Number of Pier 0
Pier and Foundation									
No	Pier Type	Height	Found. Type	Found. Size	Piles #	Piles Depth			
Components									
Type Of Expansion Joint		Cheapwood							
Type Of Guard Railing		RC							
Type of Abutment Bearing		Bearing Plate							
Type of Piers Bearing		No Bearing							
Type Of Surface		Concrete							

Figure 3.2: Typical ERA – BMS datasheet [1]

⊕ Weather data logbook

Weather information of Sheta River Bridge location from 1953 to 2013 years, such as low & high daily temperature and relative humidity, was obtained from Ethiopia Meteorology Agency with collaboration of Information Service and the Weather Data Library at Jimma Branch Directorate.

In this study, the cracks in Sheta River Bridge deck were visually observed and assessed by non-destructive tests such as visual inspection, rebound test hammer, hammer sounding, pachometer survey and chloride ion content analysis. At certain locations on the bridge deck, the crack widths were determined using a crack comparator card and regular pocket tape rule. In addition, the previously collected bridge inspection & inventory reports, data on similarly constructed bridge (Bitino River Bridge) and weather data information for the existing bridge location were collected main source of data during data collection process.

3.5. Data Processing and Analysis

The data gathered through primary and secondary sources were analysed using different methods. To identify the causes of aging reinforced concrete Sheta River Bridge deck cracking the collected data was analysed using different methods, as shown in the Table 3.1 below. For calculations of numerical values of strength and condition evaluation of existing Sheta River Bridge deck can be used Ms Excel sheet in this thesis work.

Table 3.1: Data processing and analysis methods

Measures of deck cracking	Methods/ Models
Compressive strength of Sheta River Bridge deck at any time	ACI 209 R - 92 Model & ASTM, Designation: C 805 – 97
Dry shrinkage & Creep	Euro - International Concrete Committee, CEB MC 90 - 99 Model
Crack width	Gergely and Lutz, 1964 approach
Crack density	ACI 224.1R - 07 Model
Chloride ion content analysis	ASTM C1218 Model

3.6. Limitation of the Study

Even though the study was designed and planned carefully, there would still be certain constraints that might limit the conduct of the study. Lack of As-built drawing/ structural plans of Sheta River Bridge and also lack pneumatic concrete cutting instruments to take core sample at cracks for investigation of crack width and depth, this was limit the quality of the data were collected. However, this intensity of constraints minimized by used appropriate techniques.

3.7. Operational Definitions

Bridge deck – A flat component of a bridge, with or without wearing surface, which supports wheel loads directly and is usually supported by main bridge components

Cause of cracks – Bridge structure related factors can have a substantial affect on concrete bridge deck cracking

Cracking – is a complete or incomplete separation of concrete into two or more parts produced by breaking or fracturing

Control of cracks – Providing mitigation strategies is to extend the life of the bridge deck, and to reduce the rate of cracking of the concrete bridge deck

Reinforced concrete – is a composite material made of concrete and steel. Steel provides the tensile strength and the concrete provides the compressive strength. So, by combining these features of concrete and steel, it attains high utility and versatility

CHAPTER – FOUR

RESULTS AND DISCUSSION

4.1. General

This chapter presents the results of field investigation, causes of time-dependent bridge deck cracking, mitigation strategies to reduce transverse deck cracking and comparison of this study with others. Then results are followed by discussions of research findings and some interesting observations that were made during the field investigation.

4.2. Field investigation

Field investigation included visual walk-by evaluation mostly of the top of the bridge deck as well as the bottom of the deck slab. The researcher investigated the general information of the existing Sheta River Bridge as main concerned with superstructure of the bridge and the damage information were recorded, as presented in the table 4.1.

Table 4.1: General information of existing Sheta River Bridge

Bridge type	RC Deck Girder bridge
Structural ID. No.	E61-1-001
Year of construction	Late 1950's E.C.
Designer/ Supervisor	ERA
Total span length	20 Meter
Bridge width	8.92 Meter
Number of Span	One
Number of Lane	Two
Deck slab thickness	0.20Meter
Depth of Girder	0.85Meter
Width of Girder	0.40Meter
Spacing of Girder	2.10 Meter
Abutment	Stone masonry
Height of abutment	4.80Meter
Width of abutment	11.30Meter
Wing wall length	2 Meter
Type of abutment bearing	Steel bearing plate
Problem observed, as show in the Appendix A below	During visual inspection: <ul style="list-style-type: none"> ✓ Cracking on both abutments and wing wall ✓ Cracking, peel off and honeycomb at the bottom of deck slab and girders ✓ Scouring on the abutment and deformation masonry ✓ Spalling of concrete at the railing

4.2.1. Non-destructive tests

1. Visual inspection:

In this study, surface of the bridge deck slab cracks widths are measured by using a tape rule and crack comparator card which have lines of specified thickness marked on it. Once the underneath bridge deck was cleared of debris and dirt, the bridge deck surface was string line marked at 3 meter intervals in longitudinal and transverse direction. At the end all things were determined, the crack surveys on the bridge deck were conducted and the extension of the crack was marked if it was visible to the researcher as they mark the cracks. Cracks in bridge deck should be documented on a scaled map of the deck, as shown in the Figure 4.3 below. Additionally, the researcher was taken coloured photographs for visible concrete cracks which have occurred in the deck surface for documentation in this study.



Figure 4.1: Visible transverse bridge deck cracking and deposited silt

One of the overlook of Sheta River Bridge deck is transverse cracking, as shown in the Figure 4.1 above. These cracks are includes one predominated single crack width of 1 mm and multiple small cracks with width more than 0.2 mm width together with slight water leakage. According to ERA–Bridge Inspection Manual (2008), cracking rating for bridge deck slab categorized under rank–C, routine maintenance shall be done before causes for reduction of durability the bridge deck.

Blocked drainage and deposited silt may result in two consequences. Firstly, the reduction in the strength of the superstructure and substructure concrete elements. The constant exposure to moisture accelerates the corrosion of reinforcing steel, especially where freezing and thawing are encountered cracking; and subsequent spalling. Secondly, Corrosion seizing of the expansion bearings often creates cracks near anchor bolts and leads to further chloride absorption, deterioration, and loss of load-carrying capacity.

According to ERA–Bridge Inspection Manual (2008), damage rating for drainage are excessive standing water on the surface due to blockage, which causes serious hindrance in safety to daily traffic and traffic interruption during and after rain regarded as under rank–A with desirable intervention of urgent repair. While wide range blocked, which causes standing water during rainfall, effecting on traffic regarded as under rank–B with desirable intervention of repair but not urgent and also slight blockage drainage categorized under rank–C with desirable intervention of routine maintenance. Therefore, blocked drainage of Sheta River Bridge deck categorized under rank–B based on ERA–Bridge Inspection Manual (2008), so the researcher shall recommended that repair blocked drainage to prolonging service life the bridge.



Figure 4.2: Visible leakage at cracks underneath of deck slab

Additionally, the researcher observed that soffit of the bridge deck localized or partial water leakage through fine hair line cracks, which has negative effects on the deck slab. Visual distress data were used to formulate two types of deck condition descriptors, including crack density, and crack severity. Crack density reports the linear measurement of all cracking observed in the bridge deck slab and was calculated by dividing the sum of total length of cracking in meter by the total deck area of the surveyed Sheta River Bridge. Crack severity reports the average crack width, in millimetre, observed in the test section of the bridge deck. These parameters generated from visual inspection data therefore represent the deck area only. Sheta River Bridge deck has a total of 61 documented cracks across the length of the sections. Also, at certain locations the crack widths were measured by using a tape rule and crack comparator card has a ranged of average width from 0.08 mm to 1 mm. The lengths of these cracks ranged between 0.10 m and 1 m.

The condition of cracking in the concrete deck slab was observed and measured from the bridge deck. The cumulative crack length, which is the sum of the lengths of all cracks observed in the deck slab, and the crack density, calculated by dividing the cumulative crack length by the deck area. The information of the underneath deck surface was then transferred to the scaled AutoCAD drawing.

$$\text{Crack density} = \frac{\sum \text{Crack length}}{\text{Deck area}}$$

$$\text{Crack density} = \frac{\left(\frac{0.1\text{m} + 1\text{m}}{2}\right) \times 61}{8.92\text{m} \times 20\text{m}}$$

$$\text{Crack density} = 0.188 \text{ m/m}^2$$

This means the average length of visible cracks from waist height of a person with normal height is 0.188 m of crack length over an area of one square meter of bridge deck surface.

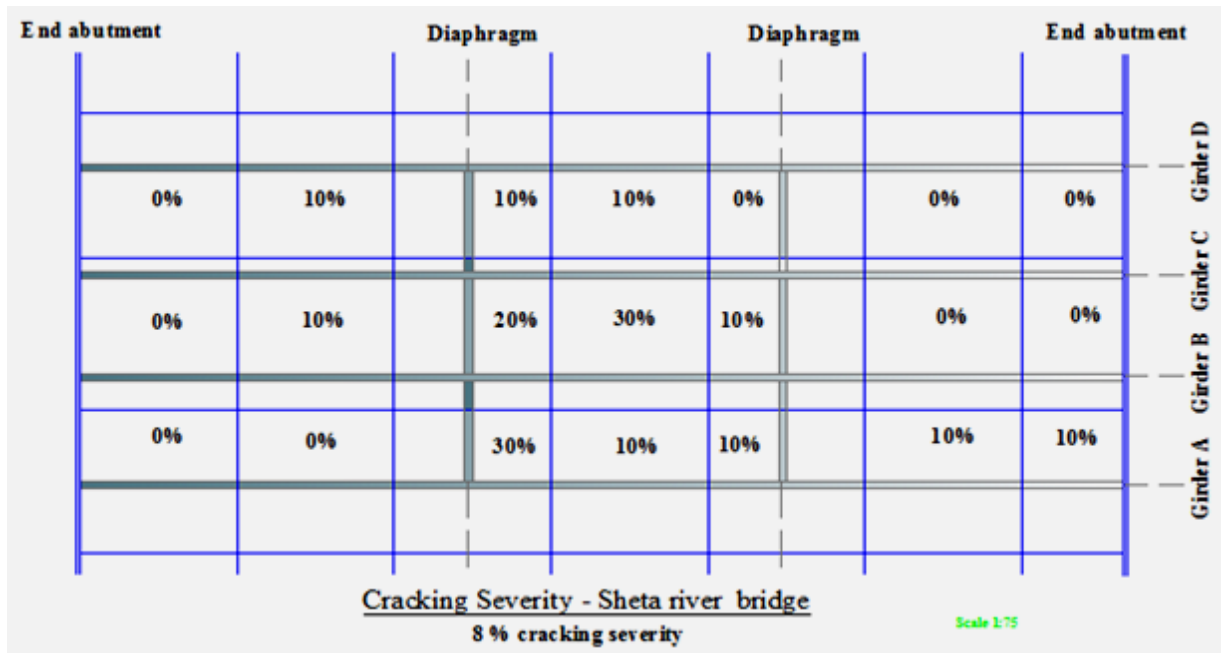
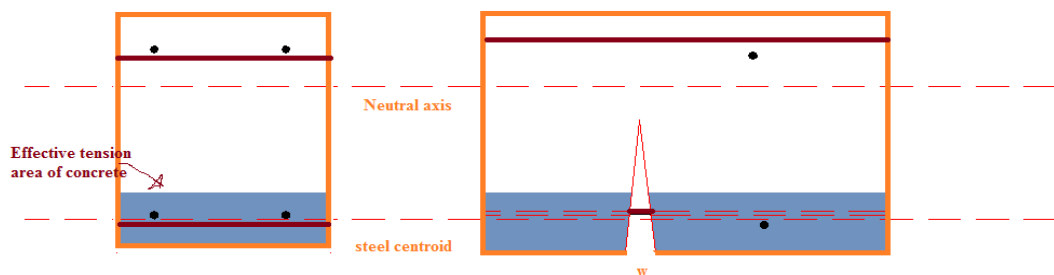


Figure 4.3: Cracking severity of Sheta River Bridge deck

2. Crack width

In this study, the crack width was computed additionally by Gergely and Lutz, 1964 approach to develop the crack width prediction equations, as shown below. Therefore, Sheta River Bridge deck crack width (w_k) is 0.297 mm ~ 0.3 mm that was tolerable crack width according to the Article 5.3.4, EBCS-2 (1995).

$$w_k = 2 \frac{f_s}{E_s} \beta \sqrt{d^2_c + \left(\frac{s}{2}\right)^2}$$



Total tensile area = $2d_c b_w$

Tensile area per bar: $A = \frac{2d_c b_w}{m}$

Where:

m = number of bars in one layer

3. Rebound test hammer

To obtain greater accuracy of test results in this study, test areas with a rough surface are ground to a uniform smoothness. This can be achieved easily with a Carborundum/abrasive stone, as shown below in the figure below.



Figure 4.4: Smoothing with a carborundum stone of underneath deck test surface



Figure 4.5: Vertical upward orientation of rebound test hammer during at deck slab

Rebound test hammer results were taken for Sheta River Bridge deck to analyzed in-place compressive strength of concrete, the data detail stipulated below.

Table 4.2: Rebound test hammer results for Sheta River Bridge deck

Test number	Test results	Estimated compressive strength (MPa)
1	35	28
2	39	40
3	37	34
4	35	28
5	34	24
6	40	44
7	39	40
8	36	31
9	38	37
10	37	34
Average		29.6

Calculation: Discard readings differing from the average of 10 readings by more than 6 units and determine the average of the remaining readings. If more than 2 readings differ from the average by 6 units, discard the entire set of readings and determine rebound numbers at 10 new locations within the test area.

References about this test procedure: ASTM, Designation: C 805 – 97

Instrument number: 1H0039

Technician: Mr. Enamrit Mulatu

Jimma University, JIT, Construction workshop assistance

Checked by: Mr. Berhanu Tefera (Researcher of this thesis)

Estimated in – place compressive strength of deck slab: 29.6MPa ~ 30MPa

Date and time of testing: 10 – 09 – 2008 E.C. at 4:00 AM (Local time)

However, limit of validity of the rebound test hammer the age of concrete should be start from 7 days up to 56 days with smooth and dry concrete surface. With old dried-out (aged) concrete the surface is always disproportionately hard. Therefore, in-place mean compressive strength of concrete is lower than is indicated by the rebound test hammer. According to the Laboratory for Building Materials of the University of Genoa carried out more than 30 wide testing campaigns on existing buildings on behalf of private third parties. In these cases, no cubic or cylindrical strength could be obtained from moulded specimens, so that the “actual strength” had to be deduced from field test from the structures. In the following, we assume a correction factor, for obtaining the cubic strength from the rebound test hammer result strength, linearly ranging from 0.93 for C10 concrete to 0.83 for C70 concrete [12]. Therefore, estimated in-place compressive strength at time $t = 28$ days of Sheta River Bridge deck is 24 MPa, as discuss in the above. Additionally, According to ACI 209R-92 model, the general equation for predicting compressive strength of concrete at any time t is given by:

$$f_{cmt} = \left[\frac{t}{a + bt} \right] \times f_{cm28}$$

Where:

f_{cmt} = Concrete mean compressive cylinder strength at age t , MPa

f_{cm28} = Concrete mean compressive cylinder strength at 28 days, MPa

Table 4.3 – Values of the constant a and b

	Moist – cured concrete		Steam – cured concrete	
	a	b	a	b
I	4.0	0.85	1.0	0.95
III	2.3	0.92	0.70	0.98

(Source: Article 5.4.1. ACI 209R- 92 model)

The constants a and b are functions of both the type of cement used and the type of curing employed. The predicted compressive strength at any time, t concrete of Sheta river bridge deck slab is;

$$f_{cmt} = \left[\frac{t}{a + bt} \right] \times f_{cm28}$$

$$f_{cmt} = \left[\frac{18,250}{4 + (0.85 \times 18,250)} \right] \times 24 \text{MPa}$$

Therefore : $f_{cmt} = 28 \text{MPa}$, for $t = 50$ years

Furthermore, followed the same basic procedure was to predicted in-place compressive strength for the girder of bridge; initially, give a code for girders just like G1, G2, G3 and G4 from upstream to downstream, respectively, and then tests performed on the smooth texture of girders independently by took more than 24 readings for one girder, Finally, estimated in-place compressive strength of bridge deck test at time $t = 28$ years is 35 MPa, as shown in the Appendix A.1. In general, it can concluded that according Article 14.1, ERA Bridge design manual – 2002 edition, the strength of sound concrete shall be assumed to be equal to either the values taken from the structural plans and specifications or the average of construction test values. When these values are not available, the ultimate stress of sound concrete shall be assumed to be 25 MPa. A reduced ultimate strength shall be assumed no less than 15 MPa. Therefore, in-place compressive strength of Sheta River Bridge deck is 24 MPa in line with the above mentioned range.

4. Hammer Sounding :

Hitting it with carpentry hammer is generally used for this study; the operator struck the concrete with a standard carpentry hammer and listened to the response. This method has two limitations that applied to hammer sounding including the subjective judgment and hearing sense of the operator. Areas of delaminations are then marked directly on the surface of the concrete. After delaminated areas are marked on the Sheta River Bridge deck, the percentage of delaminated areas can be computed. Therefore, 150 cm² of delaminated areas Sheta River Bridge deck slab surface was recorded during site investigation.



Figure 4.6: Marked delaminated areas of Sheta River Bridge deck

According to ERA–Bridge Inspection Manual (2008), damage rating for bridge deck slab are total delaminated area is more than 900 cm^2 ranking–A with desirable intervention of urgent repair, total delaminated area is between 400 to 900 cm^2 ranking–B with desirable intervention of repair but not urgent, and total delaminated area is between 100 to 400 cm^2 ranking–C with desirable intervention of routine maintenance. Additionally, AASHTO recommends maintenance of the bridge deck slab if 10 to 50 percent is affected by delaminations. Therefore, the delaminated areas of Sheta River Bridge deck ranking categorized under rank–C with desirable intervention shall be done routine maintenance, as per ERA–Bridge Inspection Manual (2008).

5. Pachometer survey:

In this study, depth of concrete cover easily obtained after measuring bare undeformed reinforcement bar projected at the end of wing wall, as shown in the figure below and peels off concrete at the bottom of deck slab.




Figure 4.7: Measuring bare undeformed steel reinforcement bars

The measured depth of concrete cover at the bottom of deck slab is 50 mm. However, different values are proposed as the optimum value of the concrete cover depth over top main reinforcing bars show AASHTO 2005 edition in the Table 5.12.3-1. Therefore, Sheta River Bridge deck satisfied the minimum concrete cover depth to main steel reinforcement bars including bars protected by epoxy coating, as per LRFD – AASHTO 2005 edition.

6. Chloride content analysis:

Concrete cores are not removed in this study, powder samples can be taken for chloride analyses. This is usually done with a Carborundum/ abrasive stone. Samples are taken at various depths, down to and slightly beyond the depth of the steel reinforcement bars, as shown in the Figure 4.4 above. The currently accepted test for water-soluble chloride content in concrete is described in ASTM C1218 was used in this thesis. The computed water soluble chloride content in the concrete bridge deck, expressed as percentage relative to the weight of sample (% C1).

Table 4.4: Chloride ion content analysis

General data	
Identification of the sample	Nature of sample: Chloride ion analysis Location of sample: At the bottom of bridge deck Sampling date: 10 – 09 – 2008 E.C. <div style="text-align: center;">  </div> Sample powder was taken for analysis
Date of the test	Date of the test: 20 – 09 – 2008 E.C.
Location of the test	Bonga complete secondary school, Chemistry laboratory
Name of the person in charge of the test	Mr. Berhanu Tefera (Researcher of this thesis)
	Mr. Adugna Adelo
References about this test procedure	ASTM C1218
Results (% C1):	8 % Water soluble chloride ion content was taken sample from underneath bridge deck slab (Percentage in weight)

High concentrations of water-soluble chloride ion in recycled concrete have been shown to contribute to accelerated corrosion of steel reinforcement bar embedment. However, the results of water-soluble tests are greatly affected by the degree of grinding of the sample and by the length and temperature of leaching.

According to the Table R4.3.1, ACI 318-05, maximum water soluble chloride ion (Cl^-) in reinforced concrete by mass of cement includes limits of 0.3 and 0.15 percent subjected to exposure classes C1 (concrete exposed to moisture but not to external sources of chlorides) and C2 (concrete exposed to moisture and an external sources of chlorides from de-icing chemicals, salt, brackish water, seawater, or spray from these sources), respectively. Therefore, Sheta River Bridge deck water-soluble chloride ion content is 8 % that was subjected to exposure classes C2, the result indicates the steel reinforcement bar was less suspected to chloride ions (Cl^-).

4.3. Cause of time – dependent concrete deck cracking

It is well-known that concrete has relatively low tensile strength, and this characteristic is one of the important causes of cracking. Many studies [3 and 7] have been done in order to determine the factors that lead to time-dependent concrete bridge deck cracking by using various methodologies like analytical modelling, field survey and testing in the laboratory. The finding of this study show that factors that lead to cracking in bridge deck can be classified into the following four categories: Environment and Site conditions, material properties (i.e. reinforced concrete and steel reinforcement bars), structural design parameters, and excessive traffic overloading and age of the bridge.

4.3.1. Environment and Site conditions

4.3.1.1. Maximum daily temperature

The effect of maximum temperature changes was assessed with the daily and seasonal temperature ranges specific to the environment surrounding Kaffa Zone, Bonga town in Sheta River Bridge location, maximum daily temperature plotted in the figure below.

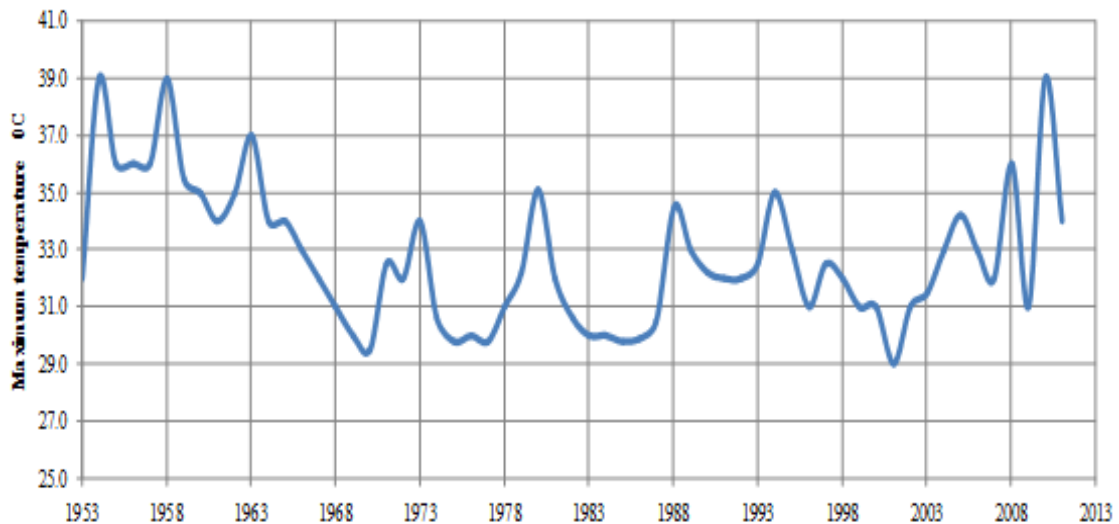


Figure 4.8: Maximum daily temperature in Kaffa Zone, Bonga town

The thermal load on concrete is due to the daily temperature cycles on the bridge deck. Once the heat of hydration process is complete, the weather and daily temperature influence the thermal stresses. Temperature gradients which produce the thermal stresses develop between the top of the bridge deck and girder of the bridge. The temperature effect was determined that the maximum tensile stress to produce transverse cracking takes place at the top of the bridge deck. The relationship between this variable and the mean crack density of bridge deck show that cracking tends to increase with increases in daily temperature.

4.3.1.2. Relative humidity

Relative humidity has a major influence on ultimate shrinkage and the rate of shrinkage. Low relative humidity is generally thought to contribute to bridge deck cracking by increasing the rate at which surface moisture evaporates from hardened concrete. According weather data logbook of Ethiopian Meteorology Agency, Jimma Branch Directorate data, the maximum low relative humidity Kaffa Zone, Bonga is 31 mm.

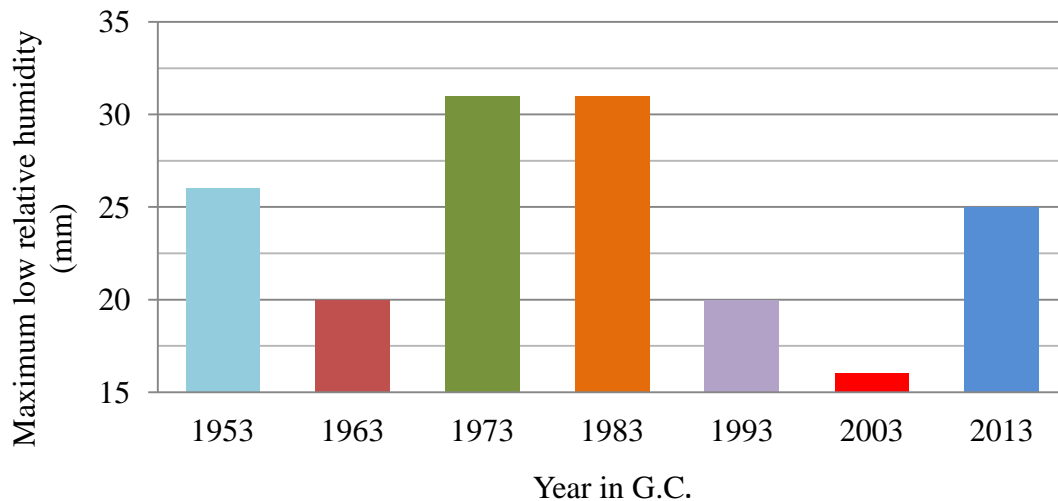


Figure 4.9: Maximum low relative humidity in Kaffa Zone Bonga town

The expansion occurs if concrete is exposed to a continuous supply of water; this process is known as swelling. Swelling is small compared with shrinkage in ordinary concrete and occurs only when the relative humidity is maintained above 94% [22].

4.3.2. Material properties

The long term material behaviour of reinforced concrete bridge deck is primarily characterized by volume change which may cause cracking leading to the impact on the in-service behaviour of concrete bridge deck. Most time-dependent variables are shrinkage and creep. These time-dependent properties of concrete are influenced by the conditions at time of placement and the environment that surrounds it throughout its service life. Prediction of the exact effect of all of the conditions is difficult, but estimates can be made of the trends and changes in behaviour.

4.3.2.1. Shrinkage

Shrinkage of an unrestrained reinforced concrete bridge deck was focused in this study. However, reinforcement embedded in the concrete provides restraint to shrinkage. As the concrete shrinks, the reinforcement is compressed and imposes an equal and opposite tensile force on the concrete at the level of the reinforcement. In this study, the time-dependent total shrinkage strain of reinforced concrete $\varepsilon_{sh}(t, t_c)$ of Sheta River Bridge deck calculated based on Euro-International Concrete Committee, CEB MC 90-99 models. Therefore, 8.2 mm reduce from 20 m span due to total shrinkage strain, detail calculation as shown in the Appendix A.3.

For anytime-dependent dry shrinkage strain of Sheta River Bridge deck for calculated strength of concrete is plotted as a function of time, in the following figure.

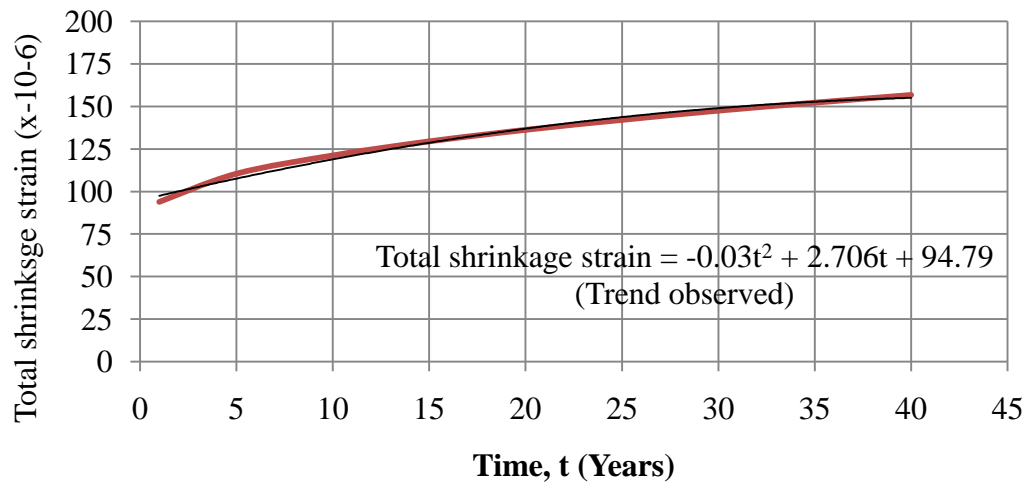


Figure 4.10: Total shrinkage strain prediction of Sheta River Bridge deck

According to the Article 1.2.2, ACI 209.1R-05; value of long – term concrete shrinkage are typically between 150 and 800 micro strain (150 and 800 x 10⁻⁶ strain). Therefore, dry shrinkage strain prediction of Sheta River Bridge deck is 155 x 10⁻⁶ strain was satisfied per ACI 209.1R- 05.

4.3.2.2. Creep

The bridge deck subjected to load responds instantaneously and time-dependently. When deck is subjected to a sustained load, deformation gradually increases with time due to creep. Any increase in deformation over time directly attributable to creep and shrinkage significantly affects the service load behaviour. According to the Gilbert research [2], the creep coefficient is assumed to approach a final value $\phi(t,t_0)$, as time approaches infinity, which usually falls within 1.2 - 4.0. Therefore, the computed creep coefficient $\phi(t,t_0)$ of Sheta River Bridge deck is 1.28, as coincided with above mentioned research result, as shown in the appendix A.4 below.

4.3.2.3. Steel reinforcement bars

Steel reinforcement bars are usually round with regularly spaced rib-shaped deformations on the surface to provide a better bond between the concrete and steel. However, Sheta River Bridge was constructed by undeformed steel reinforcement bars that leads weak bond between concrete and steel reinforcement bar. Moreover, undeformed steel reinforcement it may cause of bridge deck cracking.



Figure 4.11: Undeformed bare rebar

Corrosion to reinforcement is signs rather than reason for concrete damage. Corrosion occurs due to electrochemical oxidation of reinforcement bars in existence of moisture and electron flow inside metal. After corrosion the volumes of reinforced bars get increased. Due to increase in volume of reinforced bars a bursting radial stresses are produced around bars which result in local radial cracks around bars.

4.3.3. Structural design parameters

Structural design factors are extremely important issues for the cause of concrete bridge deck cracking. These factors are deck thickness, concrete cover, design vehicle load, girder end restraint condition, and bridge length; they are directly related to concrete bridge deck cracking.

4.3.3.1. Deck thickness

A deck thickness of the Sheta River Bridge is 200 mm. According, AASHTO (LRFD, 2005), unless approved by the owner, the depth of a concrete deck, excluding any provision for grinding, grooving, and sacrificial surface, should not be less than 175 mm.

4.3.3.2. Concrete cover

The cover thickness has also been found to affect the corrosion rates of cracked concrete. This is because an increased cover reduces the availability of oxygen at the reinforcement level by increasing the thickness which oxygen must pass through. This effect largely depends on the type of binder used. The most important consideration in bridge deck design is the thickness of protective concrete cover over the top reinforcement.

It is recommended that 60 mm of concrete, measured from top of bar, be the minimum amount of protective cover over the main reinforcement in bridge deck surfaces subject to tire stud or chain wear. Increased cover depth reduces risk of cracking, however, excessive increase in cover depth increases probability of settlement cracks over reinforcement. Proper concrete cover is necessary for durability and prevention of splitting due to bond stresses and to bond stresses and to provide for placing tolerance.

4.3.3.3. Design vehicle load

During the design period of the existing Sheta River Bridge design vehicle live load used in Ethiopia was based on the older AASHTO HS20–44 design vehicle load (320KN). However, the current design vehicle live load used in Ethiopia is HL–93 vehicle load, which also includes a design lane load of 9.3 KN/m. Thus an existing structure shall be checked for this design vehicle load. The highway load–93 or HL–93 designation consists of a design truck (identical to HS20-44) or design tandem plus design lane load, if a worse condition is created than with the design truck. To concluded that the new loads may affect existing designs, but the difference between old and new does not mean that all designs need to be updated. The small increases will affect designs that have not excess capacity.

4.3.3.4 Girder end restraint condition

Restraint condition is denotes the restraint against free deformation of the deck slab, provided by the structural system. Specifically; in this study, mainly the primary restraint parameter of the girder end restraints associated with abutment connections of the corroded steel line plate bearing.



Figure 4.12: Girder end restraint condition



Figure 4.13: Corrosion of steel plate bearing

In general terms, restraints are the direct cause of cracking in concrete. In the field investigation, computed crack density is $0.188 \text{ m} / \text{m}^2$ form one-span T - girder of Sheta River Bridge this indicates the volumetric changes in the deck slab were minimally restrained. However, the girder end bearing steel plate was highly corroded, that might have caused for the transverse cracks of deck slab.

According to ERA–Bridge Inspection Manual (2008), damage rating for bearing plate of Sheta River Bridge categorized under rank–C (corrosion of bearing steel plate, which causes a reduction of sliding functions), routine maintenance shall be done before causes for reduction of durability the bridge deck.

4.3.4. Excessive traffic overloading and Age of bridge

4.3.4.1 Excessive traffic overloading

During service life of reinforced concrete highway bridge deck slab, it is subjected to various types of loading conditions (i.e. static loading/or cyclic loading). The comparison between traffic volume, in terms of the average annual daily traffic (AADT), and mean crack density indicates some tendency for increased cracking with increases in AADT. In this study, structural cracks and bulging noted at the wing wall has may be occurred when a heavy armoured fighting vehicles (military tank) passed on during a war in the previous regime. However, the observed crack pattern suggests that live-load stresses alone play a relatively minor role in transverse cracking.

4.3.4.2 Age of bridge

As bridges are designed to withstand fatigue loading (which increases with time), age is an important parameter involved in structural condition assessment. The life expectancy of current bridges is about 50 years and for major concrete bridges is around 100 years. The service life of a bridge brings to end when one of the key components fails to function as designed. In this study, even though researcher couldn't get a formal document that indicate the exact year of construction for Sheta River Bridge, but from the informal information gathered from elderly people residing in the Bonga town and other concerned governmental offices of the Kaffa Zone, researcher come to understand that the bridge was constructed in the late 1950's (Ethiopian calendar) by then empower highway authority, which shows that it was served for past 50 years and thus might indicate that the design life of the bridge is almost completed.

4.4 Comparison of the study with others

The review design works of Sheta River Bridge was originally carried out in 1999 by an international consultant, SAUTI Consulting Engineers in association with SAVA Engineering and later on reviewed by an international Consultant BKS Global (Pty) Ltd of South Africa in association with BEZA Consulting Engineers P.L.C. of Ethiopia in 2009–2010. Currently, the design has been reviewed by the supervision consultant, DANA and Associate Engineering Consultants P.L.C. [2]. According to the conclusion of the study report of DANA & Associates Engineering Consultants P.L.C., Sheta River Bridge demolishes and replace by same 26 m span new bridge. One of the main concerns from structural perspective to demolish the bridge was designed by older AASHTO HS20-44 truck load, which is less by about 25% of current design vehicle loading, HL-93 [2].

The term design lane load is new and applies to design of above grade bridge decks. The HL-93 design truck wheel load is the same as the HS20-44 wheel load, as shown in the Figure 4.14 below. To concluded that the new loads may affect existing designs, but the difference between old and new does not mean that all designs need to be updated. The small increases will not affect designs that have excess capacity. Those designs that minimized reinforcing steel and slab thickness to create a structure that was just good enough may need to be reviewed. These conclusions are based on demonstrates that old designs are not inferior to new designs using LRFD. Sheta River Bridge was using the older load factor design (LFD), while this thesis was checked by using the newer LRFD design. Some of the steel reinforcement areas required in the newer specifications are less than steel reinforcement areas required in the older specification, However, that was compensated the bridge have enough section than the design required.

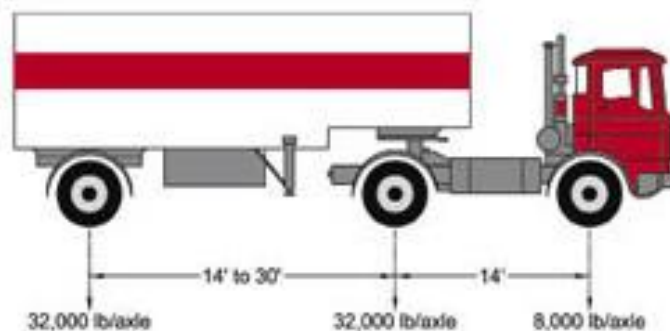


Figure 4.14: HS20-44 Truck

Additionally, DANA & Associates Engineering Consultants P.L.C. does not included Sheta River Bridge strength analysis in their 26 pages of review study reports. How could be believed the bridge was structurally good condition without strength analysis? In this study, bridge rating through structural analysis is by far the most common (and most economical) procedure for rating existing Sheta River Bridge. The strength limit state as shown in the Appendix–B below, is fundamental for public safety and is the main determining factor for bridge posting, closure and repairing.

The rating of bridges without plans is typically performed in one of four ways: using plans from a similar bridge built at about the same time; by load testing the bridge; using results of load tests from a similar bridge structure; or by professional judgment. Rating of Sheta River Bridge can be done for this study by combination of using plan from a similarly constructed bridge (Bitino River Bridge) and by professional judgment. Strength-limit state (flexural or shear capacity) of Sheta River Bridge all rating factor (RF) calculated for legal truck greater than 1.0, i.e. concluded that the bridge does not need to be posted or the structure reasonably good condition.

4.5 Major finding

Phase – 1: Field investigation

In this study, field investigation result reports for Sheta River Bridge deck as mentioned in the following tabular format.

Table 4.5: Filed investigation results

Non – destructive tests	Observation
1. Visual inspection, as show in the Appendix A	<ul style="list-style-type: none"> ⊕ Accumulation of silt and blocked drainage on the surface of bridge deck ⊕ Transverse cracks on the bridge deck, its crack width ranged from 0.08 mm to 1 mm ⊕ Computed deck crack density is 0.188 m/m^2 and also its crack severity is 8 % ⊕ Highly corroded end bearing plate ⊕ Leakage underneath of bridge deck slab ⊕ Exposed undeformed rebars was observed at wing wall of Jimma town side ⊕ Structural crack at wing wall ⊕ Scouring Problem and Vegetation around abutment
2. Rebound hammer test	<ul style="list-style-type: none"> ⊕ Predicted compressive strength at any time $t = 28$ days concrete of Sheta river bridge deck slab is 24 MPa ⊕ Estimated in – place compressive strength of bridge deck test at time $t = 50$ years is 28 MPa
3. Hammer Sounding	<ul style="list-style-type: none"> ⊕ 10% of delaminated areas concrete deck slab surface was recorded during site investigation
4. Pachometer survey	<ul style="list-style-type: none"> ⊕ The depth of bottom concrete cover for deck slab is 49 mm
5. Chloride content analysis	<ul style="list-style-type: none"> ⊕ 8 % Water soluble chloride ion content in the taken sample from underneath bridge deck slab (Percentage in weight)

Phase – 2: Causes of time dependent concrete deck cracking

The factors that affected Sheta River Bridge deck cracking as mentioned in the section 4.3 above, such as environmental and site conditions, material properties, structural design parameters, excessive traffic overloading and age of the bridge have been rated from minor to major based on its significance effect for deck cracking.

Table 4.6: Rating of the causal factors for bridge deck cracking

Causal factors	Effect		
	Major	Moderate	Minor
A. Environmental & Site conditions			
Maximum daily temperature		✓	
Relative humidity		✓	
B. Material properties			
Compressive strength of aged concrete			✓
Shrinkage		✓	
Creep		✓	
Thermal expansion			✓
Alkali-silica reaction		✓	
Reinforcement bars			✓
C. Structural design parameters			
Deck thickness		✓	
Concrete cover		✓	
Design vehicle load		✓	
Girder end restraint condition			✓
Bridge Length			✓
D. Excessive traffic overloading and Age of the bridge			
Excessive traffic overloading		✓	
Age of the bridge	✓		

Phase – 3: Mitigation strategies to reduce deck cracking

The primary reason for providing mitigation strategies is to extend the life of the bridge deck, and to reduce the rate of crack of the concrete bridge deck. In this study, once the bridge has been constructed, mitigation strategies to reduce cracking bridge deck by using surface treatments, joint sealants, applying electrical-chemical principles, by modifying the Portland cement concrete overlay, topical treatment with lithium, and improve the resistance to other deleterious influences. For the purposes of bridge maintenance, cracks can be categorized as either structural or non structural. Structural cracks are repaired to restore structural integrity, and non structural cracks are sealed to minimize the potential for increased cracking. In this study, almost all manifested cracks in the Sheta River Bridge deck are non-structural cracks, therefore, its method of crack repairs include gravity fill, topical applications of sealers, rout & seal, and epoxy injection

Phase – 4: Effect of cracks on bridge deck performance

Deck cracks can allow rapid ingress of moisture and chloride ions into concrete interior leading to accelerated corrosion of rebar, deterioration and leaching of concrete. As a result of these adverse effects of concrete bridge deck cracking can be greatly reduces the service life of deck, leads to a loss of functionality, loss of stiffness and ultimately the loss of structural safety. In this study, crack widths of less than 0.6 mm have little effect on the overall corrosion of the reinforcing steel. Although wider cracks accelerate the onset of corrosion over several years, crack width has little effect on the rate of corrosion. Cracks that follow the line of a reinforcing bar are much more serious because the length of the bar equal to the length of the crack is exposed to the ingress of moisture, oxygen, and chlorides. In addition, the presence of the cracks reduces the resistance of the concrete to spalling as the reinforcement corrodes.

CHAPTER FIVE

CONCLUSIONS AND RECOMMENDATIONS

5.1. Conclusions

The following conclusions are based on the findings of the study:

1. Time-dependent deck cracking of Sheta River Bridge deck caused by many factors such as materials properties, environment and site conditions, structural design parameters, excessive traffic overloading and age of the bridge.
2. Total shrinkage strain was one of the most detrimental properties of concrete and most significant factor influencing transverse cracking in bridge deck slab, which long-term strength and durability
3. The presence of transverse deck cracks studied has no significant effect on its general structural behavior, the existence of average cracks width are small, but as the cracks become larger can have a serious effect.
4. Under the simple support condition, the degradation of girder strength caused by the existence of transverse cracks is rather small and can be ignored in most cases. On the other hand, transverse cracks can greatly reduce the strength of the bridge deck due to allow rapid ingress of moisture and chloride ions into concrete interior leading to accelerated corrosion of rebar, deterioration and leaching of concrete.
5. Mitigation strategies for non-structural deck cracks repair mechanisms include gravity fill, topical applications of sealers, rout & seal, and epoxy injection.
6. The older load factor designs (i.e. HS 20–44) are not inferior to new designs using LRFD (i.e. HL-93), while the older LFD designs was checked by using the newer LRFD design. Some of the steel reinforcement areas required in the newer specifications are less than steel reinforcement areas required in the older specification, this comparison confirms that the new HL-93 loading is not obsolete structure which is designed by older LFD.

7.2 Recommendations

From the study that has been carried out, the followings are the recommendations drawn from the result:

1. Almost all manifested cracking in Sheta river bridge deck slab are non-structural cracks, so, to prolong the service life of bridge should be preventive maintenance can be done by gravity fillycracks repair mechanism with association of lower viscosity gravity feed product. As mentioned earlier, these recommendations are valid only to the extent that the testing areas are representative of the entire deck surfaces.
2. For future concrete bridge deck condition assessments conducted by ERA as well as bridge engineering consultants should include pachometer survey, sounding, half-cell potential measurements, and chloride concentration testing for determining whether a deteriorating deck should be rehabilitated or replaced, or whether application of a preventive maintenance treatment to a relatively aged deck is appropriate; only visual in section are not as valuable for determining bridge deck condition.
3. The results of numerical analysis are felt to be conservative because many unknowns must be accounted for using assumptions. Experimental determination of material values for these unknowns would make the analysis more reliable. Core samples of the concrete girders could provide a more representative concrete strength, which would likely result in larger load-carrying capacity. X-ray technology could be used to determine the layout of any mild steel reinforcement. Load testing the bridges would be costly, but it would be the most reliable method of ascertaining the capacities.
4. Sheta River Bridge was served for past 50 years and thus might indicate that the design life of the bridge is almost completed. Therefore, the researcher recommends that the concerned body shall strengthen the girder of the bridge.

REFERENCES

- [1] Ethiopian Road Authority, Bureau of Bridge Management. Reports for Bridge Asset Management Support Service (BMS), unpublished documents
- [2] Study report on Sheta River Bridge by DANA and Associates Engineering Consultants P.L.C. to Western Region Contract Management Directorate Director of Ethiopian Road Authority, under the scope of the works contract of Bonga – Felege Selam road project
- [3] Krauss, P.D, and Rogalla, E.A., Transverse Cracking in Newly Constructed Bridge Decks, NCHRO Report 380, Transportation Research Board, National Research Council, Washington, D.C., 1996
- [4] Robert J. F., Sergio Gutierrez, and Jacob S. Hoffmam. Control and Repair of Bridge Deck Cracking, Joint Transportation Research Program, FHWA/IN/JTRP-2010/4, West Lafayette, IN 47907-1284
- [5] Radabaugh, R.D. 2001, “Investigation of Early Age Bridge Deck Cracking,” Master’s Thesis, School of Civil Engineering, Purdue University, May 2001.
- [6] Curtis, R. H., and White, H., “NYSDOT Bridge Deck Task Force Evaluation of Bridge Deck Cracking on NYSDOT Bridges.” New York State Department of Transportation, February 2007, pp. 1-26.
- [7] Schmitt, T. R., and Darwin, D., “Cracking in Concrete Bridge Decks,” Report No. K-TRAN: KU-94-1, Final Report, Kansas Department of Transportation, April 1995.
- [8] NCHRP Synthesis 333, (2004) “Concrete Bridge Deck Performance – A Synthesis of Highway Practice,” Transportation Research Board, pp. 1-87.
- [9] Hadidi, R. and Saadeghvaziri, M. A., 2002. Cause and Control of Transverse Cracking in Concrete Bridge Decks - Final Report.FHWA-NJ-2002-19.

- [10] OPSS. Prov 1350, 2010. "Material Specification for Concrete - Materials and Production". Ontario Provincial Standard Specification, Ontario, Canada.
- [11] Cussion, D. and Repette, W. L., 2000. Early Age Cracking in Reconstructed Concrete Bridge Barrier Walls. *ACI Materials Journal*, 97(4), pp. 438-446.
- [12] Susetyo, J., 2009. Fibre Reinforcement for Shrinkage Crack Control in Pre-stressed, Precast Segmental Bridges. Doctor of Philosophy. University of Toronto, Department of Civil Engineering.
- [13] Mihashi, H. and Leite, J. P. d. B., 2004. State-of-the-Art Report on Control of Cracking in Early Age Concrete. *JCI Journal of Advanced Concrete Technology*, 2-2, pp. 141-145.
- [14] Aktan, H., Fu, G., Dekelbab, W., and Attanayaka, U., 2003. Investigate Causes and Develop Methods to Minimize Early Age Cracking in Michigan Bridge Decks (MDOT Research Report RB-1437). Michigan DOT, Michigan.
- [15] ACI228.2R-98. Non - destructive Test Methods for Evaluation of Concrete in Structures, American Concrete Institute, Farmington Hills, Mich., 1998.
- [16] ACI224.1R – 07. Causes, Evaluation, and Repair of Cracks in Concrete Structures, American Concrete Institute, Farmington Hills, MI 48331, 2007.
- [17] Robert, S., Tuttle. Condition Analysis of Concrete Bridge Decks in Utah. Report UT-06-15. Department of Civil and Environmental Engineering, Brigham Young University, Provo, UT, 2005.
- [18] Ethiopian Meteorology Agency, Jimma Branch Directorate. Reports of maximum daily temperature and relative humidity data for Kaffa zone, Bonga town, unpublished documents
- [19] ACI209.2R-08. Guide for Modelling and Calculating Shrinkage and Creep in Hardened Concrete, American Concrete Institute, Farmington Hills, MI 48331, 2008.

[20] Jansen, D. C., S. P. Shah, and E. C. Rossow. Stress-Strain Results of Concrete from Circumferential Strain Feedback Control Testing. *ACI Materials Journal*, Vol. 92, No. 4, 1995, pp. 419–428.

[21] B. Fournier, M. Berubé, Alkali-aggregate reaction in concrete: a review of basic concept and engineering implications, *Can. J. Civil Eng.* 27 (2) (2000) 167–191.

[22] Darwin, D.; and Schmitt R., Tony, 1995, “Cracking in Concrete Bridge Decks”. The Kansas Department of Transportation. K-Tran Project No. KU-94-1, pp. 148-164.

[23] ACI 224R-01. Control of Cracking of Concrete Structures, American Concrete Institute, Farmington Hills, MI 48331, 2001.

[24] ACI 345.1R-06. Guide for Maintenance of Concrete Bridge Members, American Concrete Institute, Farmington Hills, MI 48331, 2006.

Appendix – A

A.1: Field recorded of in – place rebound hammer test result of Girder

Test number	Test results	Estimated compressive strength (MPa)
G1A (Side)		
1	34	28
2	38	37
3	39	39
4	40	41
5	39	39
6	40	41
7	45	50
8	37	35
9	35	30
10	38	37
Average		36
G1B (Soffit)		
1	36	33
2	42	43
3	42	43
4	40	39
5	41	41
6	39	38
7	40	39
8	45	48
9	35	30
10	38	37
Average		38
G1C (Side)		
1	40	43
2	44	54
3	45	56
4	47	61
5	41	46
6	43	51
7	39	39
8	42	49
9	42	49
10	43	51
Average		48

Calculation: Discard readings differing from the average of 10 readings by more than 6 units and determine the average of the remaining readings. If more than 2 readings differ from the average by 6 units, discard the entire set of readings and determine rebound numbers at 10 new locations within the test area.

References about this test procedure: ASTM, Designation: C 805 – 97

Instrument number: 1H0039

Technician: Mr. Enamrit Mulatu

Jimma University, JIT, Material laboratory assistance

Checked by: Mr. Berhanu Tefera (Researcher of this thesis)

Estimated in – place compressive strength of girder G1: 40 MPa

Date and time of testing: 10 – 09 – 2008 E.C. at 5:30 AM (Local time)

Generally, during in – place rebound hammer test on the girders, first coded the four girders just like G1, G2, G3 and G4 from upstream to downstream, respectively. Tests performed on the smooth texture of girders independently, take the average of about 30 readings from one girder, as shown above.



Figure A.1: Surface preparation and coding of exterior girder (G1)

A.2: Estimate compressive strength of 28 days concrete of Sheta River Bridge deck slab as follow:

1. Estimating modulus of elasticity of concrete at a concrete age t , E_{cmt} :

According CEB MC90-99 model, for the prediction of the creep function, the initial strain is based on the tangent modulus of elasticity at the time of loading [19]. The modulus of elasticity of concrete at a concrete age t different than 28 days may be estimated from

$$E_{cmt} = E_{cm28} \exp \left[\frac{s}{2} \left(1 - \sqrt{\frac{28}{t/t_1}} \right) \right]$$

Table A.12 – Coefficient s according to CEB MC90-99 models [ACI 209.2R-08]

f_{cm28}	Types of cement	S
≤ 60 Mpa	RS (rapid hardening high – strength cement)	0.20
	N or R (normal or rapid hardening cement)	0.25
	SL (slowly – hardening cement)	0.38
> 60 Mpa*	All types	0.20

*Case not considered in CEB MC90

The coefficient S depends on the type of cement and the compressive strength of concrete and may be taken from Table A.12: So, the values of reinforced concrete Sheta river bridge deck slab; $S= 0.25$ (N–Normal hardening cement, ≤ 60 Mpa); $t_1=1$ day and $t = 18,250$ days

2. Predicting compressive strength at any time t , f_{cmt} :

According ACI 209R-92 model, the general equation for predicting compressive strength of concrete at any time t is given by

$$f_{cmt} = \left[\frac{t}{a + bt} \right] \times f_{cm28}$$

Where:

f_{cmt} = Concrete mean compressive cylinder strength at age t , MPa

f_{cm28} = Concrete mean compressive cylinder strength at 28 days, MPa

This is an empirical model developed by Branson and Christiason (1971), with minor modifications introduced in ACI 209R-82 (ACI Committee 209 1982).

Table A.4 – Values of the constant a and b ; ACI 209R- 92 model

Types of cement	Moist – cured concrete		Steam – cured concrete	
	a	b	a	b
I	4.0	0.85	1.0	0.95
III	2.3	0.92	0.70	0.98

The ratio a/b is the age of concrete in days at which one half of the ultimate (in time) compressive strength of concrete is reached. The constants a and b are functions of both the type of cement used and the type of curing employed. The concrete required mean compressive strength f_{cm28} should exceed the specified compressive strength f'_c as required in Appendix B of ACI 318 (ACI Committee 318, 2005). Mechanical properties are used to check serviceability limit states and values are almost always related to the mean compressive strength and not the characteristic strength. The predicted compressive strength at any time $t = 28$ days concrete of Sheta river bridge deck slab is;

$$f_{cmt} = \left[\frac{t}{a + bt} \right] \times f_{cm28}$$

$$f_{cm28} = \left[\frac{4 + (0.85 \times 18,250)}{18,250} \right] \times 30 \text{ MPa}$$

$$f_{cm28} = 25 \text{ MPa}$$

A.3: The time – dependent total shrinkage of reinforced concrete $\varepsilon_{sh}(t,t_c)$ of Sheta River Bridge deck calculated from:

$$\varepsilon_{sh}(t,t_c) = \varepsilon_{cas}(t) + \varepsilon_{cds}(t,t_c)$$

1. The autogenous shrinkage component $\varepsilon_{cas}(t)$:

$$\varepsilon_{cas}(t) = \varepsilon_{cas0}(f_{cm28}) * \beta_{as}(t)$$

$$\varepsilon_{cas0}(f_{cm28}) = -\alpha_{as} \left(\frac{f_{cm28}/f_{cm0}}{6 + f_{cm28}/f_{cm0}} \right)^{2.5} \times 10^{-6}$$

Where:

$$f_{cm28} = 25 \text{ MPa}, f_{cm0} = 10 \text{ MPa}, \text{ and } \alpha_{as} = 700$$

$$\varepsilon_{cas0}(f_{cm28}) = -700 \left(\frac{25/10}{6 + 25/10} \right)^{2.5} \times 10^{-6} = -0.00011$$

$$\varepsilon_{cas0}(f_{cm28}) = -0.0001 \text{ mm/mm}$$

$$\beta_{as}(t) = 1 - \exp \left[-0.2 \left(\frac{t}{t_1} \right)^{0.5} \right]$$

Where:

$$t = 50 \text{ years} = 18,250 \text{ days}, \text{ and } t_1 = 1 \text{ day}$$

$$\beta_{as}(t) = 1 - \exp \left[-0.2 \left(\frac{18,250}{1} \right)^{0.5} \right] = 1$$

Therefore, Autogenous shrinkage component $\varepsilon_{cas}(t)$ is:

$$\varepsilon_{cas}(t) = \varepsilon_{cas0}(f_{cm28}) * \beta_{as}(t)$$

$$\varepsilon_{cas}(t) = -0.00011 \times 1 = -0.0001 \text{ mm/mm}$$

2. The drying shrinkage component $\varepsilon_{cds}(t, t_c)$:

$$\varepsilon_{cds}(t, t_c) = \varepsilon_{cds0}(f_{cm28}) * \beta_{RH}(h) * \beta_{ds}(t - t_c)$$

$$\varepsilon_{cds}(t, t_c) = \varepsilon_{cds0}(f_{cm28}) * \beta_{RH}(h) * \beta_{ds}(t - t_c)$$

$$\varepsilon_{cds0}(f_{cm28}) = \left[(220 + 110\alpha_{ds1}) \exp(-\alpha_{ds2} f_{cm28}/f_{cm0}) \right] \times 10^{-6}$$

Where:

$$\alpha_{ds1} = 4, \alpha_{ds2} = 0.12, f_{cm0} = 10 \text{ MPa, and } f_{cm28} = 25 \text{ MPa}$$

$$\varepsilon_{cds0}(f_{cm28}) = [(220 + (110 \times 4)) \exp((-0.12 \times 53.98)/10)] \times 10^{-6}$$

$$\varepsilon_{cds0}(f_{cm28}) = 0.000345 \text{ mm/mm}$$

$$\beta_{s1} = \left(\frac{3.5 f_{cm0}}{f_{cm28}} \right)^{0.1} \leq 1.0$$

$$\beta_{s1} = \left(\frac{3.5 \times 10}{25} \right)^{0.1} \leq 1.0 \quad \beta_{s1} = 1.0$$

$$\beta_{RH}(h) = \begin{cases} -1.55 \left[1 - \left(\frac{h}{h_0} \right)^3 \right] & \text{for } 40\% \leq h < 99\% \times \beta_{s1} \\ 0.25 & \text{for } h \geq 99\% \times \beta_{s1} \end{cases}$$

Where:

$$h = 100\% = 1.0, \text{ and } h_0 = 1$$

Therefore, $\beta_{RH}(h)$ is:

$$\beta_{RH}(h) = 0.25$$

$$\beta_{ds}(t - t_c) = \left(\frac{(t - t_c)/t_1}{350 \left[(V/S)/(V/S)_0 \right]^2 + (t - t_c)/t_1} \right)^{0.5}$$

Where:

$$V/S = 471.74 \text{ mm, } V/S_0 = 50 \text{ mm and } t_c = 14 \text{ days}$$

$$\beta_{ds}(t - t_c) = \left(\frac{(18,250 - 14)/1}{350 \left[(471.74)/(50) \right]^2 + (18,250 - 14)/1} \right)^{0.5} = 0.608$$

This means that after 50 years 60.8% of the bridge deck slab shrinkage will have occurred.

Therefore, Drying shrinkage component $\varepsilon_{cds}(t,t_c)$:

$$\varepsilon_{cds}(t,t_c) = \varepsilon_{cds0}(f_{cm28}) * \beta_{RH}(h) * \beta_{ds}(t-t_c)$$

$$\varepsilon_{cds}(t,t_c) = 0.000345 \text{ mm/mm} \times (0.25) \times 0.608 = 0.00042 \text{ mm/mm}$$

3. Compute total shrinkage of reinforced concrete bridge deck $\varepsilon_{sh}(t,t_c)$:

$$\varepsilon_{sh}(t,t_c) = \varepsilon_{cas}(t) + \varepsilon_{cds}(t,t_c)$$

$$\varepsilon_{sh}(t,t_c) = -0.00011 \text{ mm/mm} + 0.00052 \text{ mm/mm}$$

$$\varepsilon_{sh}(t,t_c) = -0.00041 \text{ mm/mm} = 8.2 \text{ mm reduce from 20 m span due to shrinkage}$$

The time-dependent shrinkage strain for above calculated strength of concrete is plotted as a function of time, in the following figure.

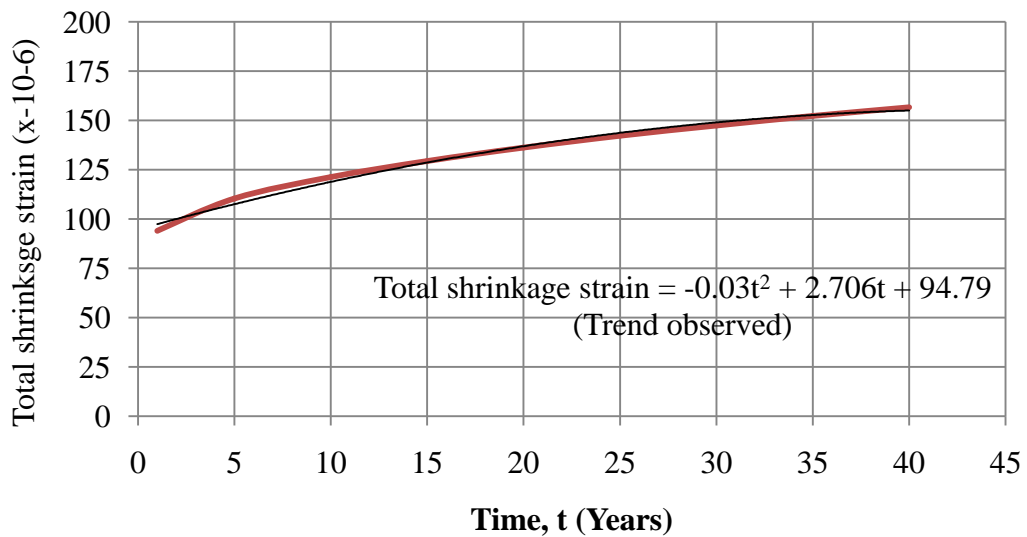


Figure A.3: Total shrinkage strain prediction

A.4: The creep coefficient $\varphi(t,t_0)$ of Sheta River Bridge may be calculated from;

$$\varphi(t,t_0) = \varphi_0 \times \beta_c(t-t_0)$$

1. Compute notational creep coefficient (φ_0)

$$\varphi_0 = \varphi_{RH}(h) \times \beta(f_{cm28}) \times \beta(t_0)$$

Where:

$$\varphi_{RH}(h) = \left[1 + \frac{1-h/h_0}{\sqrt[3]{0.1[(V/S)/(V/S)_0]}} \times \alpha_1 \right] \alpha_2$$

Thus, $h_0 = 100$, $V/S_0 = 50$ mm, $V/S = 471.74$ mm, h (i.e. relative humidity) = 100 %,

and $f_{cm0} = 10$ Mpa ; but α_1 and α_2 is:

$$\alpha_1 = \left[\frac{3.5 f_{cm0}}{f_{cm28}} \right]^{0.7} \quad \alpha_1 = \left[\frac{3.5 \times 10}{25} \right]^{0.7} = 0.74$$

and

$$\alpha_2 = \left[\frac{3.5 f_{cm0}}{f_{cm28}} \right]^{0.2} \quad \alpha_2 = \left[\frac{3.5 \times 10}{25} \right]^{0.2} = 0.92$$

$$\varphi_{RH}(h) = \left[1 + \frac{1-100/100}{\sqrt[3]{0.1 \times [471.74/50]}} \times 0.84 \right] \times 0.95$$

$$\varphi_{RH}(h) = 0.95$$

Then,

$$\beta(f_{cm28}) = \frac{5.3}{\sqrt{f_{cm28}/f_{cm0}}} = \frac{5.3}{\sqrt{25/10}}$$

$$\beta(f_{cm28}) = 2.3$$

and

$$\beta(t_0) = \frac{1}{\left(0.1 + (t_0/t_1)^{0.2} \right)}$$

The effect of type of cement and curing temperature on the creep coefficient may be taken into account by modifying the age at loading t_0 , according to below equation;

$$t_0 = t_{0,T} \times \left[\frac{9}{2 + (t_{0,T})^{1.2}} + 1 \right]^\alpha \geq 0.5 \text{ days}$$

$t_{0,T}$ is the age of concrete at loading (days) adjusted to the concrete temperature

$$t_{0,T} = \sum_{i=1}^n e^{-(4000/[273+T(\Delta t_i)]-13.65)} \times \Delta t_i$$

Where: α is a power that depends on the type of cement; $\alpha = -1$ for slowly hardening cement; $\alpha = 0$ for normal or rapidly hardening cement; and $\alpha = 1$ for rapid hardening high-strength cement, $T(\Delta t_i) = 50$ °C and $\Delta t_i = 3$ days

$$t_{0,T} = \sum_{i=1}^n e^{-(4000/[273+T(\Delta t_i)]-13.65)} \times \Delta t_i \quad t_{0,T} = 10 \text{ days then,}$$

$$t_0 = 10 \text{ days} \times \left[\frac{9}{2 + (10)^{1.2}} + 1 \right]^0 = 10 \text{ days}$$

$$\beta(t_0) = \frac{1}{\left(0.1 + (t_0/t_1)^{0.2} \right)}$$

$$\beta(t_0) = \frac{1}{\left(0.1 + (10/1)^{0.2} \right)} = 0.60$$

∴ The notational creep coefficient (φ_0) is:

$$\varphi_0 = \varphi_{RH}(h) \times \beta(f_{cm28}) \times \beta(t_0)$$

$$\varphi_0 = 0.95 \times 2.3 \times 0.6$$

$$\boxed{\varphi_0 = 1.31}$$

2. Compute development of creep with time ($\beta_c(t, t_0)$):

$\beta_c(t, t_0)$ – is a coefficient to describe the development of creep with time after loading, and may be estimated using the following expression

$$\beta_c(t, t_0) = \left[\frac{(t-t_0)/t_1}{\beta_H + (t-t_0)/t_1} \right]^{0.3}$$

$$\beta_H = 150 \times \left[1 + (1.2h/h_0)^{18} \right] \times (V/S)/(V/S)_0 + 250\alpha_3 \leq 1500\alpha_3$$

$$\alpha_3 = \left[\frac{3.5f_{cm0}}{f_{cm28}} \right]^{0.5} \quad \alpha_3 = \left[\frac{3.5 \times 10}{25} \right]^{0.5} = 0.81$$

$$\beta_H = 150 \times \left[1 + (1.2 \times (1/1))^{18} \right] \times (471.74/50) + 250 \times 0.81 \leq 1500 \times 0.81$$

$$\beta_H = 69,938 \leq 1,215$$

$$\beta_H = 1,215$$

∴ The development creep coefficient with time ($\beta_c(t, t_0)$) is:

$$\beta_c(t, t_0) = \left[\frac{(t - t_0)/t_1}{\beta_H + (t - t_0)/t_1} \right]^{0.3}$$

$$\beta_c(t, t_0) = \left[\frac{(18,250 - 10)/1}{1,215 + (18,250 - 10)/1} \right]^{0.3}$$

$$\beta_c(t, t_0) = 0.98$$

This indicates that 98 % of the total creep has occurred at the end of 50 years of Sheta River Bridge deck.

3. The creep coefficient $\varphi(t, t_0)$ is:

$$\varphi(t, t_0) = \varphi_0 \times \beta_c(t - t_0)$$

$$\varphi(t, t_0) = 1.31 \times 0.98$$

$$\varphi(t, t_0) = 1.28$$

4. Compute creep deformation of concrete ($\varepsilon_{cc}(50, t_0)$) at time $t = 50$ years for a constant compressive stress σ_c applied at the concrete age t_0 , is given by:

$$\varepsilon_{cc}(40, t_0) = \varphi(t, t_0) * (\sigma_c / E_{cca})$$

Age – adjusted effective modulus, $E_{caa}(t, t_0)$. And an age – adjsted transformed section in the calculations where:

$$E_{caa}(t, t_0) = \frac{E_c(t_0)}{1 + \chi(t, t_0) * [E_c(t_0) / E_c(28)] * \varphi(t, t_0)}$$

Where: $\chi(t, t_0)$ is an aging coefficient that can be approximated by:

$$\chi(t, t_0) = \frac{t_0^{0.5}}{1 + t_0^{0.05}}$$

A.5: Test reported for water-soluble chloride ion analysis

Structural ID. No. : E61-1-001
Bridge name : Sheta River Bridge
Location of bridge : Kaffa Zone, Bonga

General data	
Identification of the sample	Nature of sample: Chloride ion analysis Location of sample: At the bottom of bridge deck Sampling date: 10 – 09 – 2008 E.C.
Date of the test	Date of the test: 20 – 09 – 2008 E.C.
Location of the test	Bonga complete secondary school, Chemistry laboratory
Name of the person in charge of the test	Mr. Berhanu Tefera (Researcher of this thesis) Mr. Adugna Adelo
References about this test procedure	ASTM C1218
Results (% C1):	11 % Water soluble chloride ion content in the taken sample from underneath bridge deck slab (Percentage in weight)

Remark:

The chloride ions limit recommended by ACI 318–05, maximum water soluble chloride ion (Cl^-) in reinforced concrete by mass of cement is 0.3. Therefore, the result indicates the reinforcement is less suspected to chloride ions (Cl^-).

$$\%Cl = \frac{3.545C_{AgNO_3} \times V_e \times V_f}{M_{pe} \times V_p}$$
$$\%Cl = \frac{3.545C_{AgNO_3} \times (V_e - V_t) \times V_f}{M_{pe} \times V_p}$$

Where:

- ✓ Taken 5 g of sample in powder form from bottom of bridge deck
- ✓ $M_{pe} = 50$ mg or 49 mg, $V_f = 250$ ml, $V_{HCl} = 5$ ml, $C_{HCl} = 25$ ml, $V_p = 50$ ml, $V_t = 300$ ml, and $V_e = 50$ ml

1. Compute the concentration of the silver nitrate solution (C_{AgNO_3}):


$$C_{\text{AgNO}_3} = \frac{C_{\text{HCl}} \times V_{\text{HCl}}}{V_t} = \frac{25\text{ml} \times 5\text{ml}}{300\text{ml}} \quad C_{\text{AgNO}_3} = 0.42\text{ml}$$

2. Compute the percentage of chloride ion content in the taken sample % CI:

$$\% \text{CI} = \frac{3.545 C_{\text{AgNO}_3} \times V_e \times V_f}{M_{\text{pe}} \times V_p} = \frac{3.545 \times 0.41\text{ml} \times 50\text{ml} \times 250\text{ml}}{50\text{mg} \times 50\text{ml}}$$

$$\text{CI} = 7.27\% \approx 8\%$$

A.6: Bridge inspection report for Sheta River Bridge



BRIDGES INSPECTION FORMAT

District Name JIMMA Section BONGA Road Segment BONGA-TELEGESEMI Bridge No EG1-1-001 Bridge Name SHETA RIVER BRIDGE

IT. NO	Bridge parts	Damage type	Damage qty by Rank			IT. NO	Bridge parts	Damage type	Damage qty by Rank			IT. NO	Bridge parts	Damage type	Damage qty by Rank		
			A	B	C				A	B	C				A	B	C
	Super structure						Sub Structure					Ancillaries					
1	Deck Slab	Cracking, M1 Peel Off, M2 Rebar Exposure, M2 M2 Void, M2 M2				4	Pier and Foundation	Cracking, M1 Peel Off, M2 Rebar Exposure, M2 M2 Honeycomb, M2 Void, M2 M2				8	Pavement	Wave, M1 Rutting, M1 Cracking, M1 Potholes, M2			
2	Concrete Girder/Arch	Cracking, M1 Peel Off, M2 Rebar Exposure, M2 M2 Honeycomb, M2 Void, M2 M2				5	Abutment and Wingwall	Displacement Scour, M2 Cracking, M1 Peel Off / Stone deterioration, M2 Rebar Exposure, M2 Honeycomb, M2 Void, M2 Water Leakage, M2 Displacement / Bulging, M2 Scour, M2				9	Kerb & Railing	Cracking, M1 Peel Off, M2 Rebar Exposure, M2 Deformation, M1 Corrosion, M1 Missing, Each			
3	Steel Girder	Deformation, M1 Cracking, M1 Corrosion, M2 Wearing, M2 Sill Missing, Each M2				6	Embankment	Depression, M2 Erosion, M2 Missing, Each				10	Expansion Joint	Noise, M1 Water Leakage, M1 Deformation, M1 Peel Off, M1 Missing, M1			
						7	Rip rap	Erosion, M2 Missing, Each Erosion, M2 Displacement, M2				11	Bearing	Main Damage, Each Parts missing, Each Anchor Damage, Each Bed Damage, each Unusual movement, Each			
												12	Drainage	Pipe Damage, Each Blocked, Each Inlet Damage, each			

Water Way adequacy (Over flooding, Siltation, Scouring, ...)

Yes No

Inspection date 10/10/2008 EC Inspector's name and signature BERHANU TEFERA

Ethiopian Roads Authority - Bridge Management System



Bridge / Structure Type
RC Deck Girder
RC Box Girder
RC Arch
RC Slab Culvert
RC Box Culvert
PC Deck Girder
PC Box Girder
Steel Truss
Steel Girder/ Composite
Steel Panel/Bailey
Masonry Arch
Steel Struss Main and RCDG approach
RC Box Girder Main and-RCDG approach
RC Arch main and RCDG Approach
RC Deck Girder Main and-RC Slab Culvert approach
RC Deck Girder Main and-RC BOX Culvert approach

Type of slab deck
RC
Steel
Timber
Earth Filled

Type of Pier
Masonry Wall
RC Column
RC Wall
RC Rigid-Frame

Type of Foundation
CLASS 'C' CONCRETE
RC Direct/Mat
RC-Pile
PC-Pile
Steel-Pipe
Caisson

Type of Railing
Masonry
RC
Steel
RC/Steel Composite

Type of Bearing
Steel Line-Plate
Pin Connected
Bearing-Plate
Steel Roller
Rubber

Type of Abutment
Masonry
RC


Type of Expansion Joint
Blind or Dummy
Filled /cheapwood
Rubber
Steel (Finger)
Steel sheet

Type of Surface
Asphalt
Concrete
Gravel

Span Support Type
Simple Span
Multi Span
Continuous Span

A.7: Bridge inventory report for Sheta River Bridge

Bridge Management System - 2002



BRIDGES INVENTORY FORMAT

DISTRICT	SECTION	ROAD SEGMENT	ROAD CLASS	BRIDGE NAME	ROAD NUMBER	BRIDGE NO	Coordinates
JIMMA	BOUGA	BOUGA-TELEBILAN	A9	SHETA RIVER BRIDGE	E61	E61-1-001	x=199753 y=506404

IT. NO.	GENERAL INFORMATION	SUPER STRUCTURE	SUBSTRUCTURE AND FOUNDATION	COMPONENTS AND ANCILLARIES				
1	LOCATION (KM. FROM AXIS)	4.65 km	BRIDGE / STRUCTURE TYPE	Rc Beck Gordon	ABUTMENT TYPE A1	Steel Masonry	TYPE OF FOUNDATION JOINT	Chicago
2	BRIDGE LENGTH (M)	20 M	NO. OF SPAN	One	ABUTMENT TYPE A2	Steel Masonry	TYPE OF CURB RAILING	Rc
3	BRIDGE WIDTH (M)	8.92 M	SPAN COMPOSITION		HEIGHT OF ABUTMENT A1 (M)	4.5 M	TYPE OF ABUTMENTS BEARING	Steel Bearing plates
4	BEVER WIDTH (M)	7.0 M	TOTAL SPAN LENGTH (M)	20	WIDTH OF ABUTMENT A1 (M)	11.3 M	TYPE OF PIERS BEARING	
5	PERMANENT WATER LEVEL	1.20 M	LOADING WAY WIDTH (M)	7.30	HEIGHT OF ABUTMENT A2 (M)	4.6 M	TYPE OF SURFACE	Concrete
6	HIGHEST WATER LEVEL	2.50 M	SIDE WALK WIDTH (M)	0.50	WIDTH OF ABUTMENT A2 (M)	11.3 M		
7	AREA TO DRAINAGE	Rolling	NO. OF LANE	Two	WIND WALL LENGTH (M)	2 M		
8	YEAR OF CONSTRUCTION	1950s	SPAN SUPPORT TYPE	Single Span	TYPE OF PIERS			
9	CONTRACTOR		DECK SLAB TYPE	Rc	NO. OF PIERS			
10	DESIGNER / SUPERVISOR	E.R.A.	SLAB THICKNESS (cm)	0.20 mt	HEIGHT OF PIER 1.1.3			
11	COST OF THE BRIDGE, \$	Eq. 350,000	NO. OF GIRDER / BOX	4	WIDTH OF PIER 1.2			
12	LOAD CAPACITY, Ton	32 ton	DEPTH OF GIRDER / BOX	0.55 mt	TYPE OF ABUTMENT FOUNDATION	Rc Spread mat.		
13	AVERAGE DAILY TRAFFIC		SPACING OF GIRDER (M)	2.10 mt	TYPE OF PIER FOUNDATION			
14	VEHICLE POSSIBILITY, T / N	Yes	WIDTH OF GIRDER / BOX (M)	0.40 mt	ABUTMENT FOUNDATION SIZE	12 x 3		
15	ROAD ALIGNMENT, CURVE / STRAIGHT	Straight			PIER FOUNDATION SIZE			
16	ALTITUDE (M)	1,600			NO. OF ABUTMENT PILES			
17	SAFETY / LOAD LIMIT SIGN, T / N	N/D			NO. OF PIER PILES			
18					ABUTMENT PILE DEPTH			
19					PIER PILE DEPTH			
20					SOIL TYPE	Red clay		

INSPECTOR: BERHANU TEFERS Approved

Date: 10/10/2008 EC

Ethiopian Roads Authority

A.8: Bridge damage record report for Sheta River Bridge

Bridge Management System - 2002

BRIDGES RECORD FORMAT

DISTRICT JIMMA SECTION BONGA

ROAD SEGMENT BONGA-FELEGESELA BRIDGE Name and Number SHETA RIVER BRIDGE (EG1-1-001)

Comments and Remarks (OBSERVED MAJOR DEFECTS IMPROVEMENT SUGGESTION - REMEDIAL MEASURE TO BE TAKEN)

- ⊕. Deck joints are blocked.
- ⊕. Transverse cracking, Peel off and honeycomb observed at the bottom of deck slab and Girders.
- ⊕. Cracking on both abutments and Wing wall.
- ⊕. Cracking with water leakage on the deck slab.
- ⊕. There is Vegetation around abutment.
- ⊕. There is Spalling of concrete at the railing.

Bridge History , Repair History (Any kind of major events)

Sheta river bridge was constructed in the late 1950's, which shows that it is has served about more than 50 years. However, in the absence of the required information and data (such as As-built drawings) to carry out the Strenghty evaluation analysis of the bridge, to determine the available capacity of the structure to carry loads, and considering the fact that bridge was designed with the older AASHTO HS-20 loadings.

As the works of Bonga-Mizan road upgrading project, Contract-II is under full swing, the required Rehabilitation works have already been done by the executing agency.

Special Recommendation of the Inspector

Replacement	<input type="checkbox"/>
Rehabilitation	<input checked="" type="checkbox"/>
Regular Inspection	<input type="checkbox"/>

Ethiopian Roads Authority - Bridge Management Branch



BRIDGE DAMAGES RECORD FORMAT

Bridge Name	Sheta river bridge	District	Jimma	Execution Data	10/10/2008 E.C
Bridge Type	RC Deck girder bridge	Section	Bonga	Inspector	Berhanu Tefera
Bridge Length(Mt)	20 m	Road segment	Bonga - Felege selam		
Span length composition(Mt)	20 m	Locattion Bridge Length(KM)	0.3Km		



Appendix B
Strength Evaluation of Existing Sheta River Bridge Deck
(Rating Simply supported straight Cast in -place RC T - Girder bridge)

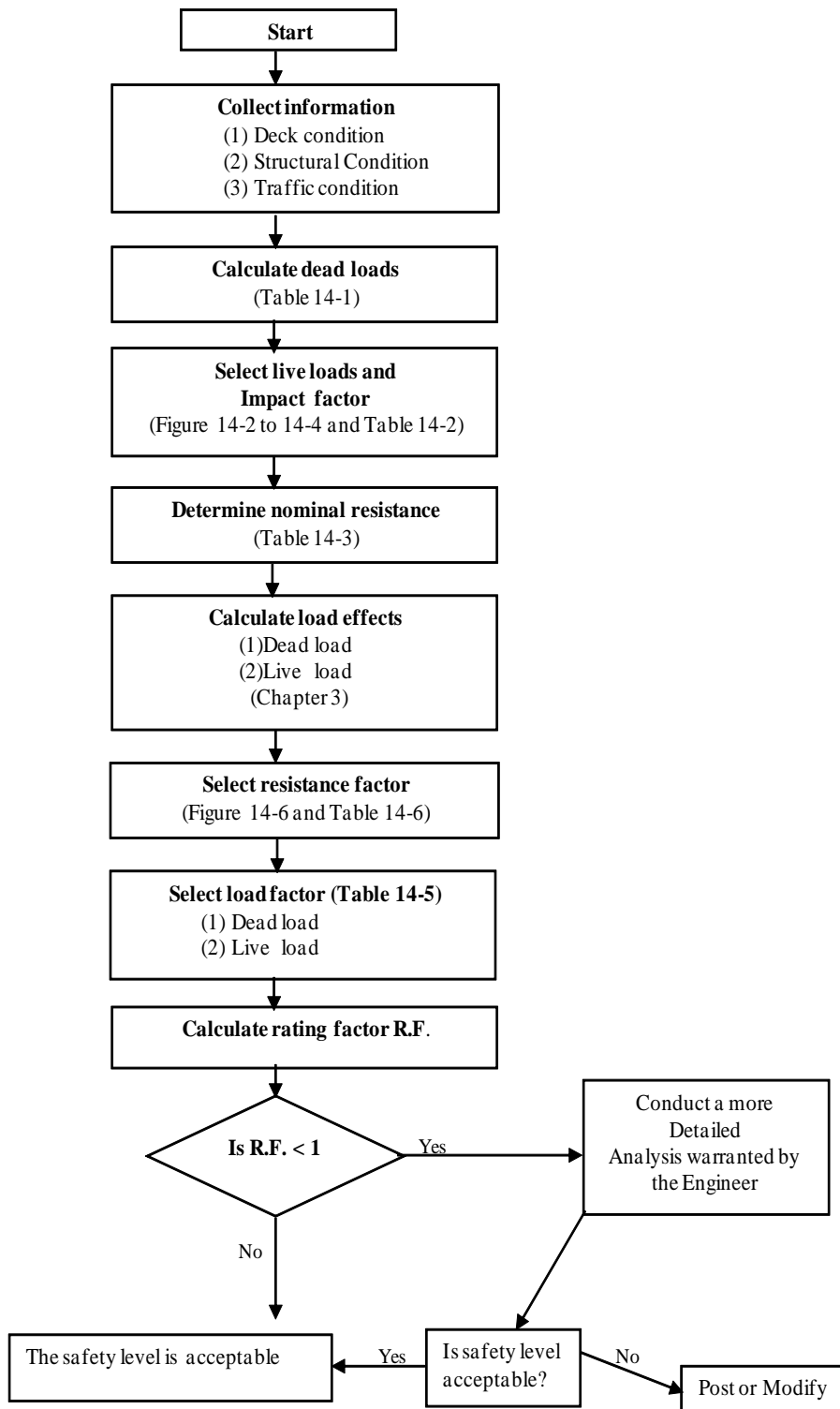


Figure B.1. Flow Chart for Rating Procedure [1]

General Information :

Name of bridge = Sheta River Bridge
Bridge Identification Number = E - 1 - 001
Year of construction = Late 1950s (Ethiopian Calander)
Design methodology = Load and Resistance Factor Design method (LRFD)
Governing Specification = ERA Bridge Design Manual 2002 (Chapter - 14)
= AASHTO LRFD Bridge design specification 2005 edition
(Manual for Strength & Condition Evaluation of Bridges. Washington, DC: AASHTO.)

Material Properties:

Type of concrete = C - 30 concrete grade

$f_{ck} = 24.00 \text{ Mpa}$ (Section 4.2.1.1. & ERA - Chapter 14 , p. 14)
 $g_c = 2,400.00 \text{ Kg/m}^3$ (ERA - Table 14.1 Unit weight of materials)
 $E_{cm} = 32,000.00 \text{ Mpa}$ (Table 2.5, EBCS - 2, 1995)

Type of steel = S - 300 Steel grade (Former grade 40)

$f_{yk} = 276.00 \text{ Mpa}$ (ERA - Table 14.3 Reinforcing steel yield stresses)
 $E_s = 200,000 \text{ Mpa}$
Density of bituminous materials = $2,250.00 \text{ Kg/m}^3$ (ERA - Table 14.1 Unit weight of materials)

Others:

Modular ratio $n = E_s/E_c = 6.25$ ”

Exsting Dimensions of Sheta river bridge :

Total span of brigde = 20.00 m
Clear roadway width = 7.32 m
Deck width = 8.92 m
Skew angle = 0.00 degree
Future wearing surface thickness = 0.075 m (assumed)
Additional curb width on both side = 0.50 m
Girders width = 0.40 m
Girders spacing @ c/c = 2.10 m
Clear bearing shelf width for bridge seats = 0.50 m
Height of abutment = 5.00 m
Deck slab thickness = 0.20 m
Girder depth = 0.85 m
Number of girder = 4.00
End of curb to outer face of exterior girder = 1.08 m
Deck overhang up to of exterior girder = 1.28 m
Number of lane = 2.00
Curb depth above slab = 0.15 m
Fillet = 0.10 m

Concrete railing and posts :

Distance b/n outer face of posts and curb end = 20.00 mm
Thickness of railing = 150.00 mm
Width of railing = 300.00 mm
Height of posts = 700.00 mm
Thickness of posts = 100.00 mm

Bridge Conditions :

Traffic Condition = The bridge exposed to heavy traffic volumes (>AADT = 1000) and for bridge do not have reasonable enforcement and apparent control of overloads

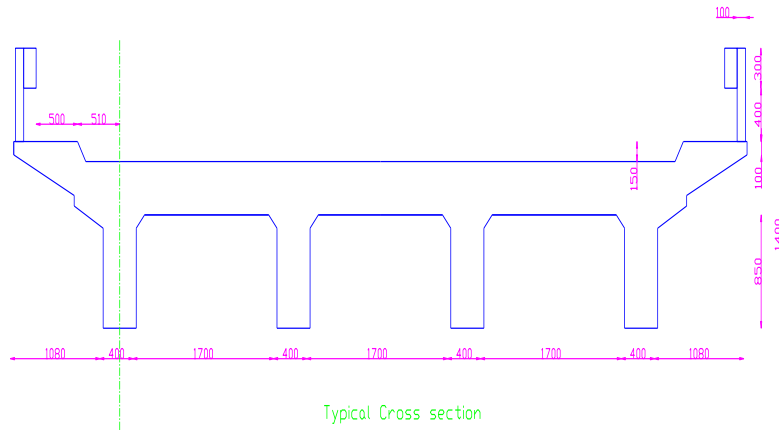


Figure B.1 Typical cross section of Sheta river bridge

B. LOADS

B.1. Permanent Loads

The dead load supported by the outside stringers or beams shall be the portion of the floor slab carried by the stringer or beam. Curbs, railings, and wearing surfaces if placed after the slab has cured, may be distributed equally to all roadway girders.

B.1.1. Interior girder loads

- ♣ Weight of railing and posts

$$W_{\text{rails \& posts}} = (0.15\text{m} \cdot 0.3\text{m} \cdot 2400\text{Kg/m}^3 \cdot 9.8\text{N/Kg}) + (0.70\text{m} \cdot (0.10\text{m} + 0.25\text{m}) / 2 \cdot 2400\text{Kg/m}^3 \cdot 9.8\text{N/Kg})$$

$$= \underline{\underline{3.94 \text{ KN/m}}}$$

- ♣ Weight of future wearing surface

$$W_{\text{wearing}} = 2,250\text{Kg/m}^3 \cdot 9.81 \text{ N/Kg} \cdot 0.075 \text{ m} \cdot 2.10\text{m}$$

$$= \underline{\underline{3.48 \text{ KN/m}}}$$

- ♣ Weight per linear meter of the reinforced concrete deck slab

$$W_{\text{slab}} = 2,400\text{Kg/m}^3 \cdot 9.81 \text{ N/Kg} \cdot 0.20 \text{ m} \cdot 2.10 \text{ m}$$

$$= \underline{\underline{9.89 \text{ KN/m}}}$$

- ♣ Weight per linear meter of cast-in-place interior girders

$$W_{\text{interior web}} = 0.5 \cdot 2,400\text{Kg/m}^3 \cdot 9.81 \text{ N/Kg} \cdot (0.40 \cdot 0.85) \text{ m}^2$$

$$= \underline{\underline{4.00 \text{ KN/m}}}$$

Weight of curb (150 mm above structural slab)

$$W_{\text{curb}} = 2,400\text{Kg/m}^3 \cdot 9.81 \text{ N/Kg} \cdot 0.15 \text{ m} \cdot 0.50\text{m}$$

$$= \underline{\underline{1.77 \text{ KN/m}}}$$

- ♣ Total dead load for interior girder ($DL_{\text{Interior beam}}$)

$$= \underline{\underline{23.07 \text{ KN/m}}}$$

B.1.2. Exterior girder loads

- ♣ Weight of railing and posts

$$W_{\text{rails \& posts}} = (0.15\text{m} \cdot 0.3\text{m} \cdot 2400\text{Kg/m}^3 \cdot 9.8\text{N/Kg}) + (0.70\text{m} \cdot (0.10\text{m} + 0.25\text{m}) / 2 \cdot 2400\text{Kg/m}^3 \cdot 9.8\text{N/Kg})$$

$$= \underline{\underline{3.94 \text{ KN/m}}}$$

- ♣ Weight of future wearing surface

$$W_{\text{wearing}} = 2,250\text{Kg/m}^3 \cdot 9.81 \text{ N/Kg} \cdot 0.075 \text{ m} \cdot 1.58 \text{ m}$$

$$= \underline{\underline{2.62 \text{ KN/m}}}$$

- ♣ Weight per linear meter of the reinforced concrete deck slab

$$W_{\text{slab}} = 2,400\text{Kg/m}^3 \cdot 9.81 \text{ N/Kg} \cdot 0.20 \text{ m} \cdot 1.58 \text{ m}$$

$$= \underline{\underline{7.44 \text{ KN/m}}}$$

- ♣ Weight per linear meter of cast-in-place interior girders

$$W_{\text{exterior web}} = 2,400\text{Kg/m}^3 \cdot 9.81 \text{ N/Kg} \cdot (0.40 \cdot 0.85) \text{ m}^2$$

$$= \underline{\underline{8.00 \text{ KN/m}}}$$

- ♣ Weight of curb (150 mm above structural slab)

$$W_{\text{curb}} = 2,400\text{Kg/m}^3 \cdot 9.81 \text{ N/Kg} \cdot 0.15 \text{ m} \cdot 0.50\text{m}$$

$$= \underline{\underline{1.77 \text{ KN/m}}}$$

- ♣ Total dead load for exterior girder ($DL_{\text{Exterior beam}}$)

$$= \underline{\underline{23.77 \text{ KN/m}}}$$

B.2. Vehicular Live Loads

Three legal trucks is believed that these typical vehicles correspond better to existing traffic and will provide more uniform reliability than the old standard AASHTO H or HS-20 design trucks. Each of the rating loads are applied at the bridge and the maximum of all the loads are taken. The three legal truck is shown below.

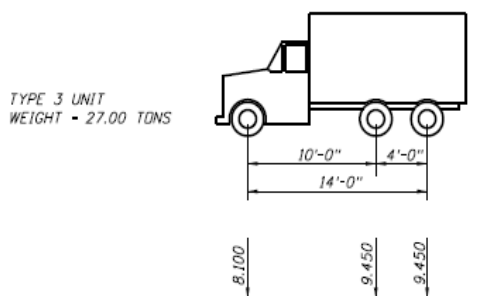


Figure B.2 Truck Type 3 Unit Weight 227KN

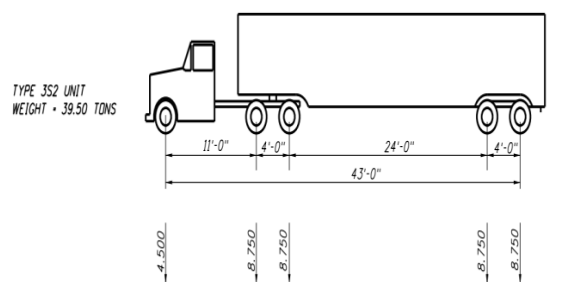


Figure B.3 Truck Type 3 S 2 Unit Weight 325 KN

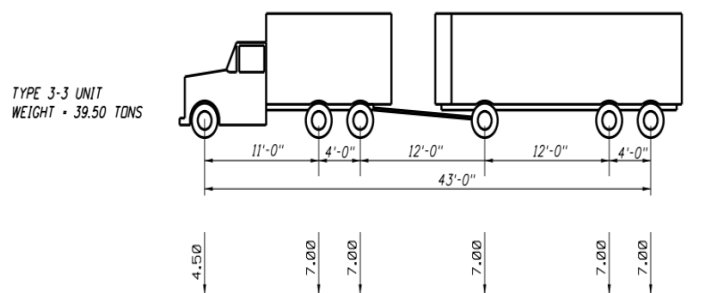


Figure B.4 Truck Type 3 - 3 Unit Weight 364 KN

B.3. Impact Factor

From Table 14 - 2 of the ERA - Bridge design manual, Impact factors are provided by correlating the roughness of the surface to the deck conditions survey values. However, Sheta river bridge is minor deficiency, item still functioning as designed.

Thus, the impact factor to be applied to the static load is:

$$\text{Impact Factor} = (1 + I) = 1.10$$

B.4. Live Load Distribution Factors

B.4.1 Interior Beams

B.4.1 - 1 Distribution Factor for moment in interior longitudinal beams

As per Table 4.6.2.2.2b-1 of AASHTO LRFD Bridge Design Specifications (AASHTO, 2005), the distribution of live loads per lane for moment in interior longitudinal beams, g_M , is specified as follows

♣ When one design lane is loaded:

$$g_M^{SI} = 0.06 + \left(\frac{G_S}{4300} \right)^{0.4} \times \left(\frac{G_S}{L} \right)^{0.3} \times \left(\frac{K_g}{L t_s^3} \right)^{0.1}$$

The longitudinal stiffness parameter:

$$K_g = n(I + A e_g^2)$$

In which $n = \frac{E_B}{E_D}$

Where:

E_B = modulus of elasticity of the beam material

E_D = modulus of elasticity of the deck material

e_g = the distance between the centers of gravity of the beams and deck

I = moment of inertia of the beam

A = area of beam

$$n = \frac{E_B}{E_D} = 1$$

$$e_g = \frac{6.7\text{m}}{2} + \frac{0.20\text{m}}{2} = 3.45\text{m}$$

$$I = \frac{bh^3}{12} = \frac{0.4\text{m} \times (0.85\text{m})^3}{12} = 0.0205\text{m}^4$$

$$A = (0.40\text{m} \times 0.85\text{m}) = 0.34\text{m}^2$$

$$K_g = n(I + A e_g^2) = 1 \times (0.0205\text{m}^4 + (0.34\text{m}^2 \times 3.45^2\text{m}^2))$$

$$K_g = 4.08\text{m}^4$$

Thus:

$$g_M^{SI} = 0.06 + \left(\frac{G_S}{4300} \right)^{0.4} \times \left(\frac{G_S}{L} \right)^{0.3} \times \left(\frac{K_g}{L t_s^3} \right)^{0.1}$$

$$g_M^{SI} = 0.06 + \left(\frac{2,100}{4,300} \right)^{0.4} \times \left(\frac{2,100}{20,000} \right)^{0.3} \times \left(\frac{4,080,000,000,000}{20,000 \times 200 \times 200 \times 200} \right)^{0.1} = 0.59$$

$$g_M^{SI} = \boxed{0.59} \quad (\text{With one design lane loaded})$$

♣ **When two or more design lane are loaded:**

$$g_M^{MI} = 0.075 + \left(\frac{G_S}{2900}\right)^{0.6} \times \left(\frac{G_S}{L}\right)^{0.2} \times \left(\frac{K_g}{L_s^3}\right)^{0.1}$$

$$g_M^{MI} = 0.075 + \left(\frac{2,100}{2,900}\right)^{0.6} \times \left(\frac{2,100}{20,000}\right)^{0.2} \times \left(\frac{4,080,000,000,000}{20,000 \times 200 \times 200 \times 200}\right)^{0.1} = 0.80$$

$g_M^{MI} =$ **0.80** (With two or more design lane loaded)

Therefore: Distribution factor for moment in interior longitudinal beams

$$g_M = \max(g_M^{SI}, g_M^{MI}) = \max(0.59, 0.80)$$

Two or more design lane loaded distribution factor for moment in interior longitudinal beams to be govern the rating:

$g_M =$ **0.80**

B.4.1 -2 Distribution Factor for shear in interior longitudinal beams

The distribution of live load per lane for shear in interior beams is specified in Table 4.6.2.2.3a-1 of AASHTO LRFD Bridge Design Specifications (AASHTO, 2005) as follows

♣ **When one design lane is loaded:**

$$g_V^{SI} = 0.36 + \frac{G_S}{7600} = 0.36 + \frac{2100}{7600} = \quad \mathbf{0.64}$$

♣ **When two or more design lane are loaded:**

$$g_V^{MI} = 0.2 + \frac{G_S}{3,600} - \left(\frac{G_S}{10,700}\right)^2 = 0.2 + \frac{2,100}{3,600} - \left(\frac{2,100}{10,700}\right)^2 = \quad \mathbf{0.74}$$

Therefore: Distribution factor for shear in interior longitudinal beams

$$g_V = \max(g_V^{SI}, g_V^{MI}) = \max(0.64, 0.74)$$

Two or more design lane loaded distribution factor for shear in interior longitudinal beams to be govern the rating:

$g_V =$ **0.74**

B.4.2 Exterior Beams

B.4.2 -1 Distribution Factor for moment in exterior longitudinal beams

As per Table 4.6.2.2d-1 of AASHTO LRFD Bridge Design Specifications (AASHTO, 2005), the distribution of live loads per lane for moment in exterior longitudinal beams, g_M , is specified as follows

♣ **In the case of one design lane loaded:**

When one design lane is loaded, the lever rule is used to determine the distribution factor, mg
 For computing the distribution factor by the lever rule, a simple structural member such as the one shown below is analyzed

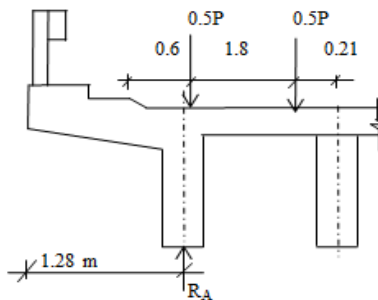


Fig B.2: Definition of Lever rule

$$\sum M_B = 0$$

$$R_A = \frac{0.5P \times (510 + 1800)}{2100} = \mathbf{0.53 P}$$

(Thus, $R_A = 0.5P + 0.5P = P$)

Article 3.6.1.1.2 of AASHTO LRFD Bridge Design Specification (AASHTO, 2005) states that a multiple presence factor $m = 1.20$ must be used when computing girder distribution factors by the lever rule. Thus, when one lane is loaded the distribution factor for the moment in exterior beams is:

$$g_M^{SE} = 1.2 \times 0.53 = \mathbf{0.63}$$

$$g_M^{SE} = \underline{\mathbf{0.63}}$$

♣ **In the case of two or more design lane loaded:**

$$g_M^{ME} = e \times g_M^{SE}$$

Where;

$$e = 0.77 + \frac{d_e}{2800}$$

The parameter d_e shall be taken as positive if the exterior web is in board of the curb or traffic barrier and negative if it is out board.

$$d_e = \underline{\mathbf{-0.51 m}}$$

(d_e = distance from the exterior web of exterior beam to the interior edge of curb or traffic barrier)

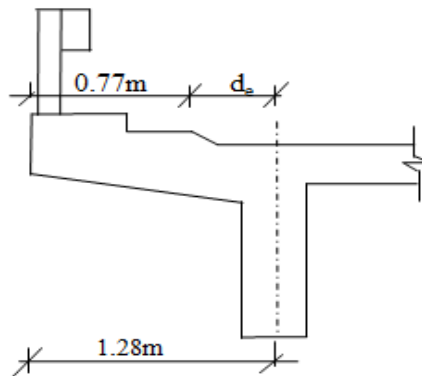


Fig. B.5: Deck overhang

Thus:

$$e = 0.77 + \frac{d_e}{2800} = 0.77 - \frac{510}{2800} = \mathbf{0.95}$$

$$g_M^{ME} = \underline{\mathbf{0.60}}$$

Therefore: Distribution factor for moment in exterior longitudinal beams

$$g_M = \max(g_M^{SE}, g_M^{ME}) = \max(0.63, 0.60)$$

One design lane loaded distribution factor for moment in exterior longitudinal beams to be govern the rating:

$$g_M = \boxed{\mathbf{0.63}}$$

B.4.2 -2 Distribution Factor for shear in exterior longitudinal beams

As per Table 4.6.2.2.3b-1 of AASHTO LRFD Bridge Design Specifications (AASHTO, 2005), the distribution of live loads per lane for shear in exterior longitudinal beams, mg , is specified as follows

♣ **In the case of one design lane loaded:**

When one design lane is loaded, the lever rule is used to determine the distribution factor, mg

For computing the distribution factor by the lever rule, a simple structural member such as the one shown above is analyzed

$$mg_v^{SE} = \underline{\mathbf{0.63}}$$

♣ In the case of two or more design lane loaded:

$$g_v^{ME} = e \times g_v^{SE}$$

Where; $e = 0.60 + \frac{d_e}{3,000}$

$$e = 0.77$$

Thus: $g_v^{ME} = \underline{0.49}$

Therefore: Distribution factor for shear in exterior longitudinal beams

$$g_v = \max(g_v^{SE}, g_v^{ME}) = \max(0.63, 0.49)$$

One design lane loaded distribution factor for shear in exterior longitudinal beams to govern the rating:

$$g_v = \boxed{0.63}$$

B.4.3 Summary Results of Load Distribution Factors

The following table summarizes the results of calculations concerning the live load distribution factors:

Action	Interior Beam	Exterior Beam
Bending Moment	0.80	0.63
Shear	0.74	0.63

Table B.1: Live Load Distribution Factors

B.5 Analysis

Three legal trucks is believed that these typical vehicles correspond better to existing traffic and will provide more uniform reliability than the old standard AASHTO H or HS design trucks. Each of the rating loads are applied at the bridge and the maximum of all the loads are taken.

B.5.1 Maximum Bending Moment Analysis

Case - I

A rudimentary structural analysis of a simply supported beam subjected to a Legal truck type 3 - 1 having two rear axles and one front axle as shown in Figure B.6 shows that the maximum moment occurs under the middle axle when such an axle is positioned at a distance of 0.52m to the left of the beam centerline.

♣ **Bending Moment Influence Line for truck - Type 3 -1 Unit weight 227 KN**

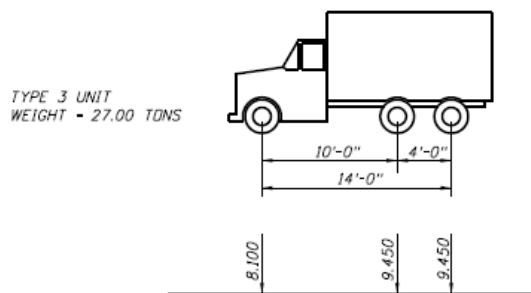


Figure B.6 Truck Type 3 Unit Weight 227KN

P	X*	P * X
73	0	0
77	4.5	346.50
77	5.7	438.90
♣ = 227		785.40

$$X' = \frac{\sum PX}{\sum P} = 3.46$$

$$X = 4.50m - 3.46m = \underline{\underline{1.04}}$$

Note: Take half of X to place the centerline of the span halfway between the center of gravity of loads and the nearest concentrated load, so that:

Distance from centerline (C_L) = 0.52 m

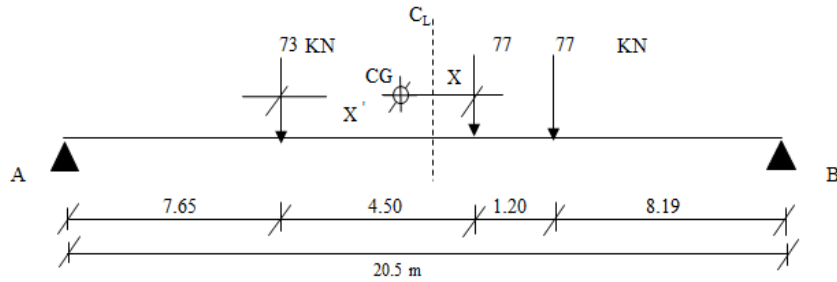


Figure B.7 Truck Type 3 Moving on a Bridge (Move from Right to Left side)

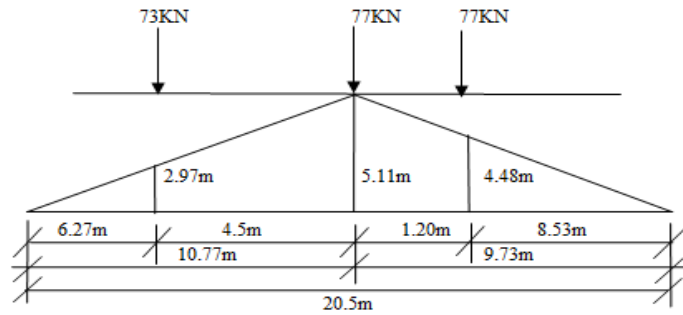


Figure B.5 Influence Line for Truck Type 3 - 1 Unit Weight 227 kN

$$M_{\text{Truck - Type 3-1}} = (73 \times 2.97) + (77 \times 5.11) + (77 \times 4.48) = 955.24 \text{ kN} - \text{m}$$

$$M_{\text{Truck - Type 3-1}} = \underline{\underline{955.24 \text{ kNm}}}$$

Case - II

A rudimentary structural analysis of a simply supported beam subjected to a Legal truck type 3 - 2 having four rear axles and one front axle as shown in Figure B.8 shows that the maximum moment occurs under the middle between rear axles when such an axle is positioned at a distance of 1.1 m to the right of the beam centerline.

♣ **Bending Moment Influence Line for truck - Type 3 - 2 Unit weight 325 kN**

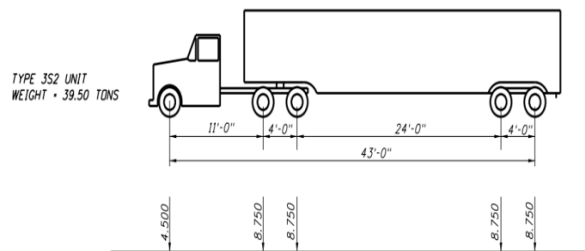


Figure B.8 Truck Type 3 - 2 Unit Weight 325 kN

P	X*	P * X
70	0	0
70	1.2	84
70	7.8	546
70	9.00	630
45	12.30	553.50
325		1,814

$$X' = \frac{\sum PX}{\sum P} = \underline{\underline{5.58}}$$

$$X = 7.80\text{m} - 5.58\text{m} = \underline{\underline{2.22}}$$

Note: Take half of X to place the centerline of the span halfway between the center of gravity of loads and the nearest concentrated load, so that:

Distance from centerline (C_L) = 1.11 m

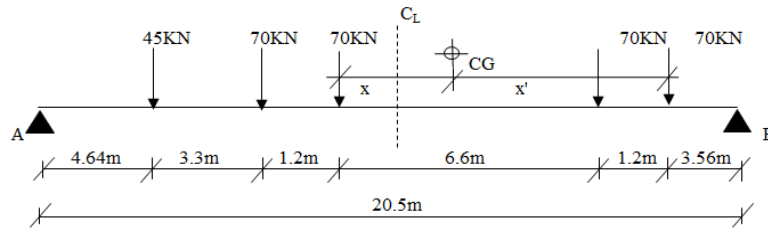


Figure B.6 Truck Type 3 - 2 Moving on a Bridge (Move from Right to Left side)

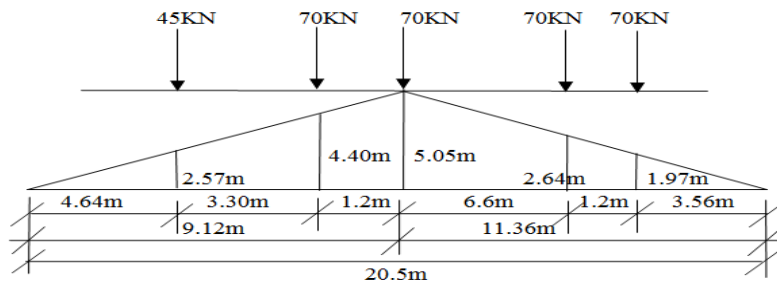


Figure B.6 Influence Line for Truck Type 3 - 2 Unit Weight 325 kN

$$M_{\text{Truck - Type 3-2}} = (45 \times 2.57) + (70 \times 4.40) + (70 \times 5.05) + (70 \times 2.64) + (70 \times 1.97) = 1,099.85 \text{ kN-m}$$

$$M_{\text{Truck - Type 3-2}} = \underline{\underline{1,099.85 \text{ kN-m}}}$$

Case - III

A rudimentary structural analysis of a simply supported beam subjected to a Legal truck type 3 - 3 having five rear axles and one front axle as shown in Figure B.9 shows that the maximum moment occurs under the middle between rear axles when such an axle is positioned at a distance of 0.59m to the left of the beam centerline.

♣ **Bending Moment Influence Line for truck - Type 3 - 3 Unit weight 364 kN**

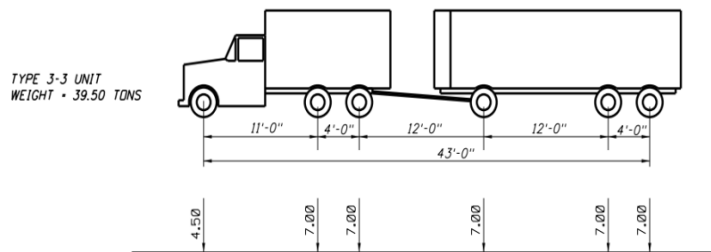


Figure B.9 Truck Type 3 - 3 Unit Weight 364 kN

P	X*	P * X
55	0	0
55	4.5	247.50
55	5.7	313.50
73	10.20	744.60
63	15.10	951.30
63	16.3	1026.90
364		3,284

$$X' = \frac{\sum PX}{\sum P} = \underline{\underline{9.02}}$$

$$X = 10.20\text{m} - 9.02\text{m} = \underline{\underline{1.18}}$$

Note: Take half of X to place the centerline of the span halfway between the center of gravity of loads and the nearest concentrated load, so that:

$$\text{Distance from centerline (C}_L\text{)} = \underline{\underline{0.59 \text{ m}}}$$

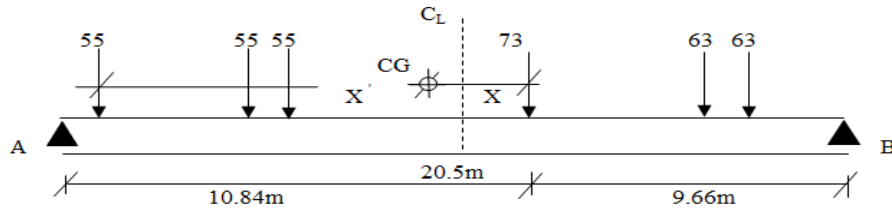


Figure B.7 Truck Type 3 - 3 Moving on a Bridge (Move from Right to Left side)

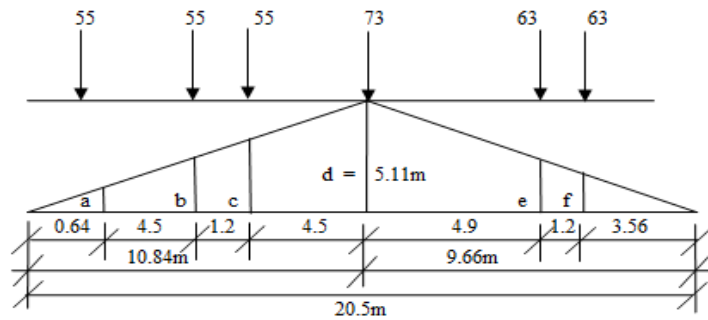


Figure B.7 Influence Line for Truck Type 3 - 3 Unit Weight 364 KN

Where:

$$\begin{aligned} a &= 0.30\text{m} & d &= 5.11\text{m} \\ b &= 2.42\text{m} & e &= 2.52\text{m} \\ c &= 2.99\text{m} & f &= 1.88\text{m} \end{aligned}$$

$$M_{\text{Truck - Type 3-3}} = (55 \times 0.30) + (55 \times 2.42) + (55 \times 2.99) + (73 \times 5.11) + (63 \times 2.52) + (63 \times 1.88) = 964.28 \text{ KN-m}$$

$$M_{\text{Truck - Type 3-3}} = \underline{\underline{964.28 \text{ KN - m}}}$$

herefore: From those the three Legal truck rating loads are applied at the bridge and the maximum live load moment of all the loads are taken.

$$M_{\text{Truck}} = \max(M_{\text{Truck Type 3-1}}, M_{\text{Truck Type 3-2}}, M_{\text{Truck Type 3-3}})$$

$$M_{\text{Truck}} = \max(955.4 \text{ KN - m}, 1,099.85 \text{ KN - m}, 964.28 \text{ KN - m})$$

$$M_{\text{Truck}} = \boxed{1,099.85 \text{ KN - m}} \quad (\text{Legal Truck 3 - 2 Unit weight 325KN to be govern the rating of bridge})$$

B.5.1 - 1 Maximum live load moment for an interior beam

By applying the impact factor and the distribution factor for moment of interior beams, we can then compute the maximum live load under the following loads:

With unfactored live load moment of $M_{\text{Truck}} = 1,099.85 \text{ KN - m}$, $g_m = 0.80$, and $I = 1.10$, M_{LL+I} can be computed at the location of the maximum live load moment (at 9.12m from the left support) to be:

$$M_{LL+I} = g_m \times (1.10 \times M_{\text{Truck}})$$

$$M_{LL+I} = 0.80 \times (1.10 \times 1,099.85 \text{ KN - m})$$

$$M_{LL+I} = \underline{\underline{967.87 \text{ KN - m}}}$$

♣ **Live load moment (at midspan):**

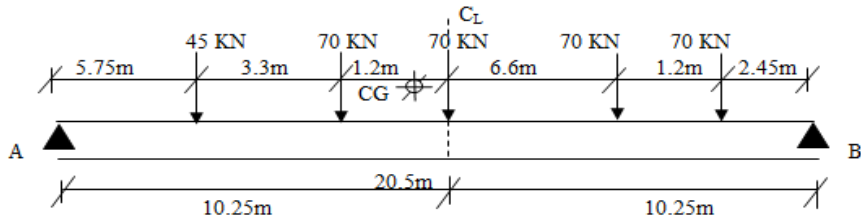


Figure B.10 Truck Type 3 - 2 Moving on a Bridge (@ Mid - span)

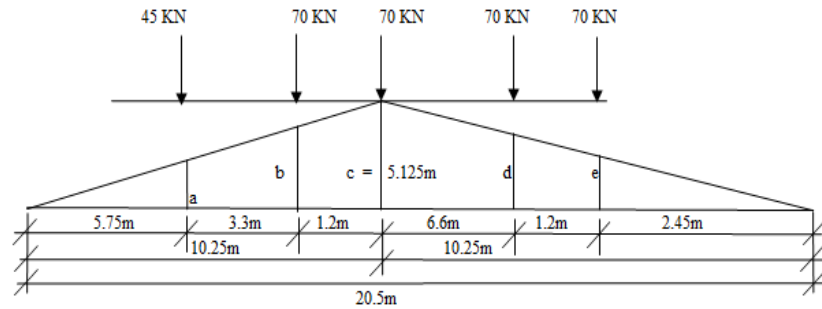


Figure B10 Bending Moment Influence Line for Truck Type 3 -2 (@ Mid - Span)

$$\begin{aligned} a &= 2.875\text{m} & d &= 1.825\text{m} \\ b &= 4.525\text{m} & e &= 1.225\text{m} \\ c &= 5.125\text{m} \end{aligned}$$

$$M_{\text{Truck}(\text{mid})} = (45 \times 2.875) + (70 \times 4.525) + (70 \times 5.125) + (70 \times 1.825) + (70 \times 1.225) = 1,018.38 \text{ KN} \cdot \text{m}$$

$$M_{\text{Truck}(\text{mid})} = \underline{\underline{1,018.38 \text{ KN} \cdot \text{m}}}$$

With unfactored live load moment of $M_{\text{Truck}(\text{mid})} = 1,018.38 \text{ KN} \cdot \text{m}$, $g_m = 0.80$, and $I = 1.10$, $M_{\text{LL}+I(\text{mid})}$ can be computed at the location of at the mid span (at 10.25m from the left support) to be:

$$M_{\text{LL}+I(\text{mid})} = g_m \times (1.10 \times M_{\text{Truck}(\text{mid})})$$

$$M_{\text{LL}+I(\text{mid})} = 0.80 \times (1.10 \times 1,018.38 \text{ KN} \cdot \text{m})$$

$$M_{\text{LL}+I(\text{mid})} = \underline{\underline{896.17 \text{ KN} \cdot \text{m}}} \quad (\text{Live load moment at midspan for interior beams})$$

B.5.1 - 2 Maximum live load moment for an exterior beam

By applying the dynamic allowance factor and the distribution factor for moment of exterior beams, we can then compute the maximum live load under the following loads:

With unfactored live load moment of $M_{\text{Truck Type 3-2}} = 1,099.85 \text{ KN} \cdot \text{m}$, $g_m = 0.63$, and $I = 1.10$, $M_{\text{LL}+I}$ can be computed at the location of the maximum live load moment (at 9.12m from the left support) to be:

$$M_{\text{LL}+I} = g_m \times (1.10 \times M_{\text{Truck}})$$

$$M_{\text{LL}+I} = 0.63 \times (1.10 \times 1,099.85 \text{ KN} \cdot \text{m})$$

$$M_{\text{LL}+I} = \underline{\underline{762.20 \text{ KN} \cdot \text{m}}}$$

♣ **Live load moment (at midspan):**

$$M_{\text{LL}+I(\text{mid})} = g_m \times (1.10 \times M_{\text{Truck}(\text{mid})})$$

$$M_{\text{LL}+I(\text{mid})} = 0.63 \times (1.10 \times 1,018.38 \text{ KN} \cdot \text{m})$$

$$M_{\text{LL}+I(\text{mid})} = \underline{\underline{705.74 \text{ KN} \cdot \text{m}}} \quad (\text{Live load moment at midspan for exterior beams})$$

B.5.1 - 3 Maximum dead load moment for an interior beam

- ♣ The dead load moment at the location where the live load produces the maximum effect is

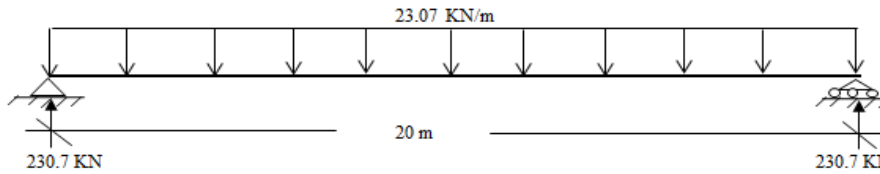


Figure B.11 Interior Girder Dead Load Moment

$$M_{DL} = 230.70 \text{ kN} \times 9.12 \text{ m} - 23.07 \text{ kN/m} \times \frac{(9.12 \text{ m})^2}{2}$$

$$M_{DL} = \underline{\underline{1,144.57 \text{ kN} \cdot \text{m}}}$$

- ♣ The dead load moment at midspan for interior beam is:

$$M_{DL} = \frac{DL_{\text{Interior beam}} \times L^2}{8}$$

$$M_{DL} = \frac{23.07 \text{ kN/m} \times (20 \text{ m})^2}{8}$$

$$M_{DL} = \underline{\underline{1,153.50 \text{ kN} \cdot \text{m}}} \quad (\text{Dead load moment at midspan for interior beams})$$

B.5.1 - 4 Maximum dead load moment for an exterior beam

- ♣ The dead load moment at the location where the live load produces the maximum effect is

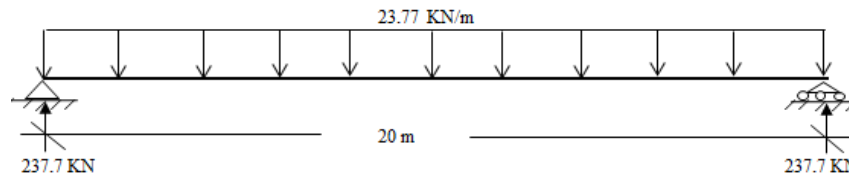


Figure B.12 Exterior Girder Dead Load Moment

$$M_{DL} = 237.70 \text{ kN} \times 9.12 \text{ m} - 23.77 \text{ kN/m} \times \frac{(9.12 \text{ m})^2}{2}$$

$$M_{DL} = \underline{\underline{1,179.30 \text{ kN} \cdot \text{m}}}$$

- ♣ The dead load moment at midspan for exterior beam is:

$$M_{DL} = \frac{DL_{\text{Exterior beam}} \times L^2}{8}$$

$$M_{DL} = \frac{23.77 \text{ kN/m} \times (20 \text{ m})^2}{8}$$

$$M_{DL} = \underline{\underline{1,188.50 \text{ kN} \cdot \text{m}}} \quad (\text{Dead load moment at midspan for exterior beams})$$

B.5.2 Maximum Shear Force Analysis

Based on the shear reinforcement details of the bridge girders, it is necessary to perform shear rating calculations of the bridge at two locations along both the interior and exterior girders. These two critical locations as stipulated in Article 8.15.5.1.4 of AASHTO Standard Specifications for Highway Bridges (AASHTO, 2002) are:

- ♣ At d_v from either support
- ♣ At 2.29 m from either support at which the stirrup spacing changes from 350mm to 450mm

B.5.2.1 Interior Beam Shear Analysis

♣ Interior beam maximum live load shear force at d_v

$$\text{Effective shear depth } d_v \text{ is maximum of } = \begin{cases} 0.9d_c = 0.90 \times 0.98 \text{ m} = 0.88 \text{ m} \\ 0.72h = 0.72 \times 1.05 \text{ m} = 0.76 \text{ m} \end{cases}$$

Where:

d_v = effective shear depth (mm)

d_c = the corresponding effective depth from the extrem compression fiber to the centroid of the tensile force in the tensile reinforcement (mm)

Case - I

A rudimentary structural analysis of a simply supported beam subjected to a Legal truck type 3 - 1 having two rear axles and one front axle as shown in Figure B.6 shows that the maximum shear force occurs under the rear axle when such an axle is positioned at a distance of $d_v = 0.88 \text{ m}$ from the left support.

♣ Shear Force Influence Line for truck - Type 3 -1 Unit weight 227 KN

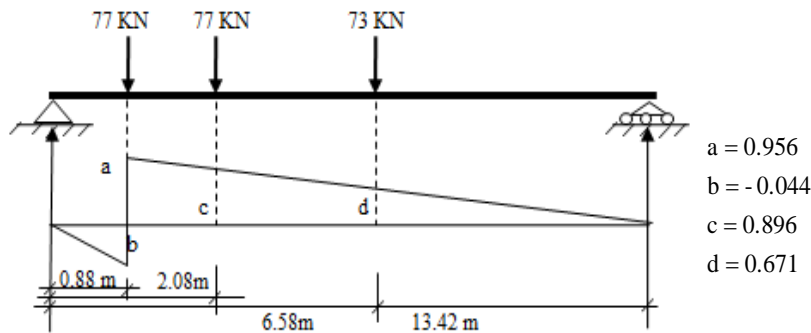


Figure B.12: Shear force Influence line diagram: Case - I

$$V_{\text{Truck Type 3-1}} = (77 \times 0.956) + (77 \times 0.896) + (73 \times 0.671) = 191.59 \text{ KN}$$

$$V_{\text{Truck Type 3-1}} = \underline{\underline{191.59 \text{ KN}}}$$

Case - II

A rudimentary structural analysis of a simply supported beam subjected to a Legal truck type 3 - 2 having four rear axles and one front axle as shown in Figure B.8 shows that the maximum shear force occurs under the rear axle when such an axle is positioned at a distance of $d_v = 0.88 \text{ m}$ from the left support.

♣ Shear Force Influence Line for truck - Type 3 -2 Unit weight 325 KN

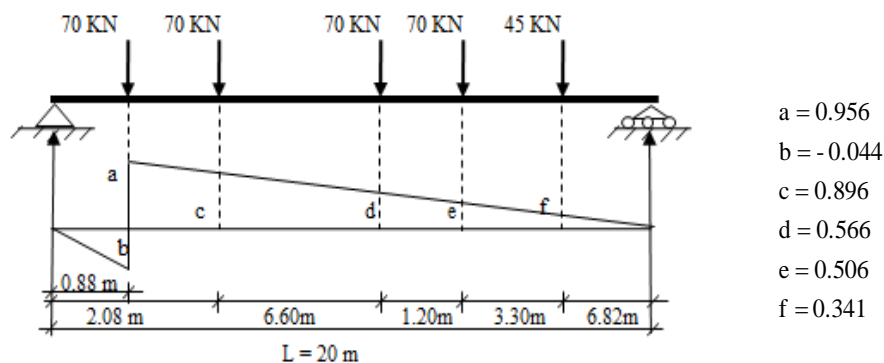


Figure B.13: Shear force Influence line diagram: Case - II

$$V_{\text{Truck Type 3-2}} = (70 \times 0.956) + (70 \times 0.896) + (70 \times 0.566) + (70 \times 0.506) + (45 \times 0.341) = 220.03 \text{ KN}$$

$$V_{\text{Truck Type 3-2}} = \underline{\underline{220.03 \text{ KN}}}$$

Case - III

A rudimentary structural analysis of a simply supported beam subjected to a Legal truck type 3 - 3 having five rear axles and one front axle as shown in Figure B.9 shows that the maximum shear force occurs under the rear axle when such an axle is positioned at a distance of $d_v = 0.88$ m from the left support.

♣ **Shear Force Influence Line for truck - Type 3 - 3 Unit weight 364 KN**

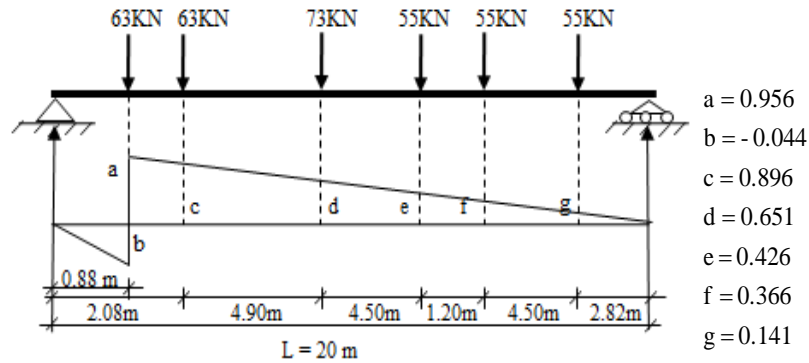


Figure B.14: Shear force influence line diagram: Case - III

$$V_{\text{Truck Type 3-3}} = (63 \times 0.956) + (63 \times 0.896) + (73 \times 0.651) + (55 \times 0.426) + (55 \times 0.366) + (55 \times 0.141) = 215.51 \text{ KN}$$

$$V_{\text{Truck Type 3-3}} = \underline{215.51 \text{ KN}}$$

Thus: From those the three Legal truck rating loads are applied at the bridge and the maximum live load shear force of all the loads are taken.

$$V_{\text{Truck}} = \max(V_{\text{Truck Type 3-1}}, V_{\text{Truck Type 3-2}}, V_{\text{Truck Type 3-3}})$$

$$V_{\text{Truck}} = \max(191.59 \text{ KN}, 220.03 \text{ KN}, 215.51 \text{ KN})$$

$$V_{\text{Truck}} = \underline{220.03 \text{ KN}} \quad (\text{Legal Truck 3 - 2 Unit weight 325KN to be govern the rating of bridge})$$

Therefore:

By applying the dynamic allowance factor and the distribution factor for shear force of interior beams, we can then compute the maximum live load under the following loads:

With unfactored live load shear force of $V_{\text{Truck}} = 220.03 \text{ KN}$, $g_v = 0.74$, and $I = 1.10$, $V_{\text{LL+I}}$ can be computed at the location of the maximum live load shear force (at $d_v = 0.88$ m from the left support) to be:

$$V_{\text{LL+I}} = g_v \times (1.10 \times V_{\text{Truck}})$$

$$V_{\text{LL+I}} = 0.74 \times (1.10 \times 220.03 \text{ KN})$$

$$V_{\text{LL+I}} = \underline{179.10 \text{ KN}}$$

♣ **Interior beam dead load shear force at d_v**

As stated in section B.5.2.1 since the dead load is a distributed load the shear computed at a distance $d_v = 0.88$ m from the support.

$$V_{\text{DL}} = \text{DL}_{\text{Interior beam}} \times \left(\frac{L}{2} - d_v \right)$$

$$V_{\text{DL}} = 23.07 \text{ KN/m} \times \left(\frac{20 \text{ m}}{2} - 0.88 \text{ m} \right)$$

$$V_{\text{DL}} = \underline{210.40 \text{ KN}}$$

♣ **Interior beam live load shear force at 2.29 m from the support**

An influence line analysis shown in Figure B.15 is used to compute the shear force at 2.29 m from the support where the stirrup spacing changes from 350 mm to 450 mm.

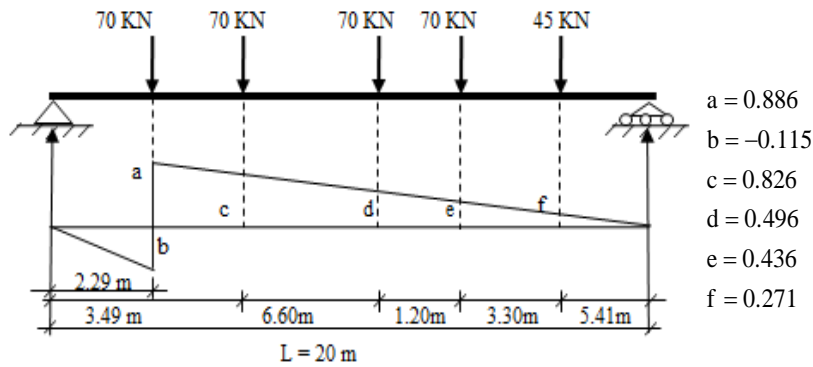


Figure B.15: Shear force Influence line diagram: @ 2.29 m

$$V_{\text{Truck} (@ 2.29\text{m})} = (70 \times 0.886) + (70 \times 0.826) + (70 \times 0.496) + (70 \times 0.436) + (45 \times 0.271) = 197.28 \text{ KN}$$

$$V_{\text{Truck} (@ 2.29\text{m})} = \underline{197.28 \text{ KN}}$$

Therefore:

With unfactored live load shear force of $V_{\text{truck} (@ 2.29\text{m})} = 197.28 \text{ KN}$, $g_v = 0.74$, and $I = 1.10$, $V_{\text{LL}+I} (@ 2.29 \text{ m})$ can be computed at the location of the maximum live load shear force (at 2.29 m from the left support) to be:

$$V_{\text{LL}+I} (@ 2.29\text{m}) = g_v \times (1.10 \times V_{\text{Truck} (@ 2.29\text{m})})$$

$$V_{\text{LL}+I} (@ 2.29\text{m}) = 0.74 \times (1.10 \times 197.28 \text{ KN})$$

$$V_{\text{LL}+I} (@ 2.29\text{m}) = \underline{160.59 \text{ KN}}$$

♣ **Interior beam dead load shear force at 2.29 m from the support**

As stated in section B.5.2.1 since the dead load is a distributed load the shear computed at a distance 2.29 m from the support.

$$V_{\text{DL} (@ 2.29\text{m})} = DL_{\text{Interior beam}} \times \left(\frac{L}{2} - 2.29 \text{ m} \right)$$

$$V_{\text{DL} (@ 2.29\text{m})} = 23.07 \text{ KN/m} \times \left(\frac{20 \text{ m}}{2} - 2.29 \text{ m} \right)$$

$$V_{\text{DL} (@ 2.29\text{m})} = \underline{177.87 \text{ KN}}$$

B.5.2.2 Exterior Beam Shear Analysis

♣ **Exterior beam maximum live load shear force**

The exterior beam shear force due to live load at $d_v = 0.88 \text{ m}$ from the support is computed in a manner similar to that presented in Section B.5.2.1.

With unfactored live load shear force of $V_{\text{Truck}} = 220.03 \text{ KN}$, $g_v = 0.63$, and $I = 1.10$, $V_{\text{LL}+I}$ can be computed at the location of the maximum live load shear force (at $d_v = 0.88 \text{ m}$ from the left support) to be:

$$V_{\text{LL}+I} = g_v \times (1.10 \times V_{\text{Truck}})$$

$$V_{\text{LL}+I} = 0.63 \times (1.10 \times 220.03 \text{ KN})$$

$$V_{\text{LL}+I} = \underline{152.48 \text{ KN}}$$

♣ **Exterior beam dead load shear force at d_v**

As stated in section B.5.2.1 since the dead load is a distributed load the shear computed at a distance $d_v = 0.88$ m from the support.

$$V_{DL} = DL_{\text{Exterior beam}} \times \left(\frac{L}{2} - d_v \right)$$

$$V_{DL} = 23.77 \text{ KN/m} \times \left(\frac{20 \text{ m}}{2} - 0.88 \text{ m} \right)$$

$$V_{DL} = \underline{\underline{216.78 \text{ KN}}}$$

♣ **Exterior beam live load shear force at 2.29 m from the support**

With unfactored live load shear force of $V_{\text{truck}(@ 2.29\text{m})} = 197.28 \text{ KN}$, $g_v = 0.63$, and $I = 1.10$, $V_{LL+I} (@ 2.29 \text{ m})$ can be computed at the location of the maximum live load shear force (at 2.29 m from the left support) to be:

$$V_{LL+I} (@ 2.29\text{m}) = g_v \times (1.10 \times V_{\text{Truck} (@ 2.29\text{m})})$$

$$V_{LL+I} (@ 2.29\text{m}) = 0.63 \times (1.10 \times 197.28 \text{ KN})$$

$$V_{LL+I} (@ 2.29\text{m}) = \underline{\underline{136.72 \text{ KN}}}$$

♣ **Exterior beam dead load shear force at 2.29 m from the support**

As stated in section B.5.2.1 since the dead load is a distributed load the shear computed at a distance 2.29 m from the support.

$$V_{DL(@ 2.29\text{m})} = DL_{\text{Exterior beam}} \times \left(\frac{L}{2} - 2.29 \text{ m} \right)$$

$$V_{DL(@ 2.29\text{m})} = 23.77 \text{ KN/m} \times \left(\frac{20 \text{ m}}{2} - 2.29 \text{ m} \right)$$

$$V_{DL(@ 2.29\text{m})} = \underline{\underline{183.27 \text{ KN}}}$$

B.6 Load Combination

B.6.1 Interior Girder

	Moment @ Mid - span	Moment at 9.12 m from support
M_{LL+I}	896.17 KN - m	967.87 KN - m
M_{DL}	1,153.50 KN - m	1,144.57 KN - m
$M_{DL} + M_{LL+I}$	2,049.67 KN - m	2,112.44 KN m

Table B.2 Bending Moment Interior Girder load combinations

	Shear @ $d_v = 0.88\text{m}$	Shear @ 2.29m
V_{LL+I}	179.10 KN	160.59 KN
V_{DL}	210.40 KN	177.87 KN
$V_{DL} + V_{LL+I}$	389.50 KN	338.46 KN

Table B.3 Shear force Interior Girder load combinations

B.6.2 Exterior Girder

	Moment @ Mid - span	Moment at 9.12 m from support
M_{LL+I}	705.74 KN - m	762.20 KN - m
M_{DL}	1,188.50 KN - m	1,179.30 KN - m
$M_{DL} + M_{LL+I}$	1,894.24 KN - m	1,941.50 KN m

Table B.4 Bending Moment Exterior Girder load combinations

	Shear @ $d_v = 0.88\text{m}$	Shear @ 2.29m
V_{LL+I}	152.48 KN	136.72 KN
V_{DL}	216.78 KN	183.27 KN
$V_{DL} + V_{LL+I}$	369.26 KN	319.99 KN

Table B.5 Shear force Exterior Girder load combinations

B.7 Member Capacity

Sheta River Bridge there is no structural plans, however, Engineering judgment can be used, along with historical records and plans of similarly constructed RC deck girder bridges in Ethiopia nearest to the year of construction of Sheta river bridge (Bitino River Bridge) and after measuring undeformed bare rebars size to arrive at possible reinforcing details, as shown as below;

B.7.1 Interior Girders

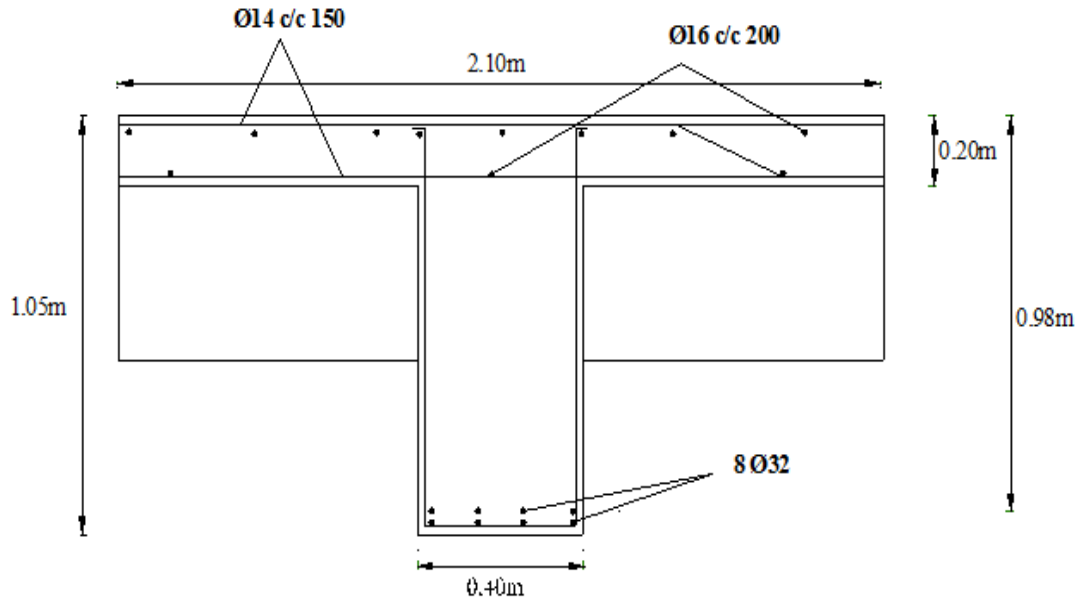


Figure B.16 Member Dimensions

Effective flange width of interior beams Article 4.6.2.6 of AASHTO Standard Specifications for highway bridges (AASHTO, 2005):

The interior beams, the effective flange width may be taken as the least of: $b_e = 2.10 \text{ m}$

$$\text{Effective width of interior girder, } b_{\text{eff}} = \begin{cases} 0.25 \times L_{\text{eff}} = 0.25 \times 20 \text{ m} = 5.0 \text{ m} \\ 12t_s + b_w = 12 \times 0.2 \text{ m} + 0.4 \text{ m} = 2.8 \text{ m} \\ \text{Spacing of adjacent beams} = 2.10 \text{ m} \end{cases}$$

Distance from the extreme compression fiber to centroid of tension reinforcement $d_c = 0.98 \text{ m}$

Concrete strength $f'_c = 24 \text{ N/mm}^2$

Steel reinforcement yield strength $f_y = 276 \text{ N/mm}^2$ (ERA - Table 14.3 Reinforcing steel yield stresses)

Stirrup spacing $S = 300 \text{ mm}$

Stirrup area $A_v \geq 0.083 \sqrt{f'_c} \frac{b_v S}{f_y}$ $A_v = 176.79 \text{ mm}^2$

Shear width (taken as the minimum web width in the depth d_v) $b_v = 400 \text{ mm}$

Angle of inclination of Diagonal Compression Stress $\theta = 44^\circ$

$\beta = 2.0$ (taken as $\theta = 44^\circ$ and $\beta = 2.0$ traditionally used for evaluation of shear resistance)

Area of steel $A_{st} = 10,456 \text{ mm}^2$

Layer	$A_s \text{ (mm}^2\text{)}$	Depth from top of slab to center of each reinforcement layer (mm)
1 st Layer of steel includes 10 \times 16 mm bars	2,011	75
2 nd Layer of steel includes 10 \times 16 mm bars	2,011	145
3 rd Layer of steel includes 4 \times 32 mm bars	3,217	959
4 th Layer of steel includes 4 \times 32 mm bars	3,217	1,000

Table B.6 Longitudinal steel layer details

Check our historical records and plans of similarly constructed RC deck girder bridges

- ♣ Maximum and Minimum area of steel reinforcement

Balance Failure

- ♣ Balance neutral axis depth, X_b

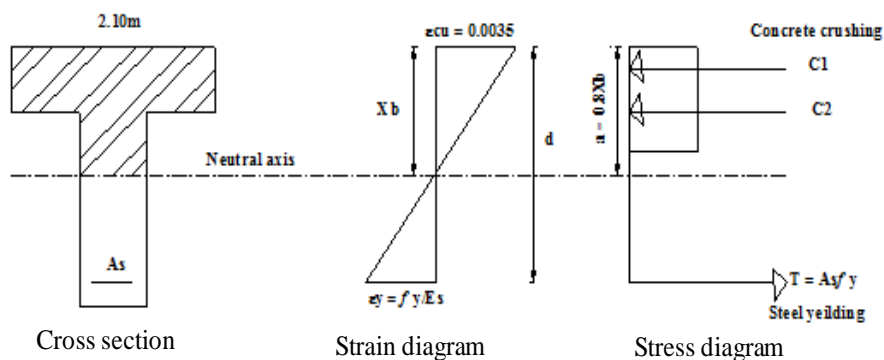
$$\frac{X_b}{d} = \frac{\epsilon_{cu}}{\epsilon_y + \epsilon_{cu}} \quad \epsilon_y = \frac{f_y}{E_s}, \quad \frac{X_b}{d} = \left(\frac{\epsilon_{cu}}{\epsilon_y + \epsilon_{cu}} \right) = \left(\frac{700}{f_y + 700} \right) = 0.72$$

$$X_b = \left(\frac{\epsilon_{cu}}{\epsilon_y + \epsilon_{cu}} \right) \times d = \left(\frac{700}{276 + 700} \right) \times 980 \text{ mm}$$

$$X_b = 0.72d = 0.7 \times 980 \text{ mm} = \underline{705.6 \text{ mm}}$$

Thus: $a = 0.8X_b = 0.8 \times 705.6 \text{ mm} = 564.48 \text{ mm}$

$a > t_s = 200 \text{ mm}$



- ♣ Balance Area of steel reinforcement, A_{sb}

$$C = C_1 + C_2$$

$$C = 0.85f'_c b_w a_b + 0.85f'_c (b_{eff} - b_w) t_s$$

$$C = (0.85 \times 24 \text{ N/mm}^2 \times 400 \text{ mm} \times 564.48 \text{ mm}) + (0.85 \times 24 \text{ N/mm}^2 (2,100 \text{ mm} - 400 \text{ mm}) \times 200 \text{ mm})$$

$$C = 11.54 \text{ MN}$$

$$A_{sb} = \frac{C}{f_y} = \frac{11.54 \times 10^6 \text{ N}}{276 \times 10^6 \text{ N/m}^2} = 0.0418 \text{ m}^2 = 41,811.60 \text{ mm}^2$$

Therefore: Maximum area of steel reinforcement $A_{s,max}$

$$A_{s,max} = 0.75A_{sb} = 0.75 \times 41,811.60 \text{ mm}^2 = 31,358.70 \text{ mm}^2$$

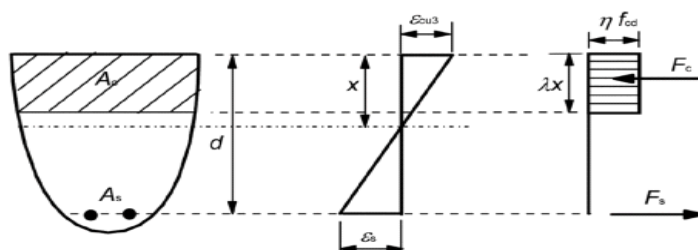
$$A_{s,max} = \underline{31,358.70 \text{ mm}^2}$$

$$A_{s,min} = \rho_{min} bd = \left(\frac{0.4}{f_y} \right) \times 2,100 \text{ mm} \times 980 \text{ mm} = 2,982.21 \text{ mm}^2$$

i.e.

$$A_{s,min} < A_s < A_{s,max}$$

Ok!



<p style="text-align: center;">Flexure</p>	<p>$\eta = 1.0$ for $f'_{ck} \leq 50$ MPa</p> <p>$\lambda = 0.8$ for $f'_{ck} \leq 50$ MPa</p> $x = \frac{A_{st} f_y}{\eta 0.85 f_c \lambda b_e} = \frac{10,456 \text{ mm}^2 \times 276 \text{ N/mm}^2}{1.0 \times 0.85 \times 24 \text{ N/mm}^2 \times 0.8 \times 2,100 \text{ mm}} = \underline{84.20 \text{ mm}}$ <p>$x = 84.20 \text{ mm} < t_s = 200 \text{ mm}$ Ok!</p> <p>Thus: $a = \lambda x = 0.8 \times 84.20 \text{ mm} = \underline{67.36 \text{ mm}}$</p> $M_n = A_{st} f_y \left(d - \frac{a}{2} \right)$ $M_n = 10,456 \text{ mm}^2 \times 276 \text{ N/mm}^2 \times \left(980 \text{ mm} - \frac{67.36 \text{ mm}}{2} \right) = \underline{2,730.94 \text{ KN} - \text{m}}$
<p style="text-align: center;">Shear (@ $d_v = 0.88$)</p>	<p>The nominal shear resistance, V_n, shall be determined as the lesser of:</p> $V_n = V_c + V_s \qquad V_n = 0.25 f'_c b_v d_v$ <p>in which $V_c = 0.083 \beta \sqrt{f'_c} b_v d_v$ $V_s = \frac{A_v f_y d_v \text{Cot}\theta}{s}$</p> $V_c = 0.083 \times 2.0 \times \sqrt{24 \text{ N/mm}^2} \times 400 \text{ mm} \times 880 \text{ mm}$ $V_c = \underline{286.26 \text{ KN}}$ $V_s = \frac{176.79 \text{ mm}^2 \times 276 \text{ N/mm}^2 \times 880 \text{ mm} \times \text{Cot } 45^\circ}{300 \text{ mm}} = \underline{221.65 \text{ KN}}$ <p>Thus:</p> $V_n = 0.25 \times 24 \text{ N/mm}^2 \times 400 \text{ mm} \times 880 \text{ mm} = \underline{2,112 \text{ KN}}$ $V_n = 286.26 \text{ KN} + 221.65 \text{ KN} = \underline{507.91 \text{ KN}}$ <p>Therefore: $V_n = \underline{507.91 \text{ KN}}$ (Nominal shear resistance @ $d_v = 0.88m$)</p>
<p style="text-align: center;">Shear (@ 2.29 m from the support)</p>	$V_c = 0.083 \times 2.0 \times \sqrt{24 \text{ N/mm}^2} \times 400 \text{ mm} \times 880 \text{ mm}$ $V_c = \underline{286.26 \text{ KN}}$ $V_s = \frac{A_v f_y d_v \text{Cot}\theta}{s}$ $V_s = \frac{176.79 \text{ mm}^2 \times 276 \text{ N/mm}^2 \times 880 \text{ mm} \times \text{Cot } 45^\circ}{450 \text{ mm}} = \underline{147.76 \text{ KN}}$ $V_n = 286.26 \text{ KN} + 147.76 \text{ KN} = \underline{434.02 \text{ KN}}$

B.7.2 Exterior Girders

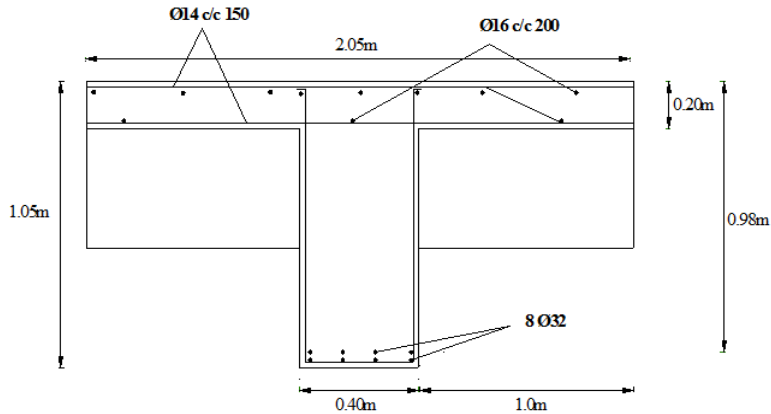


Figure B.17 Member Dimensions

Effective flange for exterior beams width Article 4.6.2.6 of AASHTO Standard Specifications for highway bridges (AASHTO, 2005):
The exterior beams, the effective flange width may be taken as one - half the effective width of the adjacent interior beam, plus the least of:

$$= \begin{cases} 0.125 \times L_{\text{eff}} = 0.125 \times 20 \text{ m} = 2.5 \text{ m} \\ 6t_s + 0.5b_w = 6 \times 0.2 \text{ m} + 0.5 \times 0.4 \text{ m} = 1.4 \text{ m} \\ \text{Width of the overhang} = 1.28 \text{ m} \end{cases}$$

$$b_{\text{eff}} = 0.5(2.10 \text{ m}) + 1.28 \text{ m} = 2.30 \text{ m}$$

Distance from the extreme compression fiber to centroid of tension reinforcement $d_c = 0.98 \text{ m}$

Concrete strength $f'_c = 24 \text{ N/mm}^2$

Steel reinforcement yield strength $f_y = 276 \text{ N/mm}^2$ (ERA - Table 14.3 Reinforcing steel yield stresses)

Stirrup spacing $S = 300 \text{ mm}$

Stirrup area $A_v \geq 0.083 \sqrt{f'_c} \frac{b_v S}{f_y}$ $A_v = 176.79 \text{ mm}^2$

Shear width (taken as the minimum web width in the depth d_v) $b_v = 400 \text{ mm}$

Angle of inclination of Diagonal Compression Stress $\theta = 45^\circ$

$\beta = 2.0$ (taken as $\theta = 45^\circ$ and $\beta = 2.0$ traditionally used for evaluation of shear resistance)

Area of steel $A_{st} = 10,456 \text{ mm}^2$

Layer	A_s (mm ²)	Depth from top of slab to center of each reinforcement layer (mm)
1 st Layer of steel includes 10 \times 16 mm bars	2,011	75
2 nd Layer of steel includes 10 \times 16 mm bars	2,011	145
3 rd Layer of steel includes 4 \times 32 mm bars	3,217	959
4 th Layer of steel includes 4 \times 32 mm bars	3,217	1,000

Table B.7 Longitudinal steel layer details

<p style="text-align: center;">Flexure</p>	$\eta = 1.0 \text{ for } f'_{ck} \leq 50 \text{ MPa}$ $\lambda = 0.8 \text{ for } f'_{ck} \leq 50 \text{ MPa}$ $x = \frac{A_{st} f_y}{\eta 0.85 f_c \lambda b_e} = \frac{10,456 \text{ mm}^2 \times 276 \text{ N/mm}^2}{1.0 \times 0.85 \times 24 \text{ N/mm}^2 \times 0.8 \times 2,300 \text{ mm}} = \underline{76.88 \text{ mm}}$ <p>$X = 76.88 \text{ mm} < t_s = 200 \text{ mm} \quad \text{Ok!}$</p> <p>Thus: $a = \lambda X = 0.8 \times 76.88 \text{ mm} = \underline{61.50 \text{ mm}}$</p> $M_n = A_{st} f_y \left(d - \frac{a}{2} \right)$ $M_n = 10,456 \text{ mm}^2 \times 276 \text{ N/mm}^2 \times \left(980 \text{ mm} - \frac{61.50 \text{ mm}}{2} \right) = \underline{2,739.40 \text{ KN} - \text{m}}$
<p style="text-align: center;">Shear (@ $d_v = 0.88$)</p>	<p>The nominal shear resistance, V_n, shall be determined as the lesser of:</p> $V_n = V_c + V_s \quad V_n = 0.25 f_c b_v d_v$ <p>in which $V_c = 0.083 \beta \sqrt{f'_c} b_v d_v$ $V_s = \frac{A_v f_y d_v \text{Cot}\theta}{s}$</p> $V_c = 0.083 \times 2.0 \times \sqrt{24 \text{ N/mm}^2} \times 400 \text{ mm} \times 880 \text{ mm}$ $V_c = \underline{286.26 \text{ KN}}$ $V_s = \frac{176.79 \text{ mm}^2 \times 276 \text{ N/mm}^2 \times 880 \text{ mm} \times \text{Cot } 45^0}{300 \text{ mm}} = \underline{221.65 \text{ KN}}$ <p>Thus:</p> $V_n = 0.25 \times 24 \text{ N/mm}^2 \times 400 \text{ mm} \times 880 \text{ mm} = \underline{2,112 \text{ KN}}$ $V_n = 286.26 \text{ KN} + 221.65 \text{ KN} = \underline{507.91 \text{ KN}}$ <p>Therefore: $V_n = \underline{507.91 \text{ KN}}$ (Nominal shear resistance @ $d_v = 0.88\text{m}$)</p>
<p style="text-align: center;">Shear (@ 2.29 m from the support)</p>	$V_c = 0.083 \times 2.0 \times \sqrt{24 \text{ N/mm}^2} \times 400 \text{ mm} \times 880 \text{ mm}$ $V_c = \underline{286.26 \text{ KN}}$ $V_s = \frac{A_v f_y d_v \text{Cot}\theta}{s}$ $V_s = \frac{176.79 \text{ mm}^2 \times 276 \text{ N/mm}^2 \times 880 \text{ mm} \times \text{Cot } 45^0}{450 \text{ mm}} = \underline{147.76 \text{ KN}}$ $V_n = 286.26 \text{ KN} + 147.76 \text{ KN} = \underline{434.02 \text{ KN}}$

B.8 Rating Calculation

The following factors are defined thus:

Live load factor for heavy volume traffic	$\gamma_{LL} = 1.45$	(ERA Table 14 - 5 based on ADTT)
Resistance Factor (for shear and flexure)	$\phi = 0.95$	

Table B.8 Load and Resistance Factor Rating (LRFR) Calculation for legal truck load
(Using the Impact factor and load distribution factors stipulated in the ERA - Bridge Design Manual - 2002)

Flexure Rating	Interior girder	Legal Level $\gamma_{DC} = 1.20$ $\gamma_{LL} = 1.45$	$RF = \frac{\phi M_n - \gamma_{DC} \times M_{DL}}{\gamma_{LL} M_{LL+I}}$ $RF = \frac{0.95 \times 2,730.94 - 1.20 \times 1,144.57}{1.45 \times 967.87} = 1.59$
	Exterior girder	Legal Level $\gamma_{DC} = 1.20$ $\gamma_{LL} = 1.45$	$RF = \frac{\phi M_n - \gamma_{DC} \times M_{DL}}{\gamma_{LL} M_{LL+I}}$ $RF = \frac{0.95 \times 2,739.40 - 1.20 \times 1,179.30}{1.45 \times 762.20} = 1.07$
Shear Rating (@ $d_v = 0.88$ m)	Interior girder	Legal Level $\gamma_{DC} = 1.20$ $\gamma_{LL} = 1.45$	$RF = \frac{\phi V_n - \gamma_{DC} \times V_{DL}}{\gamma_{LL} V_{LL+I}}$ $RF = \frac{0.95 \times 507.91 - 1.20 \times 210.40}{1.45 \times 179.10} = 1.89$
	Exterior girder	Legal Level $\gamma_{DC} = 1.20$ $\gamma_{LL} = 1.45$	$RF = \frac{\phi V_n - \gamma_{DC} \times V_{DL}}{\gamma_{LL} V_{LL+I}}$ $RF = \frac{0.95 \times 507.91 - 1.20 \times 216.78}{1.45 \times 152.48} = 1.01$
Shear Rating (@ = 2.29 m)	Interior girder	Legal Level $\gamma_{DC} = 1.20$ $\gamma_{LL} = 1.45$	$RF = \frac{\phi V_n - \gamma_{DC} \times V_{DL}}{\gamma_{LL} V_{LL+I}}$ $RF = \frac{0.95 \times 507.91 - 1.20 \times 177.87}{1.45 \times 160.59} = 1.16$
	Exterior girder	Legal Level $\gamma_{DC} = 1.20$ $\gamma_{LL} = 1.45$	$RF = \frac{\phi V_n - \gamma_{DC} \times V_{DL}}{\gamma_{LL} V_{LL+I}}$ $RF = \frac{0.95 \times 434.02 - 1.20 \times 183.27}{1.45 \times 136.72} = 1.09$